2022

Reconstructing Regional Paleoenvironments and Geomorphic History of High Plains Playa-Lunette Systems

Alyssa E. Sims
Minnesota State University, Mankato

Recommended Citation

Reconstructing regional paleoenvironments

and geomorphic history of

High Plains playa-lunette systems

by

Alyssa E. Sims

A Thesis Submitted in Partial Fulfillment of the

Requirements for the Degree of

Master of Science

In

Geography

Minnesota State University – Mankato
Mankato, Minnesota
May 2022

April 25th, 2022

Reconstructing regional paleoenvironments and geomorphic history of
High Plains playa-lunette systems

Alyssa E. Sims

This thesis has been examined and approved by the following members of the
student's committee

_____

Dr. Mark Bowen

Primary Advisor

_____

Dr. Phillip Larson

Committee Member

_____

Dr. Samantha Kaplan

Committee Member

ACKNOWLEDGMENTS

Words alone are not enough to express how thankful I am to have Dr. Mark Bowen by my side as my primary advisor through this program. Not only was he there for endless rounds of writing revisions, but he has encouraged me to push myself academically, professionally, and most importantly - personally. He will be a lifelong friend and mentor. I would also like to thank my thesis committee, Dr. Phil Larson and Dr. Samantha Kaplan, for advising and encouraging this work and my future.

None of this would have been possible without the constant love and support from family, friends, and community. The daily phone calls to my mom and sister kept me clearheaded and inspired. They are both the hardest working and driven women I know. To my fiancé, Codie, who is my biggest cheerleader, comic relief, and shoulder to cry on. To my best friend, Zoe, who is my constant sounding board and voice of reason. To my wonderful support animal, Lumi, who always manages to keep a smile on my face. To geography graduate cohort, especially Brianna, which made this university feel like home. The community of Mankato will always have a huge space in my heart. Thank you all from the bottom of my heart.

FUNDING

Table of Contents

Figures and Tables

Abstract

Playas are ephemeral upland-embedded wetlands found in semiarid and arid regions worldwide. Lunettes are isolated dunes that form along the downwind margin of playas. The paleoclimatic and geomorphic history of High Plains playa-lunette systems (PLSs) are poorly understood. To address this, we characterize the stratigraphy of four PLSs in southwest Kansas, USA. Methods include: 1) collect soil-sediment cores from playa centers and windward slopes of lunettes; 2) describe cores using USDA techniques; 3) estimate age of stratigraphic units using radiocarbon (14C); and 4) reconstruct paleoenvironmental conditions using stable carbon isotopes (13C) and particle size analysis.

Playa stratigraphy is relatively simple and consists of well-developed surface soils underlain by gleyed clays. Buried soils were identified in 2 of 4 playas. Calibrated playa 14C ages range from 6,280-23,600 cal yr BP. Lunette stratigraphy is complex; buried soils and thick units of light-dark bands are common. Calibrated 14C ages for buried soils in lunettes range from 19,050-32,300 cal yr BP. Lunette 13C data are highly oscillatory, but average ~-14‰ in the lower portion of cores (i.e., prior to ~30 ka), decline to ~-20‰ in the middle portion of cores (estimated ~30-12 ka) and steadily return to ~-14‰ in the upper ~1 m (~12 ka to present). These data indicate a warm-dry period dominated with C4 plants preceded ~30 ka, and was followed by a cool-moist, C3 plant dominated period before returning to warm-dry conditions throughout much of the Holocene.

Playa records extend from marine isotope stage (MIS) 3 (i.e., prior to the Last Glacial Maximum), and lunette records extend into MIS 3. Playa stratigraphy suggests they were dominated by alluvial-lacustrine processes during the late Pleistocene and early Holocene. Alternating light-dark bands in lunettes are hypothesized to represent incipient soils and aeolian sediment resulting from small-scale shifts in climate throughout much of the late Pleistocene and early Holocene, with geomorphic processes alternating between aeolian deposition and pedogenesis. Well-developed surface soils in playas and lunettes suggest stabilization and pedogenesis dominated the mid to late Holocene under a warming and drier climate. Thus, PLS development appears linked to both global-scale and regional climate processes.

Chapter 1 Introduction

Playa wetlands are relatively small, circular to elongate, shallow wetlands found in semiarid regions worldwide and are particularly abundant on the semi-arid High Plains of the central United States. Playa wetlands differ significantly different from arid region playa lakes, as discussed below. These ephemeral playa wetlands (i.e., "playas") have distinct hydroperiods seasonally and annually but are most often dry during winter months with peak water levels in late spring to early summer (Ward and Huddleson, 1972). These shallow landforms are topographic depressions within endorheic basins (Fish et al., 1998). Great Plains playas are often composed of shrink swell clays, and infiltration rates differ by several orders of magnitude depending on moisture status (e.g., actively wet, recently wet, dry). When dry, desiccation cracks form on the surface and allow for high initial infiltration rates (Zartman et al., 1996). Once these clays become saturated, the cracks close, infiltration rates decrease, and the playa may store water.

Lunettes are low relief (up to 30 m), isolated, aeolian dunes with a sub-circular, bow, or crescentic shape with arms facing upwind (Figure 1). Lunettes form along the downwind margin of playas, ephemeral lakes, or ephemeral wetlands (Rich, 2013; Sabin and Holliday, 1995). They often develop over prolonged periods ranging from thousands of years to several tens of thousands of years. The earliest evidence of formation in Kansas is ~40 ka (perhaps as early as ~125 ka); however, on the southern High Plains (SHP), formation began as early as ~250 ka (Rich, 2013; Bowen and Johnson, 2012; Holliday, 1997; Arbogast, 1996). In Kansas, lunettes have an average height of ~3 m (9.8 ft) (Bowen et al., 2018). Lunette formation is influenced by the strength and direction of prevailing winds. For example, in Kansas predominantly northwest

winds during the late Pleistocene to Holocene have resulted in lunette formation primarily on the southeast margin of playas (Bowen et al., 2018; Laity, 2014).

Given the morpho-genetic connections between playas and lunettes, we can think of these interrelated landforms as a playa-lunette system (PLS) (Bowen and Johnson, 2012). Coupled playa-lunette systems are crucial natural resources, especially in the High Plains of Kansas. Playas provide a range of ecosystem functions including surface water storage, wetland habitat, and groundwater recharge (Smith et al., 2011), with playas being the primary source of recharge for the Ogallala Aquifer (Gurdak and Roe, 2009). Lunettes have high potential to preserve archaeological artifacts and high-resolution stratigraphic sequences. Paleoindian communities used lunettes as sites for both seasonal and permanent campsites due to the dune's ability to shield from northerly winds while allowing maximum insolation on the southern side and providing cover to stalk animals attracted to playas (Bowen et al., 2018). PLS stratigraphy provides high resolution paleoenvironmental data (Bowen and Johnson, 2015, 2012). Because playas are low spots on the landscape, they accumulate and store sediment from the surrounding watershed primarily due to runoff during wet periods (Luo et al., 1999; Bowen et al., 2018). Lunettes receive regional dust inputs and deflated sediment from playas during dry periods (Bowen and Johnson, 2015, 2012). As a result, sediment and proxy records preserved within PLSs can be used to reconstruct environmental conditions and geomorphic processes at local to regional to global scales. For example, stable carbon isotopes preserved in soil organic matter within PLSs can be used to reconstruct C3 and C4 plant concentrations throughout PLS evolution to infer regional climatic conditions, local playa hydrology, and geomorphic processes affecting PLSs (e.g., Bowen and Johnson, 2012, 2015). C3 grasses thrive in cool (15-30 °C),

moist environments whereas C4 grasses thrive in warm (24-40 °C), dry environments with lower

atmospheric CO_2 levels (Leavitt et al., 2007).

Figure 1 *Oblique aerial view of a typical playa-lunette system (Lane County, Kansas) with a large (~1.1 km x 0.5 km) shallow (<1 m deep) playa and lunette (~7.5 m tall) to the southeast (clearly visible due to agricultural terraces encircling it).*

Playa-lunette systems are also particularly useful as geochronological records of

paleoenvironmental change. Both form and process are influenced by fluvial, lacustrine, and

aeolian processes, with the dominant geomorphic process at a given time being dependent upon

prevailing environmental conditions (Bowen and Johnson, 2012). In these systems, changes in

geomorphic processes are driven by changes in temperature and precipitation regimes. The

geomorphic processes of western Kansas alternated between dissolution- and fluvial-aeolian-

driven processes as climate changed and playa development progressed (Bowen and Johnson,

2012). Dissolution processes were dominant during moist periods and initial playa development whereas aeolian processes, such as deflation, were dominant during arid periods and playa evolution (Bowen and Johnson, 2012). Dateable material such as mollusk shells, animal teeth and bones, seeds, and buried soils are commonly preserved within PLSs, which can provide age control for stratigraphic units and insight into the timing of environmental conditions and geomorphic processes during formation of those units (Bowen and Johnson, 2015, 2012; Holliday et al., 2008; Mason et al., 2008).

Our understanding of the paleoclimatic and geomorphic history of High Plains PLSs is expanding; however, few studies have investigated the coupled relationships between playas and lunettes to develop a comprehensive conceptual model for the origin of PLSs. Several hypotheses have been proposed for the potential origin of playas and lunettes; however, there has not been extensive studies into the age and geomorphic processes of these systems, especially in North America. The purpose of this study is to reconstruct regional paleoenvironments and geomorphic history of playa-lunette systems on the High Plains of western Kansas. To do this, I: 1) collected soil-sediment cores from four playa-lunette systems (located in Lane, Clark, and Scott counties, Kansas) to describe and analyze stratigraphic units; (2) determined the age of stratigraphic units in playas and lunettes using 14C dating techniques; and (3) reconstructed paleoenvironmental conditions (i.e., climate, hydrology, vegetation communities) and geomorphic processes using a variety of environmental proxy records including stable carbon isotope and particle size distribution data. The resulting data are utilized to reconstruct the timing and magnitude of environmental change and shifts in geomorphic processes throughout playa-lunette system formation and evolution.

I hypothesize that playa-lunette systems began forming during the late Pleistocene with playa formation occurring first and lunette formation following. Prior to the Last Glacial Maximum (LGM), climate on the Central High Plains (CHP) was characterized by frequent extreme shifts in temperature and precipitation regimes (Bowen and Johnson, 2012; Welch and Hale, 1987) and playas likely formed via dissolution. Once the playa formed and climate shifted to warmer and/or drier conditions (e.g., during the Pleistocene-Holocene Transition), aeolian processes (e.g., wind deflation from playas) became dominant and lunettes experienced increased sediment accumulation and development. Alternating cool and/or moist and warm and/or dry periods throughout the Holocene resulted in differing rates of playa and lunette development and dominant geomorphic processes. Climate change in the Holocene produced highly variable precipitation patterns with a warming trend, which impacted playa hydroperiod and the development of lunettes. When climate was dry, playa hydroperiods were short and playas were likely only inundated seasonally, allowing soils to develop. When playa floors were exposed, sediment was deflated and accumulated on lunettes along with regional dust inputs. Conversely, when climate was sufficiently moist and playa hydroperiods were long, sediment accumulation on lunettes decreased and pedogenesis increased. This study improves our understanding of the role that environmental change has on the geomorphic processes occurring within and surrounding playa-lunette systems and provides new insight into the timing and processes of playa-lunette system formation and evolution.

Research Questions

Few studies have focused on playa-lunette systems, especially in the High Plains of the central United States. At present, our understanding of environmental conditions during playa-

lunette system development indicates sufficient moisture for pedogenesis prior to the LGM, after the LGM, during the Pleistocene-Holocene transition, and during the middle to late Holocene, while arid conditions dominated the early Holocene. (Bowen and Johnson, 2015). Playa-lunette system geomorphic history indicates fluctuations between dissolution and fluvial-aeolian driven processes dependent on climate (Bowen and Johnson, 2012)**.** This study produced additional radiocarbon (14C), stable carbon isotope (13C), and particle size data. Broadly speaking, this study contributes additional data on playa-lunette system stratigraphy and geomorphology. More specifically, this study improves the understanding of how environmental change impacts geomorphic processes occurring within and surrounding playa-lunette systems and advances our knowledge of the timing of playa-lunette system formation and evolution.

Chapter 2 Literature Review

2.1 Playa Lakes versus Playa Wetlands

It is important to note the differences between arid region playa lakes and semi-arid region playa wetlands (Figure 2). Playa lakes are commonly found in intermountain basins throughout the arid southwest United States, including in California, Nevada, Utah, Arizona, and New Mexico (Brostoff et al., 2001). Playa lakes are generally large (>15 ha), flat, vegetation free, lower portions of arid basins that show evidence of evaporite accumulation and have a negative water balance for over half of each year (Briere, 2000). Of the ~300 playa lakes in the US, ~120 are relict large Pleistocene lakes that dried as a result of climatic change (Cooke et al., 1993). Conversely, playa wetlands are commonly found on the semi-arid High Plains of the central United States, including in western portions of Oklahoma, Kansas, and Nebraska and eastern portions of New Mexico, Colorado, and Wyoming (Smith, 2003). Playa wetlands are generally small (<2 ha), flat, vegetated, circular depressions within their own internally drained watersheds that collect runoff and focus recharge to the Ogallala Aquifer (Brostoff et al., 2001). Playa wetlands are typically flooded for 1–3 months each year, which often eliminates vegetation from the deeper portions (Gustavson et al., 1994). Playa wetlands are often clustered and dot the landscape closely together (Figure 2F). To visualize the difference between the two types of playas, figure 2 compares the well-known Racetrack Playa Lake in Death Valley, California (Figure 2A) to a typical High Plains playa wetland in western Kansas (Figure 2B). The difference in topographic profiles (Figure 2C, 2D) between the playa lake and playa wetland illustrates that both are generally shallow, while playa lakes have a much larger surface area. As illustrated in figure 2, playa lakes are often frequently situated within confined valleys with steep walls (e.g., horst and graben landscapes), while playa wetlands are typically found in unconfined

nearly level plains. There are a variety of other forms of playa-like features (referred to as pans, sabkhas, dayas, baltes, dongas, vleis, chor/sor) distributed globally that resemble these two forms (Brostoff et al., 2001). Hereafter, "playa" is used to refer specifically to playa wetlands, not playa lakes.
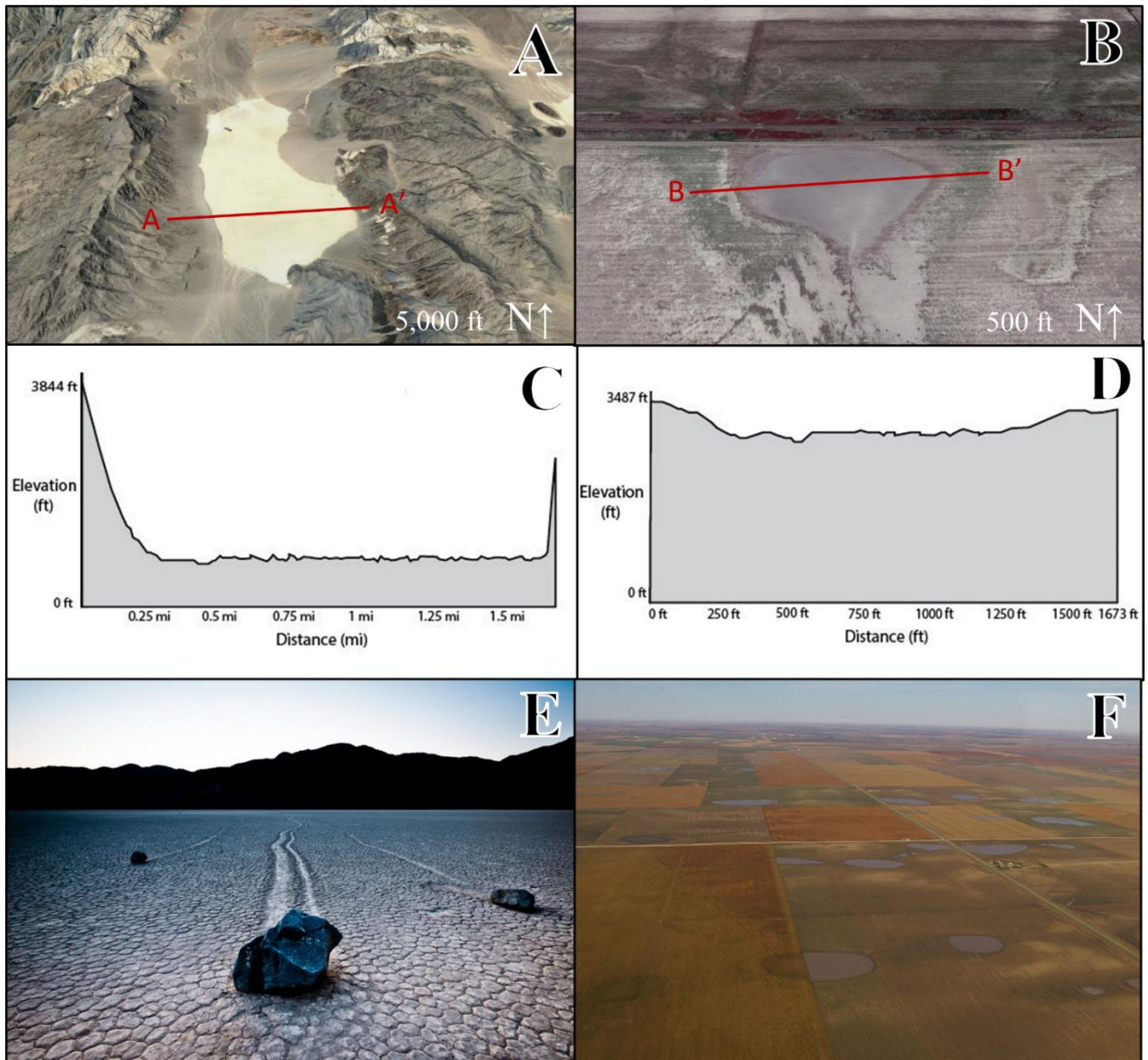
Figure 2 *A) Aerial Image of Racetrack Playa, Death Valley, CA, B) Aerial Image of a typical playa wetland in southwest Kansas C) Elevation profile of Racetrack Playa, D) Elevation profile of typical Kansas playa wetland, E) Sliding Rocks in Racetrack Playa (National Parks Service), and F) Aerial Imagery of multiple playa wetlands in rural Kansas.*

2.2 High Plains Playa-Lunette System Geomorphic Origins

2.2.1 Playa Origin

Researchers have identified three primary sections of a playa: (1) playa floor or basin, (2) playa annulus, and (3) interplaya (Bowen and Johnson, 2012). The playa floor or basin is that portion of the lowest spot in the topographic depression in which water is temporarily stored, resulting in hydric soils (Sabin and Holliday, 1995; Smith, 2003). The playa annulus is the area between the hydric soil and the edge of the topographic depression (Bowen and Johnson, 2012). The interplaya is the upland area between playas (Bowen and Johnson, 2012).

The hypotheses that are most widely accepted to have created playas are deflation, dissolution, or a combination of both. Researchers believe that playa formation is a result of a combination of geomorphic, climatic, and biogeochemical processes (Bowen and Johnson, 2012; Gustavson et al., 1995; Holliday et al., 1996).

The hypothesis of deflation suggests initial playa formation may have begun with the collection of water in a small depression which is then elongated by wave action (Reeves, 1966). Once the depression dries, it would be deepened by wind deflating sediment from the playa floor (Reeves, 1966). This lacustrine-aeolian–driven process has been proposed to produce and maintain playas. Lunettes provide direct evidence that aeolian processes such as wind deflation play an important role in playa maintenance and enlargement (Holliday et al., 1996; Holliday, 1997; Gilbert, 1895).

The dissolution hypothesis suggests that underlying carbonate or evaporite beds form voids where there are fluctuations of a high-water table. Subsequently, the voids collapse, creating the depression that evolves into a playa (Wood et al., 1992). This process is likely more important during initial playa development rather than maintenance and evolution. There are

several lines of evidence that indicate that dissolution may have been a key process in playa formation. This evidence includes the quasi-circular shape of playas, suggesting development began in the center (void) and moved outwards (subsidence) (Osterkamp and Wood, 1987). There is also a lack of surface salt crusts on playa beds and of dissolved solid concretions in shallow playa water (Osterkamp and Wood, 1987). However, Holliday et al. (1996) stated that several playas on the southern High Plains have eroded into and truncated underlying substrate but do not exhibit evidence of subsidence.

It has been hypothesized that playa evolution is dependent on regional and global climate patterns, though exact mechanisms are not well known. During moist mesic periods, playas have sufficient vegetation cover and stable land surfaces which allows them to store sediment and promote soil formation. Conversely, during dry periods, decreased vegetative cover and unstable landscapes susceptible to erosion cause playas to produce sediment, inhibiting soil formation on PLSs (Bowen et al., 2009).

2.2.2 Lunette Origin

Lunettes form along the downwind margin of some relatively large, wide, and deep playas (Arbogast, 1996). The origin of these features is less debated than playas since it is widely accepted that they are aeolian dunes. Lunettes are composed of sediment eroded from the playa floor and regional dust inputs, including aeolian sand, silt, and clay deposits containing intercalated soils (Bowen and Johnson, 2012). This geomorphic development reflects regional circulation of wind in addition to the availability of sediment for deflation from within the playa basin (Telfer and Thomas, 2006). Oscillations in temperature, precipitation, and sediment accumulation throughout lunette evolution produced alternating sequences of sediment deposits

and soils via episodic deposition (Bowen and Johnson, 2012). When precipitation is low and sediment accumulation is high, sediment is deposited, whereas when precipitation is high and temperature allows for stabilizing vegetation, pedogenesis results in at least incipient soil development. The presence of calcareous sandy loams in lunettes were likely derived by deflation of adjacent playa basins with accumulated lacustrine carbonate. Lunettes are stable and cemented in place due to this calcareous material entrained in sediment being affected by dissolution and precipitation (Rich, 2013; Holliday, 1996). It is hypothesized that depth of a playa impacts the formation of a lunette, with lunettes typically associated with larger, deeper playas (Sabin and Holliday, 1995). In Kansas, lunettes are only associated with playas with a surface area of at least 5 ha (Bowen et al., 2018). Development of lunettes supports the playa origin theory of deflation; however, a study by Gustavson et al. (1995) suggested that lunettes are too small to account for the volume of soil missing from playa basins, indicating a significant portion of the deflated sediment is completely removed from the system.

2.3 Paleoenvironments

The Quaternary Period is the most recent geologic era spanning the last ~2.6 million years (my) (Pillans and Naish, 2004). This period is divided into two epochs: the Pleistocene and the Holocene. The Pleistocene spanned from ~2.6 mya to ~11,700 yr before present (BP) and has three subdivisions: Lower- (2.588 to 0.781 Ma), Middle- (0.78 to 0.126 Ma), and Upper- (0.126 to 0.012 Ma) Pleistocene (Gibbard et al., 2010; Pillans and Naish, 2004). The Holocene, which is sub-divided into early (11,700 to 8,200 years), middle (8,200 to 4,200 years), and late (4,200 to present), is the current interglacial interval which began ~11,700 yr BP and continues today (Walker et al., 2018; Pillans and Naish, 2004). The Quaternary Period is heavily researched due

to the ubiquity of nearly complete records of proxy data. These complete records allow researchers to reconstruct past environments and explore future climate scenarios using evidence of paleo to modern environment origins.

Throughout the Pleistocene there were several glacial/interglacial cycles, including the Illinoian glaciation (191,000 to 130,000 years BP), Sangamonian interglacial (130,000 to 71,000 years ago) Wisconsinan glaciation (75,000 to 11,700 years BP), and Holocene interglacial (11,700 years BP to present) (Pillans and Naish, 2004). Climate during the Illinoian glaciation was moist with cool summers and more effective precipitation than present (Kapp, 1965). Climate in Kansas during the Sangamonian interglacial was moist with mild winter and evenly distributed precipitation throughout the year (Kapp, 1965). The Wisconsinan glaciation had a more boreal climate and favored widespread aeolian transportation and accumulation of loess (Welch and Hale, 1987). By the Late Wisconsinan, or last glacial maxima (LGM), the climate became much cooler, effective precipitation increased, and the magnitude and intensity of flooding increased. Following the Wisconsin glaciation, there was a continued cooling trend into the Younger Dryas, a cool and moist stadial period (Steffensen et al., 2008). Younger Dryas cooling began ~12,900 calendar years before present, with warming starting 11,700 calendar years before present (Holliday et al., 2011; Steffensen et al., 2008). From existing records in the central Great Plains, it has been proposed that aeolian activity was not widespread during the Younger Dryas (Mason et al., 2008).

The Pleistocene-Holocene (P-H) transition occurred ~12,000 years BP. Greenland ice core data indicates rapid warming at the beginning of this period followed by several decades of warming (Pillans and Naish, 2004). There are various lines of evidence that support conflicting interpretations of the timing, abruptness, and nature of climate change in the Great Plains region

during the P-H transition (Mason et al., 2003). Stratigraphic records of the Great Plains were

clearly produced by a host of geomorphic processes, and continuous records with plant fossil

evidence (e.g., pollen and phytoliths) for P-H transitional environments are rare (Holliday et al.,

2011).

During the Holocene, warming continued and precipitation became highly variable. Due

to the arid to mesic conditions in the Holocene, playas were frequently subaerially exposed

(Bowen and Johnson, 2015). Prolonged droughts were common; therefore, the modern Great

Plains of North America contain widespread records of Holocene drought and resulting aeolian

activity (Jacobs and Mason, 2004). In the early Holocene, conditions transitioned from mesic to

arid and aeolian processes were dominant within playas (Bowen and Johnson, 2015). In the mid

Holocene, mesic conditions returned and pedogenesis was enhanced (Bowen and Johnson,

2015). During the mid- to late Holocene, effective precipitation increased, and playa floors were

inundated for longer periods. In the late Holocene, mesic conditions continued and fluvial

processes were enhanced (Bowen and Johnson, 2015). Playa water levels during the late

Holocene were higher but still fluctuated considerably (Bowen, 2011). Although precipitation

and water levels were variable, moisture was sufficient throughout most of the Holocene to

support dense vegetation and promote pedogenesis within playas, resulting in multiple Holocene-

aged soils throughout playa-lunette systems (Bowen and Johnson, 2011).

2.4 Stratigraphy

The bedrock geology in Clark, Lane, and Scott counties includes Permian shales and

sandstone with significant evaporite deposits, Cretaceous limestone and shale, and the Ogallala

Formation (Macfarlane and Brownie, 2006). Proximal to study sites, Cretaceous and Permian

deposit are deeply buried and only the Ogallala Formation is exposed at the surface. The Tertiary

or Pliocene age Ogallala Formation is a geologic wedge composed of sand, gravel, and other

debris with a thick, highly resistant, pedogenic calcrete at the top (Prescott, 1951; Waite, 1947).

These sediments were deposited by Rocky Mountain region streams (Waite, 1947). The Ogallala

Formation has variable thickness ranging from a few feet to ~160 feet due to the uneven

depositional surface and post deposition erosion (Prescott, 1951; Waite, 1947). Quaternary

stratigraphic units that overlie the Ogallala Formation include Loveland Loess, Sangamon Soil,

Gilman Canyon Formation, Peoria Loess, Brady Soil, Bignell Loess and Holocene-aged, buried

soils in order from oldest to youngest (Welch and Hale, 1987). At all study sites, the Ogallala

Formation is buried by several meters of Pleistocene to Holocene age loess (playas and lunettes),

other aeolian deposits (lunettes), and/or lacustrine deposits (playas) (Soil Survey Staff et al.,

2019a).

2.4.1 Loveland Loess

Loveland Loess was deposited on top of thick, carbonate rich Ogallala calcrete during the

Illinoian stage (191,000 – 130,000 years ago), making it the oldest of the recognized loess units

in Kansas (Welch and Hale, 1987). It is relatively thin and discontinuous in comparison to

subsequent layers (Welch and Hale, 1987; Frye and Leonard, 1951). Frye and Leonard (1951)

described the type section of Loveland Loess as being 9 m (30 feet) thick, massive, well-sorted

fine sand and silt. The upper 6.6-7.2 m (22-24 feet) is leached of calcium carbonate but the lower

1.8-2.4 m (6-8 feet) is not (Frye and Leonard, 1951). There are few recorded fossil fauna (Welch

and Hale, 1987). Loveland Loess has not been identified at any playa-lunette system locations

(Bowen and Johnson, 2012).

2.4.2 Sangamon Soil

The Sangamon Soil developed on the uppermost, leached zone of Loveland Loess (Frye and Leonard, 1951). It is described as pink to red-brown in color due to weathering (Welch and Hale, 1987). This paleosol typically features a structural and argillic B horizon, carbonate-rich B or C horizons, and yellow-red hues (Johnson et al., 2007). The soil formed during and following the Sangamonian interglacial stage (130,000 – 71,000 years ago) between the Illinoian and Wisconsinan glacial stages (Welch and Hale, 1987). Regional climate during Sangamon Soil formation was warm and dry (Feng et al., 1994) or warm and humid (Karlstrom et al., 2008; Muhs and Bettis, 2003). The Sangamon Soil has been identified in only interplayas and lunettes, not within playas (Bowen and Johnson, 2012).

2.4.3 Gilman Canyon Formation

Gilman Canyon Loess was deposited in the early Wisconsinan glacial stage (79,000 – 65,000 years ago) (Welch and Hale, 1987). The unit was developed 60,000 and 25,000 years ago (Bowen and Johnson, 2012). There are three distinct loess units and three soils within the formation in Nebraska (Johnson et al., 2007). Loess deposition occurred slowly, and the unit is frequently characterized by pedogenic alteration throughout (Jacobs and Mason, 2007; Johnson et al., 2007). Texture is principally silty clay loam, though sand and clay content are lower and silt content greater compared to the underlying Sangamon Soil (Bowen and Johnson, 2012). The Gilman Canyon Formation is commonly identified in lunettes and has been identified in playas (Bowen and Johnson, 2012).

2.4.4 Peoria Loess

Peoria Loess was deposited primarily during later portions of the Wisconsinan glacial stage and overlies the Gilman Canyon Formation (Welch and Hale, 1987). The unit was developed 25,000 and 12,000 years ago and is composed of massive, yellow-tan to buff-colored, well-sorted, calcareous, very fine sands, silts, and clays (Welch and Hale, 1987). It is the thickest and most widely distributed loess unit on the central Great Plains (Muhs et al., 1999). Peoria Loess deposition accumulated more rapidly than underlying loess units (Martin, 1993; Feng et al., 1994; Maat and Johnson, 1996) during a colder and/or drier climate than today (Jacobs and Mason, 2007; Muhs et al., 1999). Past studies have suggested that "dark bands" and laminations in the unit represent periods of decreased loess deposition and incipient paleosol formation (Bowen and Johnson, 2012). Peoria Loess is commonly identified throughout playa-lunette systems (Bowen and Johnson, 2012).

2.4.5 Brady Soil

The Brady Soil is a paleosol that separates Peoria and Bignell loess units. Formation began as early as 15,000 years ago but was halted by the deposition of Holocene aged Bignell loess (Bowen and Johnson, 2012). Formation of the Brady Soil has been attributed to a shift in climatic conditions that reduced dust influence and made pedogenic processes more effective (Mason et al., 2008; Jacobs and Mason, 2004; Johnson and Willey, 2000). The Brady Soil represents a broad peak of effective moisture and aeolian system stability beginning about 15–13.5 cal ka and ending around 9–10.5 cal ka (Mason et al., 2003). This unit is widely recognized as a distinct soil throughout the Great Plains. A Brady Soil equivalent is commonly identified in playa-lunette systems, particularly within lunettes (Bowen and Johnson, 2012).

2.4.6 Bignell Loess

Bignell Loess is the uppermost unit of the Great Plains loess sequence. This unit was deposited during either the late Pleistocene/Wisconsin glacial stage or early Holocene (10,000 to 9,000 years ago) (Bowen and Johnson, 2012). Clusters of OSL ages from within Bignell Loess (ranging from 10,250+610 years at 5.9 m depth to 100+10 years at 0.1 m depth) helped identify episodes of extensive aeolian activity triggered by severe drought (Miao et al., 2007). Buried soils ranging in age from ca.10 to 1.6 ka are commonly found within this unit, but are particularly common in the upper portion (Mason et al., 2008, 2003; Mason and Kuzila, 2000; Miao et al., 2007). When loess accumulates without significant post-depositional reworking, it is a near-continuous record of aeolian activity, pedogenesis, and inferred climate change in the central Great Plains (Mason et al., 2003). This deposit is morphologically similar to Peoria Loess (massive, yellow-tan to buff-colored, well-sorted, calcareous, very fine sands, silts, and clays) but is generally more friable and less compact (Welch and Hale, 1987). Modern (Holocene) soils have formed in Bignell Loess. Bignell Loess and several Holocene-age buried soils are commonly identified in playa-lunette systems (Bowen and Johnson, 2012).

Chapter 3 Study Area

Kansas is part of the Great Plains region of North America, which is known for being relatively flat, expansive land covered predominantly by agriculture with isolated patches of native prairie vegetation between the Rocky Mountains and the Mississippi River (Figure 3) (Wishart, 2004). Western Kansas is part of the High Plains, which is the westernmost subsection of the Great Plains characterized by higher elevation and lower precipitation than the eastern Great Plains (Buchanan and McCauley, 2010). Uplands between major drainages along the Colorado-Kansas border are expansive flat regions that transition to the rolling hills of the Central

Figure 3 *Map displaying the Great Plains physiographic region (green) across North America. From the "Encyclopedia of the Great Plains" (University of Nebraska Press)*

Lowlands to the east (Fenneman, 1931). Playas in western Kansas are characteristically situated in low-relief watersheds with gentle slopes (Bowen and Johnson, 2019).

This study includes four PLSs in three counties on the Central High Plains of western Kansas (Figure 4). Site "LE" is in Lane County, approximately 11.9 kilometers (7.4 miles) southwest of Dighton (Figure 5). LE land cover is agriculture (winter wheat) (Kansas Biological Society, 2017). LE playa (LE-P) has a surface area of 55.2 ha, perimeter of 2.7 m, and is <6 m (<20 ft) deep, while the lunette (LE-L) is ~711 m (2,335 ft) long and ~6 m (20 ft) tall (Table 1). Site "CA1" is located Clark County, approximately 2.4 km (1.3 miles) northwest of Minneola

(Figure 6). The primary land cover for CA1 is agriculture (winter wheat), but a portion is in the Conservation Reserve Program (CRP); playa and lunette cores were collected from the CRP portions (Kansas Biological Society, 2017). The playa at CA1 (CA1-P) has a surface area of 99.0 ha, a perimeter of 4.9 m, and is <6 m (<20 ft) deep, while the lunette (CA1-L) is ~504 m (1,655 ft) long and ~3 m (~10 ft) tall (Table 1). Site "CA2" is also located in Clark County, approximately 1.0 kilometers (0.6 miles) southeast of Minneola (Figure 7). CA2 land cover is primarily agriculture (winter wheat) (Kansas Biological Society, 2017). The playa at CA2 (CA2-P) has a surface area of 28.9 ha, a perimeter of 2.5 m, and is ~3 m (~10 ft) deep, while the lunette (CA2-L) is ~1,132 m (3,715 ft) long and ~6 m (~20 ft) tall (Table 1). Site "SC" is in Scott County, approximately 4.7 km (2.9 miles) northwest of Scott City (Figure 8). A portion of the PLS has been in CRP since at least 1991 while the remainder has been in cultivated cropland; playa and lunette cores were collected from the CRP portion. The playa at SC (SC-P) has a surface area of 29.3 ha, a perimeter of 2.7 m, and is ~6 m (~20 ft) deep, while the lunette (SC-L) is ~792 m (2,600 ft) long and ~9 m (~30 ft) tall (Table 1). Of the four playas, LE-P is the most circular (0.82) (Table 1). LE-P is also relatively large compared to its watershed - it is the 2nd largest playa but has the smallest watershed (Table 1).

All study sites are within NRCS Land Resource Region H – Central Great Plains Winter Wheat and Range Region. Region H is described as a nearly level to gently rolling fluvial plain in the north and an eroded plateau with entrenched streams in the south (NRCS, 2006). Sites SC and LE are in Major Land Resource Area (MLRA) 72 – Central High Tableland (Figure 9A). Elevation of MLRA 72 ranges from 795 m to 1,190 m (2,600 to 3,900 feet), generally decreasing from west to east (NRCS, 2006). Sites CA1 and CA2 are in MLRA 73 – Rolling Plains (Figure

9B). Elevation ranges from 505 to 915 m (1,650 to 3,000 feet), generally decreasing from west to

east (NRCS, 2006).
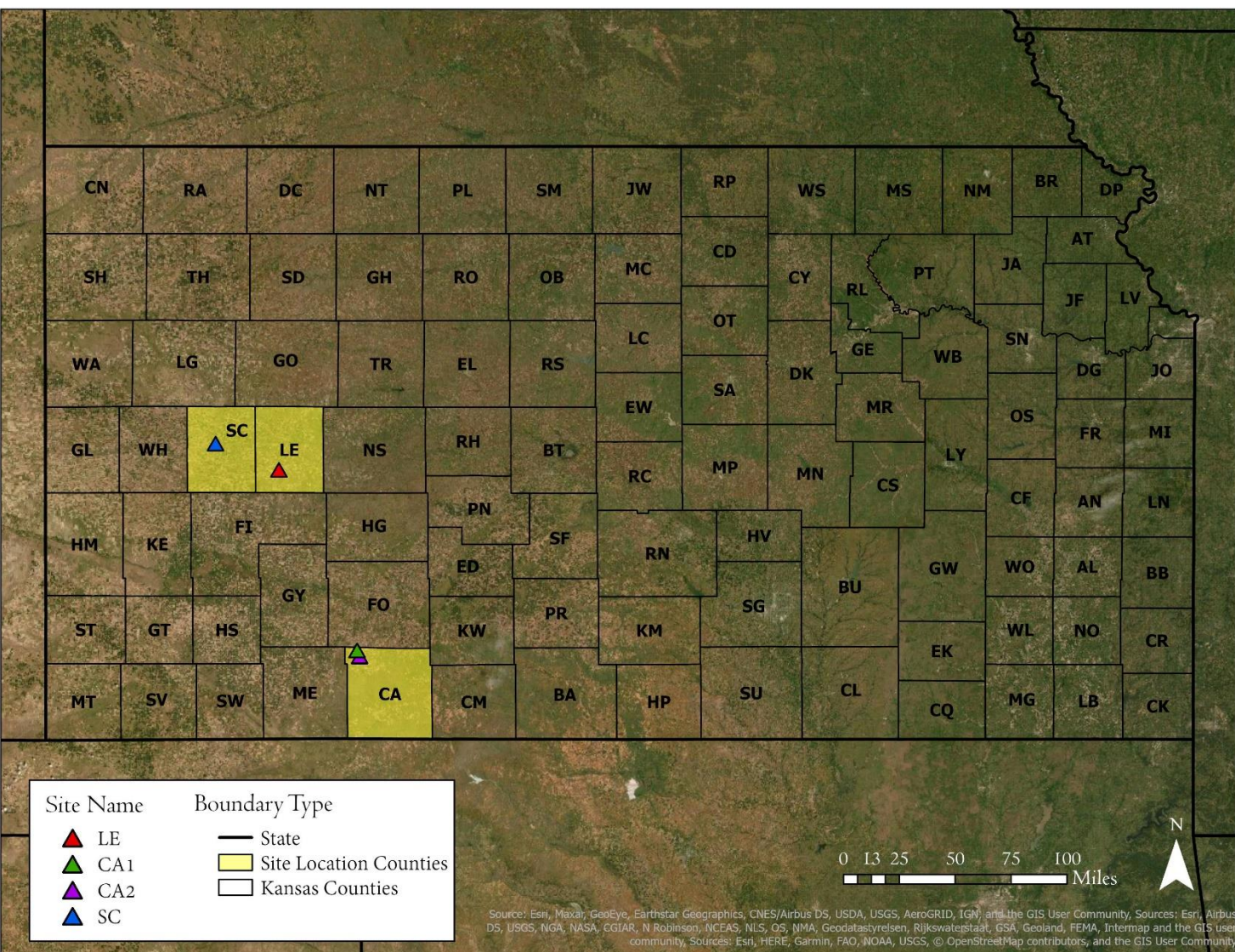
Figure 4 *Map of the state of Kansas including county boundaries, highlighted research counties (Lane, Clark, and Scott), and site locations (LE, CA1, CA2, and SC). Created with ArcGIS Pro.*
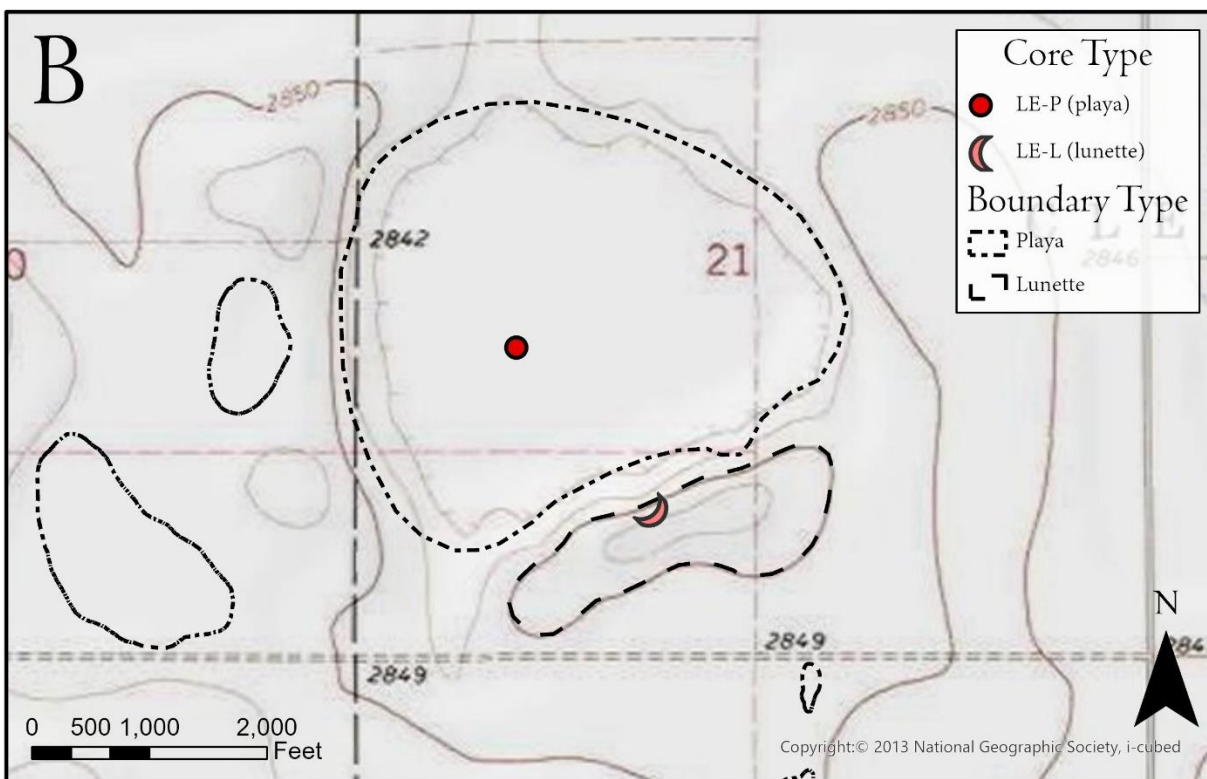
Figure 5 *Topographic and aerial imagery of research site and core locations LE2 in Lane County, Kansas, USA. Created with ArcGIS Pro.*
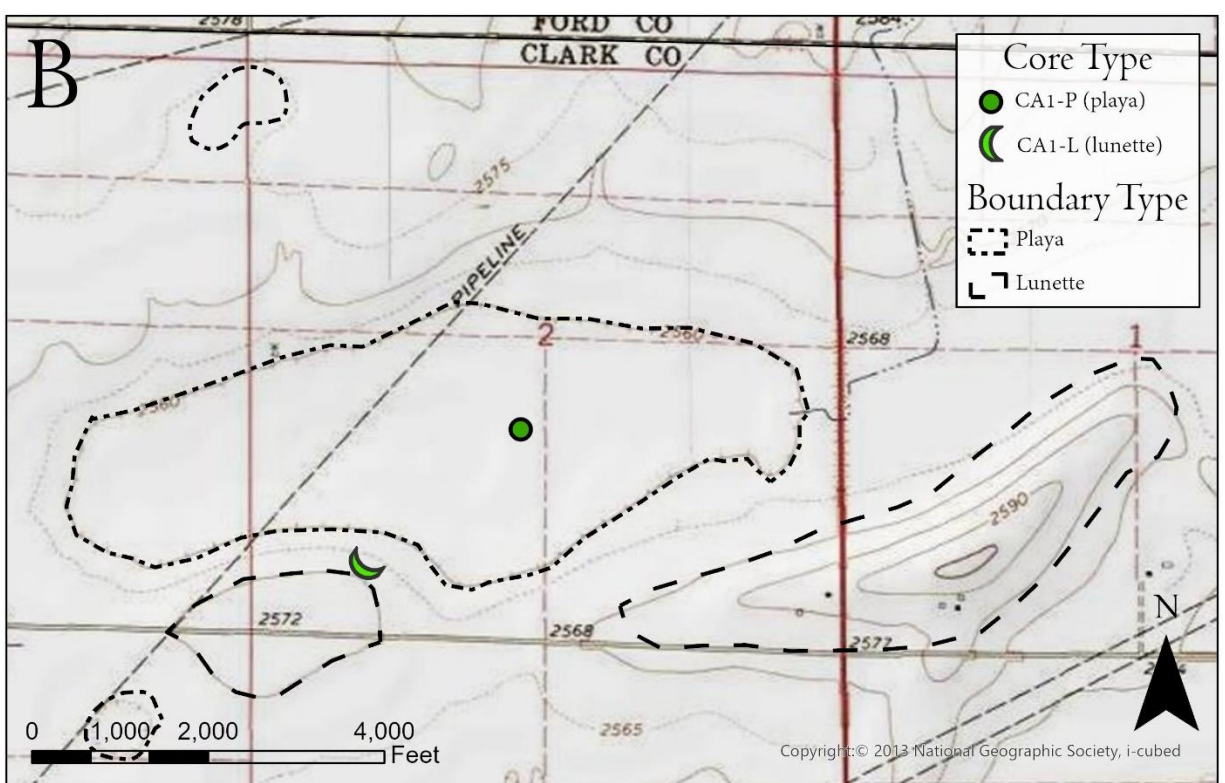
Figure 6 *Topographic and aerial imagery of research sites and core location CA1 in Clark County, Kansas, USA. Created with ArcGIS Pro.*
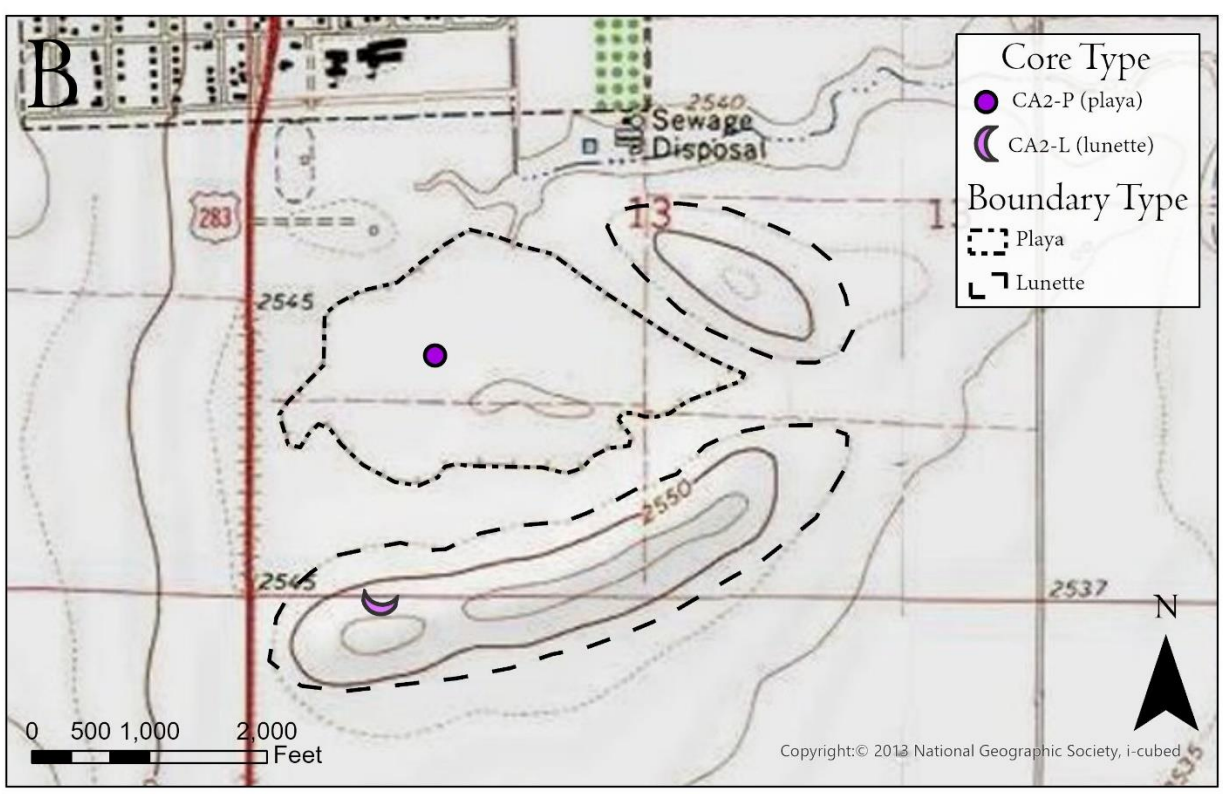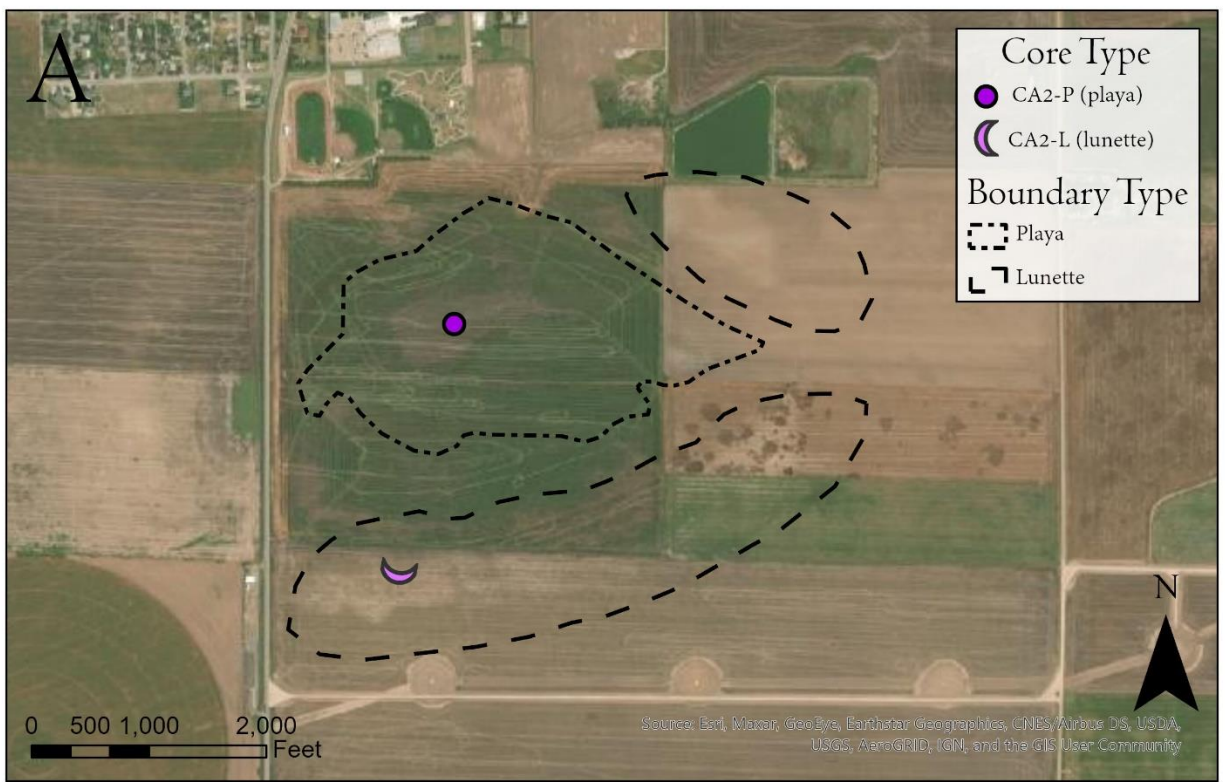
Figure 7 Topographic and aerial imagery of research sites and core locations CA2 in Clark County, Kansas, USA. Created with ArcGIS Pro.
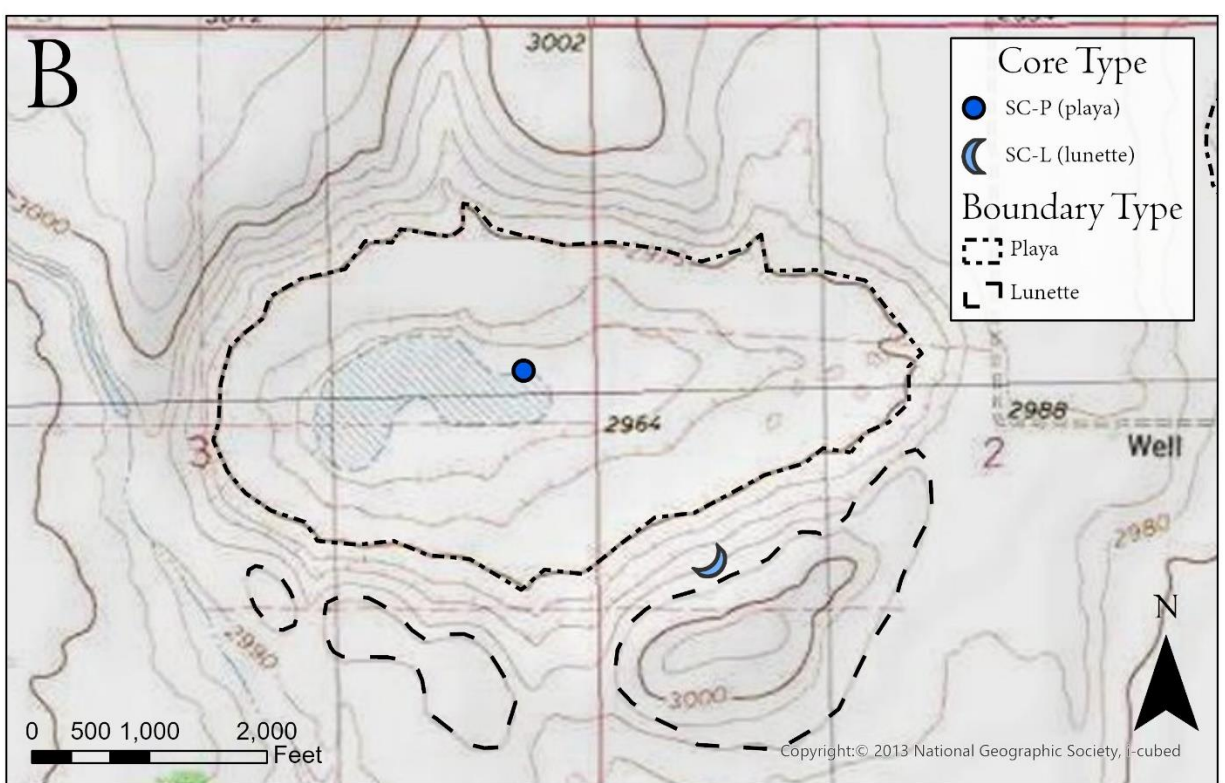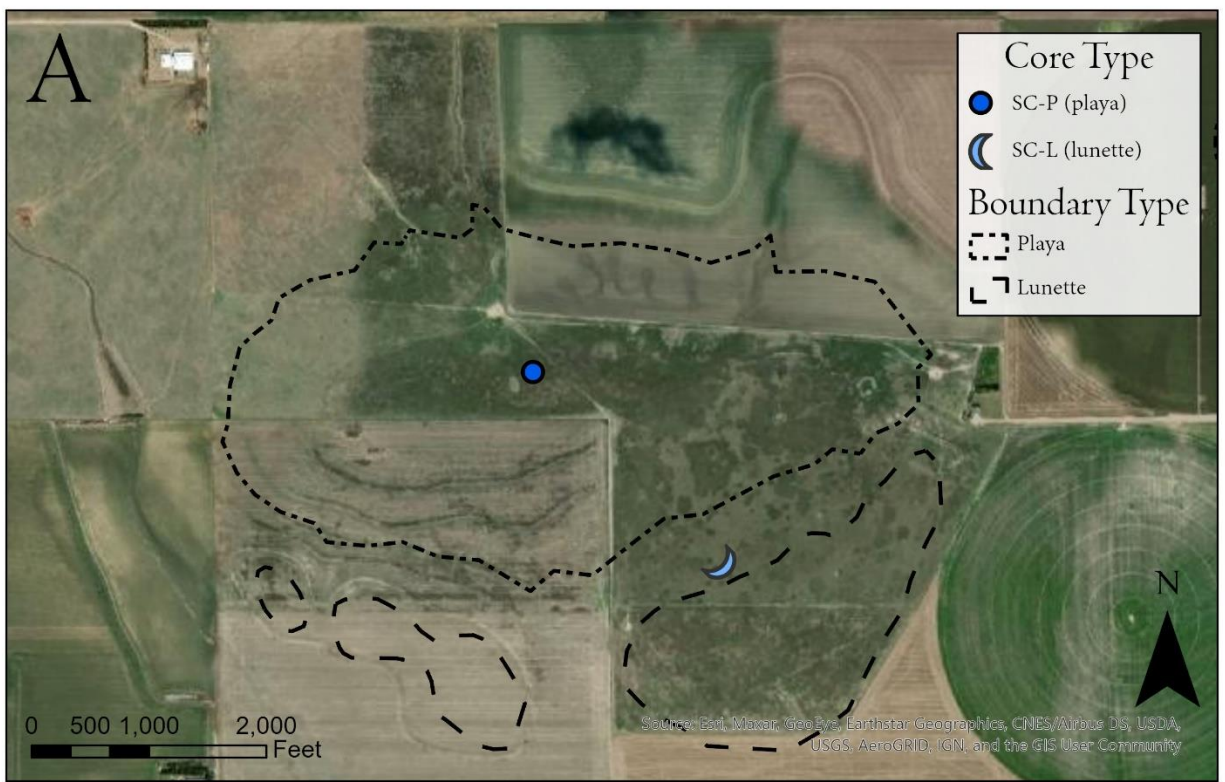
Figure 8 *Topographic and aerial imagery of research site and core locations SC in Scott County, Kansas, USA. Created with ArcGIS Pro.*
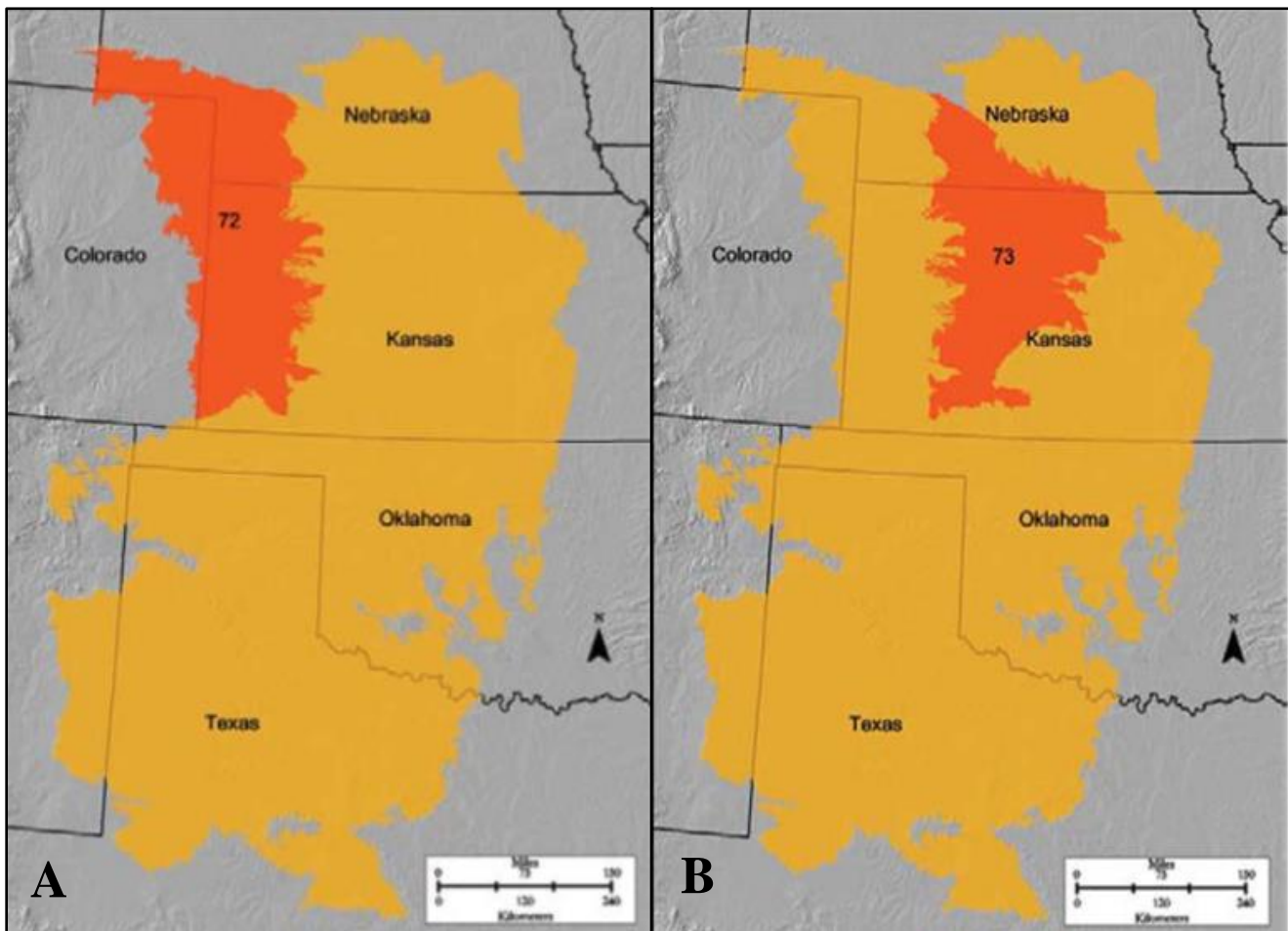
Figure 9 Map displaying NRCS Land Resource Region H in orange and MLRA 72 (A) and MLRA 73 (B) in red (NRCS, 2006).

Table 1 Summary of sites LE, CA1, CA2, and SC including location, land cover, morphology, and soils.

	LE	CA1	CA2	SC
Latitude	38.38561	37.46358	37.43345	38.51932
Longitude	-100.53548	-100.53548	-100.01130	-100.94593
County	Lane	Clark	Clark	Scott
MLRA	72	73	73	72
Land Cover	Winter Wheat	Winter Wheat and CRP	Winter Wheat	Warm-Season Grassland
Playa Area (ha)	55.2	99.0	28.9	32.7
Playa Depth (m)	<6	<6	3	6
Playa Perimeter (m)	2.9	4.9	2.5	2.7
Playa Circularity	0.82	0.52	0.58	0.57
Watershed Area (ha)	239	1,408	275	537
Watershed Perimeter (km)	5.9	21.7	8.6	9.7
Watershed Circularity	0.87	0.38	0.48	0.72
Watershed Area to Playa Area	4.3	14.2	9.5	16.4
Lunette Length (m)	711	504	1,132	792
Lunette Height (m)	6	3	6	9
Upland Soil	Harney Silt Loam	Harney Silt Loam	Harney Silt Loam	Richfield Silt Loam
Playa Soil	Ness Clay	Ness Clay	Ness Clay	Ness Clay
Lunette Soil	Buffalo Park Silt Loam	Harney Silt Loam	Uly Silt Loam	Ulysses Silt Loam

3.1 Soils

The dominant soil orders in MLRA 72 are Entisols and Mollisols (NRCS, 2006). Entisols are relatively "young" soils that exhibit little evidence of pedogenesis and lack distinct soil horizons (Schaetzl and Anderson, 2005). Mollisols are relatively deep soils with thick, organic

matter rich A horizons formed with grassland cover (Schaetzl and Anderson, 2005). These soils have a mesic soil temperature regime, an ustic or aridic soil moisture regime, mixed or smectitic mineralogy, and variable texture (NRCS, 2006).

Soils on the uplands of SC primarily consist of Richfield silt loam (*Fine, smectitic, mesic Aridic Argiustolls*) (Soil Survey Staff et al., 2019b). Richfield silt loam is characterized as a very deep, well-drained plains soil formed in calcareous loess with slopes that range from 0 to 6 percent (Natural Resources Conservation Service, 2006a). A typical profile has Ap, Bt, BCk1, BCk2, and C horizonation. (Natural Resources Conservation Service, 2006a; Soil Survey Staff et al., 2019b). Soils on the uplands of CA1, CA2, and LE are primarily mapped as Harney silt loam (*Fine, smectitic, mesic Typic Argiustolls*) (Soil Survey Staff et al., 2019b). Harney silt loam is characterized as deep, well drained, moderately slowly permeable upland soils that formed in loess with slopes that range from 0 to 8 percent (Natural Resources Conservation Service, 1997). A typical profile has Ap, AB, Bt1, Bt2, BCk, Ck, and C horizons (Natural Resources Conservation Service, 1997; Soil Survey Staff et al., 2019b).

Soils for all four playas are mapped as Ness Clay (*Fine, smectitic, mesic Ustic Epiaquerts*) (Soil Survey Staff et al., 2019b). Ness clay is characterized as deep, poorly drained soils whose parent material is clayey alluvium and aeolian sediments formed with slopes that range from 0 to 1 percent (Natural Resources Conservation Service, 2006b). A typical profile has A, Bss1, Bss2, BC, 2C1, and 2C2 horizonation (Natural Resources Conservation Service, 2006b).

Lunette soils for SC primarily consist of Ulysses silt loams (*Fine-silty, mixed, superactive, mesic Torriorthentic Haplustolls*) (Soil Survey Staff et al., 2019b). The Ulysses series is characterized as very deep, well drained soils formed in loess with slopes that range

from 0 to 20 percent (Natural Resources Conservation Service, 2017). A typical profile has Ap1,

Ap2, Bw, Bk1, Bk2, Bk3, and Bk4 horizons (Natural Resources Conservation Service, 2017).

Soils on the lunette at site CA1 were not differentiated from the surrounding uplands and were

mapped as the Harney series (see description above). Soils mapped for the lunette at CA2 are

mapped as the Uly series (*Fine-silty, mixed, superactive, mesic Typic Haplustolls)* (Soil Survey

Staff et al., 2019b). Like the Ulysses series, the Uly series consist of very deep, well drained soils

that formed in loess on uplands. Slopes range from 0 to 30 percent. A typical profile includes A,

BA, Bw, BC, and very thick C horizonation (Natural Resources Conservation Service, 2007).

The lunette at site LE is mapped as the Buffalo Park series (*Fine-silty, mixed, superactive, mesic

Aridic Haplustepts*) (Natural Resources Conservation Service, 2018). This series consists of very

deep, well drained soils that formed in loess with slopes ranging from 1 to 20 percent.

Horizonation of this series is complex, and soils typically have Ap, Bw, Bk1, Bk2, Bk3, 2Bk4,

and 2Bk5 horizons (Natural Resources Conservation Service, 2018).

3.2 Climate and Weather

The High Plains region of western Kansas has a semi-arid climate (Peel et al., 2007).

Annual precipitation in Kansas ranges from 334 mm to 1,269 mm (~13 in to 50 in) and increases

from W to E (Figure 10) (Kansas State University, 2020). Annual mean temperature ranges from

10 ℃ to 15 ℃ (50 ℉ to 59 ℉), increasing from NW to SE (Figure 11) (Kansas State University,

2020). Winds on the High Plains of western Kansas blow from the northeast at approximately 20

km/hour during the winter, and are predominantly from the south and southeast at a slightly

higher velocity during the summer (Bowen, 2011). Precipitation (rain and snow) for MLRA 72

and 73 fluctuates widely between years and mostly occurs as high-intensity thunderstorms during

the growing season (NRCS, 2006). The freeze-free period (number of consecutive days when the air temperature does not fall below -2.2°C (28°F)) averages 175-180 days and ranges from 135 to 210 days (NRCS, 2006).

Monthly temperature and precipitation data for Scott City, Kansas (proximal to sites SC and LE) and Sublette, Kansas (proximal to sites CA1 and CA2) were acquired from the High Plains Regional Climate Center (HPRCC) CLIMOD database (http://climod.unl.edu) (High Plains Regional Climate Center, 2020). Mean annual temperature (MAT) for the period of record (1985-2022) in Scott City, Kansas is 12.2°C (54.0°F), ranging from a monthly minimum of -1.1°C (30.1°F) in January to a maximum of 25.6°C (78.1°F) in July (High Plains Regional Climate Center, 2020). The MAT for the period of record (1918-2019) in Sublette, Kansas is 12.2°C (55.4 °F), ranging from a monthly minimum of 0.2°C (32.3°F) in January and a maximum of 26.2°C (79.1°F) in July (High Plains Regional Climate Center, 2020).

Mean annual precipitation (MAP) is the sum of all rainfall and liquid equivalent of snowfall for a given year. MAP for the period of record (1985-2022) in Scott City, Kansas is 505 mm (~19.9 inches), ranging from a monthly minimum of 11 mm (~0.4 inches) in January to a monthly maximum of 77 mm (~3 inches) in June (High Plains Regional Climate Center, 2020). MAP for the period of record (1918-2022) in Sublette, Kansas is 489 mm (19.3 inches), ranging from a monthly minimum of 10 mm (~0.4 inches) in January to a monthly maximum of 76 mm (~3 inches) in June (High Plains Regional Climate Center, 2020). The majority of precipitation for both the Scott City station and the Sublette station is delivered from May to August with ~57% of precipitation occurring in late spring and summer (High Plains Regional Climate Center, 2020).

Normal Annual Precipitation
based on data from 1991-2020

Total Precipitation (Inches)

13.13 – 18.00	31.00 – 33.00
18.00 – 23.00	33.00 – 36.00
23.00 – 26.00	36.00 – 39.00
26.00 – 29.00	39.00 – 44.00
29.00 – 31.00	44.00 – 49.97

0   25   50   100 Miles

Produced by Weather Data Library
Department of Agronomy
Kansas State University
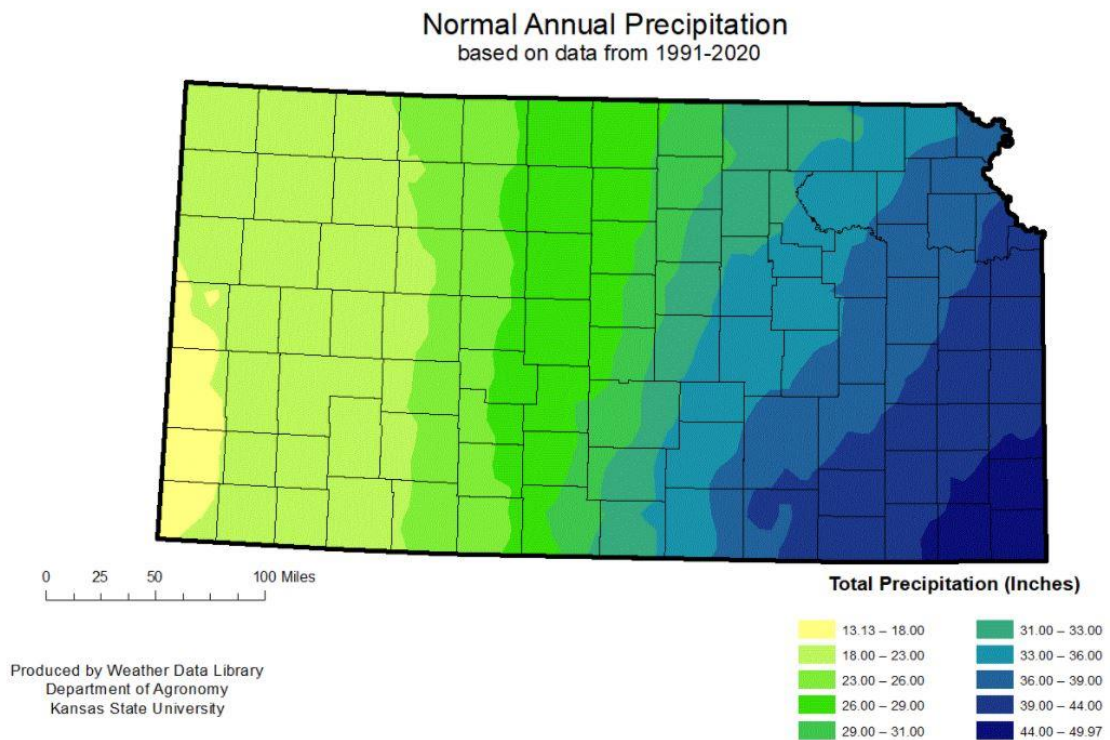
Figure 11 *Map displaying normal annual precipitation values (1991-2020). (KSU)*

Normal Annual Mean Temperatures
1991-2020

Mean Temperatures (°F)

50.0 – 52.0	54.5 – 55.5
52.0 – 53.0	55.5 – 56.0
53.0 – 54.0	56.0 – 57.0
54.0 – 54.5	57.0 – 59.0

0   25   50   100 Miles

Produced by Weather Data Library
Department of Agronomy
Kansas State University
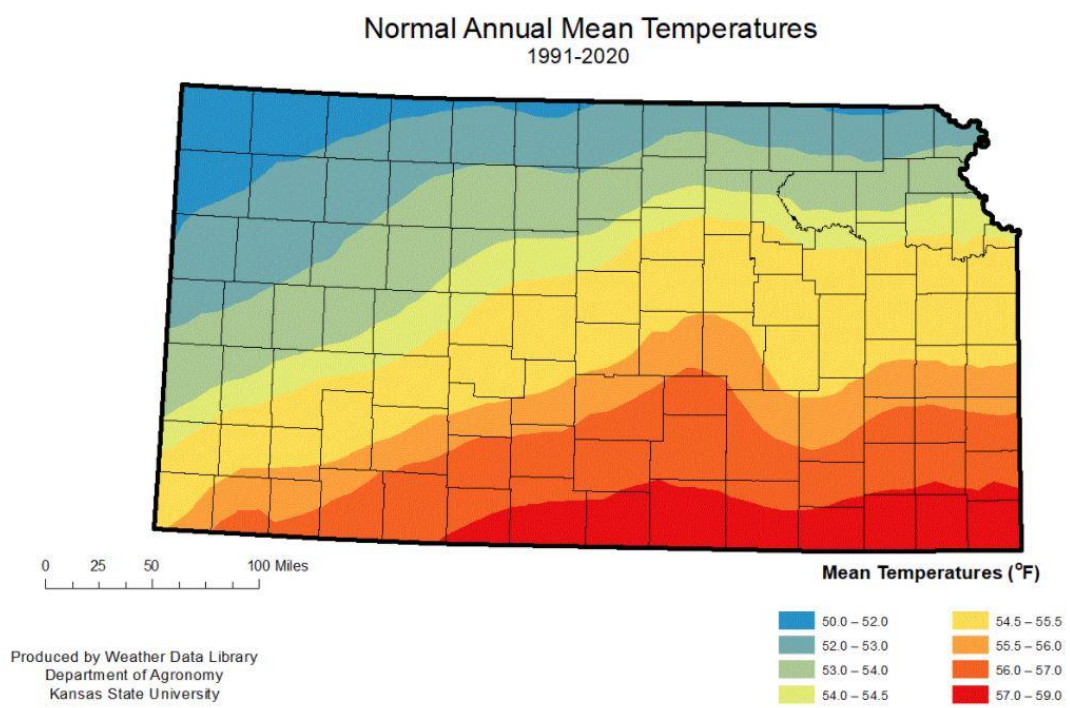
Figure 10 *Map displaying normal annual temperature values (1991-2020). (KSU)*

3.3 Groundwater and Surface Hydrology

The Ogallala Aquifer is the water bearing portion of the Ogallala Formation (Figure 12). It underlies ~110 million acres (~175,000 square miles) in parts of eight States - Colorado, Kansas, Nebraska, New Mexico, Oklahoma, South Dakota, Texas, and Wyoming (McGuire, 2017), including all four study sites. Naturally, groundwater discharges to streams and springs or is lost to evapotranspiration in areas where the water table is near the land surface (Weeks et al., 1988). The aquifer is the primary source of groundwater in the area, and provides more than 70% of all of the water in the state of Kansas (Buchanan et al., 2015). Extensive pumping of the Ogallala Aquifer for irrigation-based agriculture has led to depleted subsurface storages (Kustu et al., 2010). The aquifer as a whole has declined 5 m on average while portions in southern Kansas declined a weighted average of 8 m (~50 m for the area) (McGuire, 2017). Between 1939 and 1981, water-level declines in southwestern Kanas ranged from 3 meters to 15 meters and water in storage decreased by 8% (Spinazola and Dealy, 1983). In Scott County, wells drilled into the Ogallala recorded a drop of 0.05 meters followed a slight gain of 0.02 meters in 2017 (The KU News Service, 2020). The main source of recharge for this aquifer is infiltration of precipitation through surface soils, therefore playas on the High Plains are of crucial importance. Playas provide as much as 90% of the recharge to the Ogallala Aquifer (Gurdak and Roe, 2009).
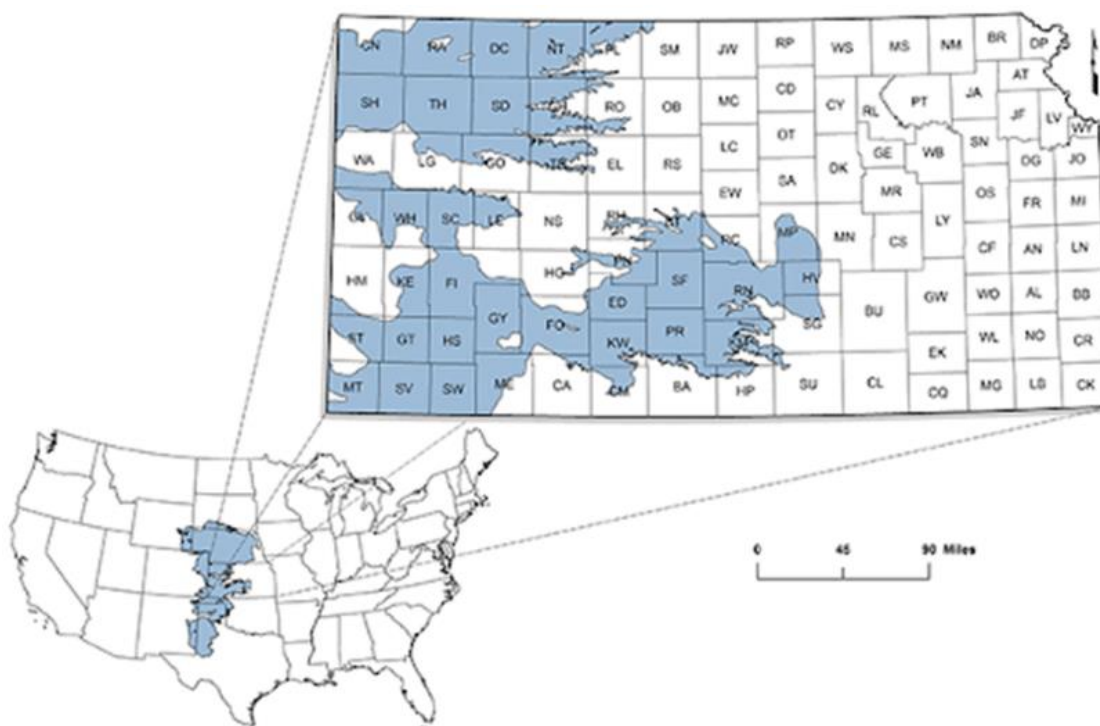
Figure 12 Map displaying the Ogallala (High Plains) Aquifer, highlighted in blue, in the United States and Kansas (Kansas Geological Society)

3.4 Land Use and Land Cover

Kansas is a highly productive agricultural state often referred to as the "Breadbasket" of the country (Figure 13). Major crops produced in Kansas include wheat, sorghum, hay, sunflowers, summer potatoes, soybeans, corn, oats, alfalfa, and cotton (Kansas Department of Agriculture, 2019). In 2018, the number one agricultural product for Kansas (livestock or crop) was wheat at 333,600,000 bushels (accounting for ~19% of all wheat produced in the US) (Kansas Department of Agriculture, 2019). Prior to the conversion to cropland, native vegetation primarily consisted of grasslands including dense short grasses like buffalo grass (*Bouteloua dactyloides*) and blue grama (*Bouteloua gracilis*) (Kuchler, 1974). Current land use in MLRA 72 includes Cropland (private) - 67%, Grassland (private) - 30%, Urban development (private) - 2%, and Other (private) - 1% (NRCS, 2006). Nearly all MLRA 72 is occupied by farms or

ranches dominated by cultivated cropland and livestock production. Current land use in MLRA

73 includes Cropland (private) – 55%, Grassland (private) 39%; (federal) 1%, Forest (private) –

1%, Urban development (private) – 2%, Water (private) – 1%, and Other (private) – 1% (NRCS,

2006). Like MLRA 72, MLRA 73 is primarily composed of farms or ranches. Sites CA2 and LE

are classified as Winter Wheat and based on examination of aerial imagery have been

continuously cultivated since at least 1985. Sites SC and CA1 are classified as Warm-Season

Grassland, and were converted to CRP as early as 1991 and 2005, respectively, based on aerial

imagery. (Kansas Biological Society, 2017).
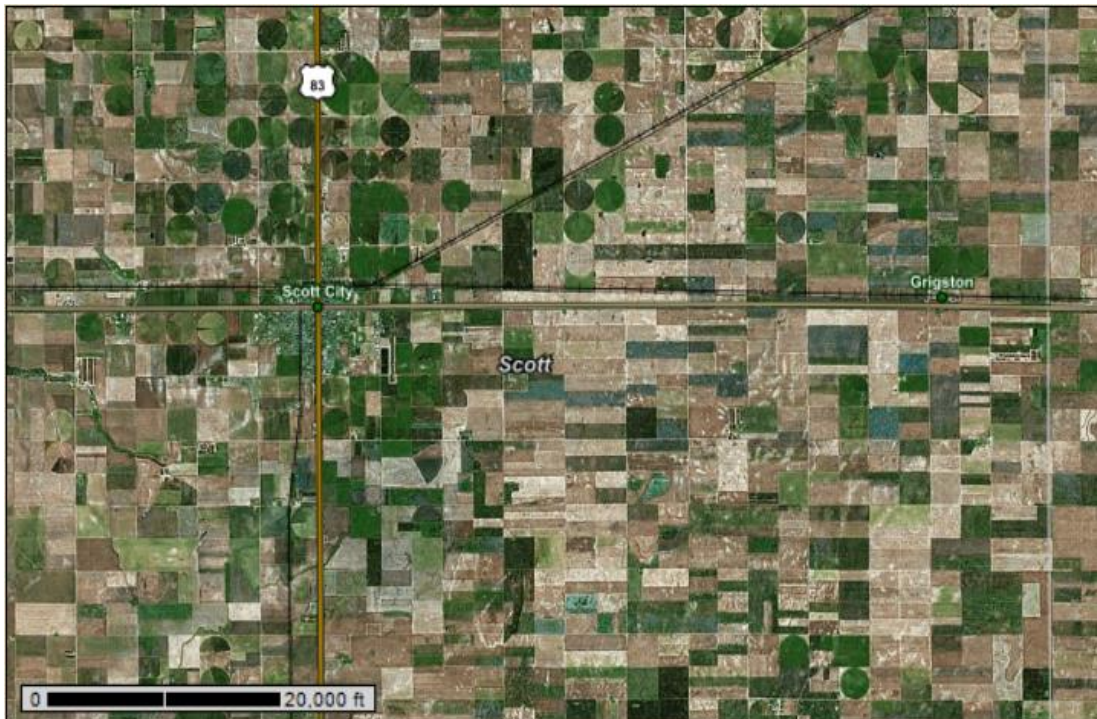
Figure 13 A 2020 aerial image of Scott City, Kansas from the Scott City AOI (Soil Survey Staff et al., 2019), with the rectilinear and circular patterns highlighting the dominance of agriculture in this region.

Chapter 4 Methods

4.1 Field Methods

Fieldwork for this project was conducted during two separate campaigns. In June 2012, Dr. Mark Bowen, Dr. William Johnson, and Chelsey Herring collected soil-sediment cores from sites CA1, CA2, and LE. In the summer of 2021, Luis Lepe, Dr. Mark Bowen, and I collected soil-sediment cores from SC. Cores at CA1, CA2, and LE were collected near the mid-point of the windward slope of lunettes and playa centers; cores were collected from multiple positions at SC, including the windward slope and crest of the lunette and the playa center using a Giddings hydraulic coring machine. This machine manually drilled into the target areas and collected soil-sediment cores ~2.5 inches (6 cm) in diameter to maximum depth possible. Cores were collected in plastic coring tubes, capped, sealed, labeled, and transported to the EARTH Systems Laboratory at Minnesota State University, Mankato (MNSU) for analysis.

4.2 GIS Methods

Playas and their watersheds were delineated and characterized to compare morphology among the four sites and evaluate potential source areas for overland flow and associated sediment delivered to the playas. Watershed and playa boundaries were digitized, and all morphometric variables were calculated using ArcGIS 10.5. Playa boundaries were digitized by outlining the innermost depression contour mapped on 1:24,000-scale digital raster graphics, which was assumed to represent the floor of the playa. Watershed boundaries were digitized by manually tracing drainage divides on 1:24,000-scale digital raster graphics. Playa and watershed perimeter and area were calculated using the "Calculate Geometry" function. Circularity was

calculated for playas and watersheds using the formula: circularity = 4π x area /perimeter2, with a value of 1 representing a perfect circle, and as the value decreases it indicates elongation.

4.3 Lab Methods

4.3.1 Core Descriptions

Soil profile descriptions were completed for cores SC-P, SC-L, CA1-P, CA1-L, CA2-P, CA2-L, LE-P, and LE-L. Using the NRCS Field Book for Describing and Sampling Soils Version 3.0, soil horizons (i.e., master horizons, subordinate horizons, and transitional horizons), redoximorphic features, texture, structure, consistence, carbonate content, Munsell color, and other key features were described. Classifying these parameters in soil profiles helps identify buried soils, changes in parent material, soil moisture, soil compaction, human alterations, etc. In this study, soil descriptions are important for correlating stratigraphic units between playas and lunettes and to identify changes in environmental conditions and geomorphic processes as reflected in the stratigraphic layers.

4.3.2 Particle Size Distribution

Particle size distribution analysis can be used to infer geomorphic processes because grain-size components reflect different transportation or depositional processes and preserve environmental information about those processes (Sun et al., 2002). The percent sand, silt, and clay in samples was measured in the EARTH Systems Lab using a Malvern Mastersizer 3000 laser diffractometer. This method utilizes a laser beam to pass through a sample dispersed in water, and reports volume percent by size class for up to 105 different size classes ranging from 0.01 µm to 2.0 mm. Samples were collected from cores SC-P and SC-L in 5 cm intervals and

from CA1-P, CA1-L, CA2-P, CA2-L, and LE-L in 8 to 12 cm intervals. Samples were not collected from core LE-P because the core was damaged. After collection, samples were prepared for analysis by drying, grinding using an agate motor and pestle, and sieving through a 2 mm screen. Roots and other organic material were manually removed during this stage. Following sample preparation, enough sediment from each sample was added to the dispersion unit of the Mastersizer to reach between 5-10% obscuration. Samples were sonicated for 180 seconds (3 minutes), particle size measurements were conducted three times, and averages were calculated; averages were used for all data analysis. Particle size textural class was determined using "TRIANGLE", an online interface for soil textural classification based on the USDA system (Gerakis and Baer, 1999). Percent sand and clay were uploaded as a .csv (comma-separated values) file, verbal classifications were generated, and size classes were plotted on a textural triangle. Results were graphed using Microsoft Excel.

4.3.3 Stable Carbon Isotope $\delta^{13}C$

Stable carbon isotope ratios ($\delta^{13}C$) can be used to reconstruct past vegetation and associated climate. ^{13}C signals preserved within a soil reflect the type of plants that grew during a given time and is maintained indefinitely in the soil record. C4 plants (i.e., those adapted to warmer, drier conditions) and C3 plants (i.e., those adapted to cooler, moister conditions) discriminate between carbon isotopes ^{13}C and ^{12}C during photosynthesis due to differing photosynthetic pathways (Schaetzl and Anderson, 2005). The data provided through this method is a measure of the ratio of stable isotopes $^{13}C:^{12}C$ compared to a standard (i.e., Pee Dee Belemnite) and is reported in parts per thousand (per mil, ‰) using the following equation (Ludlow et al., 1976; Nordt et al., 1994):

$$\delta 13C = \frac{[13C:12C(\text{sample}) - 13C:12C(\text{standard})]}{13C:13C(\text{standard}) * 1000}$$

For this study, samples were collected from soil cores SC-P, SC-L, CA1-P, CA2-P, and LE-P in 5 cm intervals. Samples from cores CA1-L, CA2-L, and LE-L were collected in 8 cm intervals. All samples were dried, ground using an agate motor and pestle, and submitted to the University of Kansas Keck Paleoenvironmental Stable Isotope Lab (KPESIL). [13]C results were used to reconstruct mean July temperature when the organic matter accumulated using the following equation (Nordt et al., 2007):

$$\text{July Temperature} = [0.685 * 13C \text{ (result)}] + 34.9$$

Temperature deviation was calculated by subtracting the reconstructed temperature value (°C) determined using the Nordt et al. equation from the 30-year mean (i.e., ~1990-2020) July temperature at the nearest HPRCC station. Percent organic matter contributed by C4 vegetation (%C4) was calculated using the following equation (Ludlow et al., 1976):

$$\%C4 = \frac{[13C \text{ (result)} - 27]}{(-12 - 27) * 100}$$

Playa δ^{13}C data was used to infer hydrology whereas lunette δ^{13}C data was used to infer regional climate (temperature and moisture conditions). Results were graphed using Microsoft Excel.

4.3.4 Radiocarbon Dating [14]C

For this study, bulk sediment samples were collected near the tops and bases of buried soils preserved within cores and one freshwater micro mollusk shell found in a playa core (SC-P). All samples were collected in a sterile environment using gloves and masks to avoid modern

human contamination. A total of 23 samples for radiocarbon analysis were collected: three from

SC-P, five from SC-L, two from CA1-P, one from CA1-L, two from CA2-P, three from CA2-L,

two from LE-P, and five from LE-L (Table 10). Bulk sediment samples were dried, ground, then

roots and other material were removed; the shell was cleaned by soaking and gently agitating in

deionized water to remove sediment. All samples were submitted to the National Ocean Sciences

Accelerator Mass Spectrometry (NOSAMS) laboratory for analysis. At NOSAMS, samples were

treated to remove inorganic carbon and mobile organic acid phases and combusted at high

temperature to produce CO_2 and converted to graphite for analysis by accelerator mass

spectrometry. Sample ages were corrected for fractionation compared to standards and reported

following conventions described by (Stuiver and Polach, 1977) and (Stuiver, 1980). Returned

sample ages were converted to calendar age using the Calib 8.20 calibration program (Stuiver et

al., 2022) and reported as mean age plus/minus two standard deviations in calendar years before

present (cal yr BP) for the highest probability distribution under the calibration curve.

Radiocarbon dating was pioneered by Dr. Willard Libby in 1949 as the first ever

radiometric technique (Walker, 2005). Since then, the technique has become widely used and

accepted by disciplines such as archeology, geology, geography, and geomorphology to

determine the numerical age of carbon-containing samples such as carbon-rich sediment,

charcoal, peat, seeds, plant remains, teeth, bones, and carbonates (Schaetzl and Anderson, 2005).

This method is relatively inexpensive compared to other dating methods and sample collection is

simple. The three main forms of isotopic carbon are ^{12}C, ^{13}C, which are both stable forms, and

^{14}C. ^{12}C comprises most of the naturally occurring carbon at ~98% (Walker, 2005). $^{14}CO_2$, a

radioactive form of carbon (C), is produced by cosmic rays in the upper atmosphere where it

rapidly mixes throughout the troposphere and exchanges with the reactive carbon reservoirs of

the oceans and biosphere (Fairbanks et al., 2005). During this process, Nitrogen (N) absorbs a

neutron and emits a proton and electron which changes the atomic number from 7 (N) to 6 (C)

(Walker, 2005). Living plants take up carbon dioxide (CO_2) during photosynthesis that contains

the various isotopes of C. Plant tissues (and the animals that eat the plants) contain the ratio of

$^{14}C:^{12}C$ in the atmosphere at the time they were alive, and this ratio is preserved indefinitely in

soil as the plant decomposes (Walker, 2005). Radiocarbon dating relies on analyzing the ratio of

the known rate of decay of ^{14}C to the constant rate of ^{12}C ($^{14}C:^{12}C$) in a dead organism (Walker,

2005). The known decay rate of ^{14}C is ~1% every 83 years, making the half-life 5,730 years, and

radiometric dating typically has a limit of approximately eight to ten half-lives (Walker, 2005).

Due to this half-life limit, the age range of radiocarbon dating is ~1,000 to ~55,000 years

(Walker, 2005). Because of the continuous incorporation of modern carbon into soil, ages from

^{14}C dating of organic matter samples are interpreted as minimal ages, or limiting ages, for the

length of soil formation (Wang et al., 1996). Additionally, due to fluctuations in atmospheric

carbon content over time, ages must be calibrated using calibration curves such as IntCal 20

which include single-year tree-ring age data for the late Holocene and Younger Dryas/GS-1 and

floating tree chronologies for the Bølling/GI-1e and the last glacial period make to increase its

accuracy and age range from the previous version – IntCal 13 (Reimer et al., 2020). IntCal 13

uses ages from tree-ring chronologies, lacustrine and marine sediments, ice cores, microfossils,

speleothems, and corals (Reimer et al., 2020). Radiocarbon calibration is used to convert

radiocarbon ages to calendar years and to compute changes in atmospheric ^{14}C ($\Delta^{14}C$) through

time (Reimer et al., 2020).

Chapter 5 Results

5.1 Soil Core Descriptions

5.1.1 LE

LE-P

The soil profile for LE-P extends 605 cm deep and is complex with many buried soils, carbonates, and accumulations of clay (Table 2). The surface A horizon is 52 cm thick and the top ~20 cm is affected by plowing. The horizon is dark grayish brown, with strong medium subangular to angular blocky structure and common very fine roots. The Bt horizon is ~50 cm thick, dark grayish brown, has strong fine angular structure, and common to few very fine roots. The C horizon is ~130 cm thick and has light gray coloring. Structure is moderate, fine subangular blocky and there are few very fine roots. Below the A, B, and C horizons are multiple alternating buried horizons and sediment horizons with high accumulation of silicate and sesquioxide clays and carbonates. Buried soils have very pale brown to light brownish gray color and moderate to fine granular or subangular blocky structure.

LE-L

The soil profile for LE-L extends to 949 cm and is complex with many buried soils (Table 3). The A horizon is ~20 cm thick and has been disturbed by plowing. It is light brownish gray in color with weak, fine subangular blocky structure with many fine roots. The AB, B, and BC horizons are 69 cm thick with pale brown to light gray coloring, moderate, fine to medium angular blocky structure, and common very fine roots. The Cstrat horizon is ~540 cm thick and is composed of a series of 2-5 cm thick weakly developed pale brown A horizons separated by 2-10 cm thick very pale brown sedimentary layers (i.e., stacks of alternating A-C horizons). The lower 322 cm of the profile consists of two buried soils separated by ~215 cm of two distinct

sediment layers with strong gleying in the upper sediment layer. The upper buried soil consists of Ab-C horizonation, and the lower buried soil consists of Ab-Bb-BC horizonation; both soils have moderate subangular blocky structure.

5.1.2 CA1

CA1-P

The soil profile for CA1-P extends 359 cm deep and is relatively simple (Table 4). There is a distinct 6 cm sediment layer on the surface that is gray with moderate subangular blocky structure and many medium sized roots. Horizon A is 49 cm thick, dark gray, with strong angular blocky structure and common very fine roots. The Bt horizon is gray with strong, medium, angular blocky structure. The C horizon is 215 cm thick and consists of two distinct units, each with multiple horizons. The upper unit (Ck1 and Ck2 horizons) is 76 cm thick, white to pale brown in color, with moderate, medium subangular blocky structure and few roots and evidence of gleying. The 2Ck, 2Cg, and 2C horizons are 139 cm thick, pale brown to very pale brown, with moderate, medium subangular blocky structure with few roots.

CA1-L

The soil profile for CA1-L extends 564 cm deep and is complex with many buried soils (Table 5). There is a 3 cm thick sediment layer at the surface that is dark gray with weak, fine to medium granular structure and many very fine sized roots. The A horizon is 24 cm thick, has dark grayish brown color, moderate subangular blocky structure, and common very fine roots. The Bt horizon is ~80 thick and has a 10 cm thick krotovina (animal burrow) within. Bt horizon color is pale brown to brown with strong angular blocky structure and common very fine roots. The C horizon is 76 cm thick, pale brown to brown, has strong subangular blocky structure, and

common very fine roots to no roots. Underlying the surface, A, B, and C horizons, the remaining

362 cm has three buried soils with A-Bt horizonation and subangular blocky structure. Carbonate

and manganese nodules are common near the bottom of the profile.

5.1.3 CA2

CA2-P

The soil core for playa CA2-P extends to 246 cm deep and is relatively simple (Table 6).

There is a thin (~10 cm), dark gray Ap horizon that has weak granular structure and common

very fine roots. The B horizon is 100 cm thick (Bg, Bgk, and BC horizons), gray in color, has

medium to fine angular blocky structure, and common very fine roots. Underlying the solum are

two distinct parent materials. The upper Cgk and Cg horizons are 118 cm thick, light gray, with

moderate fine to medium subangular blocky structure. The 2C horizon has a distinct increase in

sand content and reddening (light reddish brown).

CA2-L

The soil profile for playa CA2-L is complex and extends to a depth of 824 cm (Table 7).

The A horizon is 56 cm thick, the upper 7 cm exhibits evidence of plowing, color is grayish

brown to dark grayish brown, with moderate to strong, fine to medium subangular blocky

structure, and fine to medium roots common. The Bt horizon is 59 cm thick, brown, with

moderate, fine, subangular blocky structure. Underlying the solum, the profile consists of ~7 m

of intercalated buried soils and sediment layers. Buried soils are typically darker (pale brown to

yellowish brown) than sediment layers (very pale brown to light yellowish brown), while buried

soils and sediment both have angular to subangular blocky structure.

5.1.4 SC

SC-P

The soil profile for playa SC-P extends to a depth of 340 cm and is relatively simple (Table 8). The surface soil A horizon is 14 cm thick, black, with strong subangular blocky structure and many very fine roots. The B horizon is 8 cm thick with dark brown color, moderate subangular blocky structure with common very fine roots. The surface soil is welded to a ~1 m thick buried soil with Ab, ABb, BAb, Bb horizonation and carbonate nodules throughout. The Ab horizon is 17 cm thick, very dark gray, with strong subangular blocky structure. The ABb horizon is 5 cm thick, very dark grayish brown, with strong subangular blocky structure and common very fine roots. Horizon BAb is 16 cm thick, brown, has moderate subangular blocky structure, and common very fine roots. Horizon Bb is very pale brown with moderate subangular blocky structure and common very fine roots. The C1 horizon is 134 cm thick, with a gleyed, light yellowish-brown color, weak subangular blocky structure, few very fine roots, and the presence of shells. Horizon C2, which is 89 cm thick, was similar to C1 but had iron staining throughout while there was no evidence of iron staining in C1.

SC-L

The soil core for lunette SC-L is complex and extends to a depth of 481 cm (Table 9). The surface horizon, Ap, was disturbed by plowing, cultivation, pasturing, or other human activity. It is 7 cm thick, has dark brown coloring, moderate granular to subangular blocky structure, and many very fine to fine roots. Horizon A is 17 cm thick, very dark brown, with moderate subangular blocky structure and many very fine to fine roots. The B horizon is 15 cm thick, dark grayish brown, with moderate subangular blocky structure and common very fine roots. The transitional BC horizon is 5 cm thick with brown coloring, weak subangular blocky

structure, and common very fine roots. Transitional horizon CB is 46 cm thick, brown, has weak subangular blocky structure, and few very fine roots. The C horizon is 391 cm thick, with a light brown matrix, weak subangular blocky structure, and very few to no roots present. The entire C horizon has slight pedogenic modification with alternating light and dark bands throughout. There were particularly distinct dark bands at 88 to 90 cm, 126 to 131 cm, 145 to 147 cm, 222 to 236 cm, 257 to 262, cm, 281 to 284 cm, 302 to 310 cm, 317 to 318 cm, 324 to 328 cm, 336 to 343 cm, 370 cm, 373 to 375 cm, 388 to 395 cm, 410 to 416 cm, 437 to 440 cm, 453 to 456 cm, and 457 to 480 cm. Two gravel-sized pink to light red rock fragments were found in this horizon. Core SC-L had carbonate nodules and/or carbonate roots traces at 60 cm, 66 to 80 cm, 109 cm, 114 cm, 125 to 133 cm, 312 to 355 cm, 447 cm, 455 cm, and 462 cm.

Table 2 *Soil core profile description for LE-P. Soil core description completed 9/5/2012.*

Depth	Soil Horizon	Description
LE-P (playa) Soil Core Description		
0-20	Ap	10YR 4/2 (dark grayish brown); strong, medium, subangular blocky structure; common very fine roots
20-52	A	10YR 4/2 (dark grayish brown); strong, medium, angular blocky structure; gradual horizon boundary; common very fine roots
52-102	Bt	10YR 4/2 (dark grayish brown); strong, fine to medium, angular blocky structure; gradual horizon boundary; common very fine roots
102-112	BC	10YR 5/2 (grayish brown); strong, fine, angular blocky structure; gradual horizon boundary; few very fine roots
112-341	Cgk	2.5Y 7/2 (light gray); moderate, fine, subangular blocky structure; clear horizon boundary; few fine roots
341-365	2Ab	10YR 7/3 (very pale brown); moderate, fine, subangular blocky structure; gradual horizon boundary; few very fine roots
365-408	2Bb	10YR 6/3 (pale brown); moderate, medium, subangular blocky structure; gradual horizon boundary; few very fine roots
408-478	2Bb2	10YR 6/2 (light brownish gray); moderate, fine, granular to subangular blocky structure; gradual horizon boundary; few roots
478-493	2Co	10YR 7/4 (very pale gray); moderate, very thin, platy structure; clear horizon boundary; few roots
493-503	3Ab	10YR 6/3 (pale brown); strong, medium, subangular blocky structure; gradual horizon boundary; few roots
503-541	3Ck	10YR 8/2 (very pale brown); moderate, fine, angular blocky structure; gradual horizon boundary; few roots
541-567	4Ak	10YR 7/2 (light gray); strong, medium, subangular blocky structure; clear horizon boundary; few roots
567-605	4Btk1	10YR 7/3 (very pale brown); moderate to strong, fine, subangular blocky structure; gradual horizon boundary; few roots

Table 3 *Soil core profile description for LE-L. Soil core description completed 10/30/2012.*

Depth	Soil Horizon	Description
0-20	Ap	10YR 6/2 (light brownish gray); weak, fine, subangular blocky structure; many fine roots
20-36	AB	10YR 6/3 (pale brown); moderate, medium, subangular blocky structure; gradual horizon boundary; common very fine roots
36-77	B	10YR 6/3 (pale brown); moderate, medium, angular blocky structure; diffuse horizon boundary; common very fine roots
77-89	BC	10YR 7/2 (light gray); moderate, fine, angular blocky structure; diffuse horizon boundary; common very fine roots
89-627	Cstrat *	10YR 7/3 (very pale brown) to 10YR 6/3 (pale brown); moderate, medium, subangular blocky structure; diffuse horizon boundary; common very fine roots
627-633	2Ab	10YR 6/4 (light yellowish brown); moderate, fine, subangular blocky structure; clear horizon boundary; few roots
633-668	2C	10YR 5/4 (yellowish brown); moderate, fine, subangular blocky structure; gradual horizon boundary; few roots
668-687	2Cg	5Y 7/1 (light gray); strong, medium, angular blocky structure; clear horizon boundary; few roots
687-766	3C	10YR 6/3 (pale brown); moderate, medium, subangular blocky structure; gradual horizon boundary; few roots
766-795	3Ck1	10YR 6/3 (pale brown); strong, medium, angular blocky structure; gradual horizon boundary; few roots
795-848	3Ck2	10YR 6/1 (gray); moderate, fine, subangular blocky structure; clear horizon boundary; few roots
848-859	4Ab	10YR 5/3 (brown); moderate, medium, subangular blocky structure; clear horizon boundary; few roots
859-904	4Bb	10YR 5/4 (yellowish brown); moderate, medium, subangular blocky structure; gradual horizon boundary; few roots
904-949	4BC	10YR 6/4 (light yellowish brown); moderate, coarse, subangular blocky structure; clear horizon boundary; few roots

Table 4 *Soil core profile description for CA1-P. Soil core description completed 4/24/2013.*

		CA1-P (playa) Soil Core Description
Depth	**Soil Horizon**	**Description**
0-6	Sed	10YR 5/1 (gray); moderate, fine, subangular blocky structure; gradual horizon boundary; many medium roots
6-55	A	10YR 4/1 (dark gray); strong, medium, angular blocky structure; gradual horizon boundary; common very fine roots
55-144	Bt	10YR 5/1 (gray); strong, medium, angular blocky structure; gradual horizon boundary; common fine roots
144-180	Ck1	10YR 8/1 (white); moderate, medium, subangular blocky structure; clear horizon boundary; few roots
180-220	Ck2	10YR 6/3 (pale brown); moderate, medium, subangular blocky structure; gradual horizon boundary; few roots
220-286	2Ck	10YR 6/3 (pale brown); moderate, medium, subangular blocky structure; clear horizon boundary; few roots
286-312	2Cg	2.5Y 7/3 (pale brown); moderate, medium, subangular blocky structure; clear horizon boundary; few roots
312-359	2C	10YR 7/3 (very pale brown); moderate, medium, subangular blocky structure; few roots

Table 5 *Soil core profile description for CA1-L. Soil core description completed 4/15/2013.*

Depth	Soil Horizon	Description
0-3	Sed	10YR 4/1 (dark gray); weak, fine to medium, granular structure; diffuse horizon boundary; many very fine roots
3-27	A	10YR 4/2 (dark grayish brown); moderate, fine, subangular blocky structure; gradual horizon boundary; common very fine roots
27-46	Bt	Matrix – 10YR 6/3 (pale brown), Carbonate – 10YR 4/2 (dark grayish brown); strong, medium, angular blocky structure; diffuse horizon boundary; common very fine roots
82-92	Krot	Matrix – 10YR 6/3 (pale brown), Carbonate – 10YR 4/2 (dark grayish brown); strong, medium, subangular blocky structure; diffuse horizon boundary; common very fine roots
92-126	Bt'	10YR 5/3 (brown); strong, medium, subangular blocky; diffuse horizon boundary; common very fine roots
126-202	C	10YR 5/3 (brown) to 10YR 6/3 (pale brown); strong, medium, subangular blocky structure; gradual horizon boundary; common very fine roots
202-262	Ab1	10YR 5/4 (yellowish brown); strong, medium, subangular blocky structure; diffuse horizon boundary; no roots
262-310	Btb1	10YR 4/3 (brown); moderate, fine, subangular blocky structure; gradual horizon boundary; no roots
310-332	Ab2	10YR 5/4 (yellowish brown); moderate, fine, subangular blocky structure; gradual horizon boundary; no roots
332-366	Btb2	7.5YR 5/4 (brown); strong, medium, subangular blocky structure; gradual horizon boundary; no roots
366-390	2Ck	10YR 6/4 (light yellowish brown); strong, medium, angular blocky structure; gradual horizon boundary; no roots
390-435	2Akb	10YR 6/4 (light yellowish brown); strong, medium, subangular blocky structure; diffuse horizon boundary; no roots
435-488	2Btkb	10YR 6/4 (light yellowish brown); strong, medium, subangular blocky structure; gradual horizon boundary; no roots
488-564	3Cg	10YR 5/2 (grayish brown); strong, medium, angular blocky structure; no roots

Table 6 *Soil core profile description for CA2-P. Soil core description completed 2/8/2013.*

Depth	Soil Horizon	Description
0-10	Ap	10YR 4/1 (dark gray); weak, fine, granular structure; diffuse horizon boundary; common very fine roots
10-44	Bg	10YR 6/1 (gray); moderate, medium, angular blocky structure; diffuse horizon boundary; common very fine roots
44-89	Bgk	10YR 6/1 (gray); strong, medium, angular blocky structure; diffuse horizon boundary; common very fine roots
89-110	BC	2.5Y 6/1 (gray); moderate, fine, angular blocky structure; gradual horizon boundary; common very fine roots
110-142	Cgk	2.5Y 7/2 (light gray); moderate, medium, subangular blocky structure; gradual horizon boundary; common fine roots
142-228	Cg	2.5Y 7/2 (light gray); moderate, fine, subangular blocky structure; gradual horizon blocky structure; very few roots
228-246	2C	7.5YR 6/4 (light reddish brown); moderate, medium, subangular blocky structure; very few roots

Table 7 Soil core profile description for CA2-L. Soil core description completed 2/8/2013.

Depth	Soil Horizon	Description
0-7	Ap	10YR 5/2 (grayish brown); moderate, fine, subangular blocky structure; diffuse horizon boundary; common medium roots
7-56	A	10YR 4/2 (dark grayish brown); moderate to strong, medium, subangular blocky structure; diffuse horizon boundary; common very fine roots
56-115	Bt	10YR 5/3 (brown); moderate, fine, subangular blocky structure; diffuse horizon boundary; common very fine roots
115-398	2C$_{strat}$	10YR 6/3 (pale brown) to 10YR 7/3 (very pale brown); moderate, fine, subangular blocky structure; clear horizon boundaries
398-523	2C	10YR 6/4 (light yellowish brown); moderate to strong, medium, subangular blocky structure; gradual horizon boundary; few roots
523-583	3Ab	10YR 5/3 (brown); moderate to strong, medium, subangular blocky structure; gradual horizon boundary; few roots
583-619	3Bb	10YR 5/3 (brown); moderate, medium, subangular blocky structure; gradual horizon boundary; few roots
619-672	3C	10YR 6/4 (light yellowish brown); moderate, medium, subangular blocky structure; gradual horizon boundary; few roots
672-703	3Ab2	10YR 5/2 (grayish brown); strong, medium, angular blocky structure; gradual horizon boundary; few roots
703-728	3Bb2	10YR 5/4 (yellowish brown); strong, medium, angular blocky structure; gradual horizon boundary; few roots
728-753	3BC	10YR 6/3 (pale brown); strong, medium, angular blocky structure; gradual horizon boundary; few roots
753-824	3Ck	10YR 6/4 (light yellowish brown) to 10YR 7/4 (very pale brown); strong, medium, angular blocky structure; gradual horizon boundary; few roots

Table 8 *Soil core profile description for SC-P. Soil core description completed 6/22/2021.*

Depth	Soil Horizon	Description
	SC-P (playa) Soil Core Description	
0-14	A	7.5YR 2.5/1 (black); strong, very fine to fine, subangular blocky structure; clear horizon boundary; many very fine to fine roots
14-22	B	7.5YR 3/2 (dark brown); moderate, very fine to fine, subangular blocky structure; abrupt horizon boundary; common very fine roots
22-39	Ab	7.5YR 3/1 (very dark gray); strong, very fine to fine, subangular blocky structure; gradual horizon boundary; common very fine roots
39-44	ABb	10YR 3/2 (very dark grayish brown); strong, very fine to fine, subangular blocky structure; gradual horizon boundary; common very fine roots
44-60	BAb	10YR 5/3 (brown); moderate, very fine to fine, subangular blocky structure; gradual horizon boundary; common very fine roots
60-117	Bb	10YR 7/3 (very pale brown); moderate, fine to medium, subangular blocky structure; gradual horizon boundary; common very fine roots
117-251	C1	2.5Y 6/3 (light yellowish brown); weak, fine to medium, subangular blocky structure; gradual horizon boundary; few very fine roots
251-340	C2	2.5Y 7/3 (pale brown); weak, fine to medium, subangular blocky structure; very few very fine roots

Table 9 *Soil core profile description for SC-L. Soil core description completed 6/23/2021.*

Depth	Soil Horizon	Description
	SC-L (lunette) Soil Core Description	
0-7	Ap	10YR 3/3 (dark brown); moderate, fine, granular to subangular blocky structure; abrupt horizon boundary; many very fine to fine roots
7-24	A	10YR 2/2 (very dark brown); moderate, very fine to fine, subangular blocky structure; clear horizon boundary; many very fine to fine roots
24-39	B	10YR 4/2 (dark grayish brown); moderate, fine, subangular blocky structure; gradual horizon boundary; common very fine roots
39-44	BC	10YR 4/3 (brown); weak, very fine, subangular blocky structure; gradual horizon boundary; common very fine roots
44-90	CB	10YR 5/3 (brown); weak, very fine to fine, subangular blocky structure; diffuse horizon boundary; few very fine roots
90-481	C$_{strat}$	7.5YR (light brown); weak, very fine to fine, subangular blocky structure; very few to no roots

5.2 Radiocarbon Dates

5.2.1 LE

Calibrated radiocarbon ages for LE-P were reported as $10{,}790 \pm 90$ cal yrs BP from the lowermost portion of the surface soil at 109 cm and $25{,}000 \pm 375$ cal yrs BP from a buried soil at 499 cm. Samples collected for LE-L were reported as $22{,}520 \pm 420$ cal yrs BP at 198 cm, $27{,}670 \pm 400$ cal yrs BP at 297 cm, $25{,}570 \pm 400$ cal yrs BP at 408 cm, $28{,}520 \pm 660$ cal yrs BP at 627 cm, and $32{,}210 \pm 1{,}120$ cal yrs BP at 872 cm. The upper four ages were collected from dark units (interpreted as incipient A horizons) in the Cstrat horizon, while the lowermost sample was collected from a distinct, well-developed buried soil. The returned age at 408 cm in core LE-L is ~2,100 years younger than the returned age at 297 cm, which could be due to potential contamination by younger carbon. Reported radiocarbon ages are generally younger than the actual soil age due to natural carbon cycling (Wang et al., 1996).

5.2.2 CA1

Calibrated radiocarbon ages for CA1-P are $8{,}380 \pm 30$ cal yrs BP at 142 cm from the base of the surface soil and $23{,}500 \pm 300$ cal yrs BP at 236 cm within the 2Ck horizon. Only one sample was collected for CA1-L at 324 cm from a deeply buried soil and has a calibrated age of $37{,}050 \pm 4{,}090$ cal yrs BP.

5.2.3 CA2

Samples from CA2-P were collected at 111 cm and 223 cm within the Cgk and Cg horizons. Calibrated ages are $7{,}210 \pm 50$ cal yrs BP at 111 cm and $27{,}760 \pm 420$ cal yrs BP at 223 cm. All samples taken from CA2-L were collected from buried soils and have calibrated

ages of 26,240 ± 290 cal yrs BP at 266 cm, 32,670 ± 780 cal yrs BP at 580 cm, and 37,560 ±

2,830 cal yrs BP at 680 cm.

5.2.4 SC

Three samples were collected from SC-P – two from buried soils (organic sediment) and

one near the top of the C horizon (mollusk shell). Radiocarbon ages are 980 ± 25 cal yrs BP at 23

cm and 1,370 ± 30 cal yrs BP at 43 cm for the two sediment samples, and 18,540 cal yrs BP at

126 cm for the shell. Core SC-L had 5 samples collected from depths ranging from 89 cm to 470

cm. The radiocarbon dates are 5,220 ± 70 cal yrs BP at 89 cm at the base of the surface soil,

27,640 ± 460 cal yrs BP at 224 cm, 28,470 ± 630 cal yrs BP at 305 cm, 30,270 ± 770cal yrs BP,

and 29,320 ± 670 cal yrs BP at 470 cm. The returned age at 470 cm in core SC-L is ~1,000 years

younger than the returned age at 326 cm but within the margin of error for these two samples.

Table 10 Radiocarbon dates organized by site, lab sample number, sample type, depth, reported 14C age ± one standard deviation, and calibrated age ± two standard deviations.

Site^	Sample No.	Sample Type	Depth (cm)	14C Age	14C Age Err (± 1 SD)	Cal YR	Cal YR Err (± 2 SD)
LE-P	OS-160888	Sediment OC*	109	9,540	35	10,790	90
LE-P	OS-160889	Sediment OC*	499	20,800	140	25,000	375
LE-L	OS-145384	Sediment OC*	198	19,050	160	22,520	420
LE-L	OS-102878	Sediment OC*	297	23,500	220	27,670	400
LE-L	OS-145385	Sediment OC*	408	21,300	210	25,570	385
LE-L	OS-102926	Sediment OC*	627	24,400	320	28,520	660
LE -L	OS-145386	Sediment OC*	872	27,900	500	32,210	1,120
CA1-P	OS-160896	Sediment OC*	142	7,560	25	8,380	30
CA1-P	OS-160887	Sediment OC*	236	19,550	120	23,500	300
CA1-L	OS-146955	Sediment OC*	324	32,300	1,900	37,050	4,090
CA2-P	OS-160893	Sediment OC*	111	6,280	25	7,210	50
CA2-P	OS-160894	Sediment OC*	223	23,600	190	27,760	420
CA2-L	OS-160895	Sediment OC*	266	22,100	150	26,240	290
CA2-L	OS-102908	Sediment OC*	580	28,500	230	32,670	780
CA2-L	OS-103161	Sediment OC*	680	32,800	1,300	37,560	2,830
SC-P	OS-162413	Sediment OC*	23	1,110	15	980	25
SC-P	OS-162414	Sediment OC*	43	1,490	15	1,370	30
SC-P	OS-162352	Mollusk	126	15,050	70	18,540	100
SC-L	OS-162415	Sediment OC*	89	4,490	20	5,220	70
SC-L	OS-162416	Sediment OC*	224	23,400	270	27,640	460
SC-L	OS-162417	Sediment OC*	305	24,300	300	28,470	630
SC-L	OS-162418	Sediment OC*	326	26,000	370	30,270	770
SC-L	OS-162419	Sediment OC*	470	25,000	330	29,320	670

Site^ = LE – Lane, CA1 – Clark 1, CA2 – Clark 2, SC – Scott, L – lunette, P – playa

OC* = organic carbon

5.3 Stable Carbon Isotopes

5.3.1 LE

LE-P δ^{13}C values range from -27.5‰ to -19.8‰ (Figures 14 and 15). δ^{13}C is stable at ~-20% from the surface to ~110 cm and then decreases steadily to -27.5‰ at 235 cm. δ^{13}C values remain less than -26‰ until 280 cm and then exhibit a generally increasing trend to ~-22.5‰ at 370 cm. Between 370 cm and 480 cm, δ^{13}C values oscillate between -22.5‰ and -25‰ and then exhibit a generally declining trend to the bottom of the core at 605 cm. Percent total organic carbon (TOC) values for LE-P range from 0.1% to 0.7% (Figure 14). TOC ranges from ~0.5% to 0.7% from 0 to ~110 cm, decreases to 0.3% at 140 cm, and remains below 0.3% to depth for all but one sample. LE-P temperature deviation (i.e., reconstructed temperature based on ^{13}C values minus the 30-year mean July temperature) compared to the HPRCC Healy, KS weather station mean July temperature (78.1 °F, 25.6 °C), ranges from -9.5 °C to -4.2 °C (Figure 15). From the surface to 100 cm, temperature deviations range from -5.5 °C to -4.6 °C, indicating reconstructed temperatures are cooler than modern temperatures. Below 100 cm, all temperature deviation values are less than -5 °C, and they are less than -9 °C between 230 cm and 275 cm and less than -8.5 °C from 515 cm to the base of the core.

LE-L δ^{13}C values range from -21.3‰ to –11.5‰ (Figures 16 and 17). δ^{13}C values are -13.3‰ near the surface and decline to ~-20.6‰ at 98 cm. From 98 cm to 600 cm, values oscillate between -17.6‰ and -21.3‰ and then increase to -16.6‰ at 650 cm. δ^{13}C values then decline sharply to -21‰ at 674 cm and then rapidly increase to -16.2‰ at 714 cm. From 714 cm to 842 cm, δ^{13}C values decline slightly to -17.4‰ at 842 cm and then rapidly increase to -14.9‰ at 850 cm. δ^{13}C values oscillate between -11.5‰ and -18.7‰ from 842 cm to the bottom of the core at 942 cm, with values frequently shifting by 2-3‰ in less than 10 cm intervals. LE-L TOC

values range from 0.1% to 0.7% (Figure 16). TOC is greatest in the uppermost sample at 0.7% at 10 cm, declines to 0.4% at 26 cm and remains below 0.4% to depth. LE-L temperature deviation compared to the HPRCC Healy, KS weather station mean July temperature (78.1 °F, 25.6 °C) ranges from -5.6 °C to 1.1 °C (Figure 17). From 50 cm to 600 cm, reconstructed temperature is 2.9-5.6 °C cooler than modern, while from 600 cm to 858 cm reconstructed temperature is 2-4 °C cooler than modern. Below 858 cm, temperature deviations are highly oscillatory and range from 1.1 °C warmer than modern to 3.8 °C cooler.

5.3.2 CA1

CA1-P δ^{13}C values range from -27.6‰ to –22.3‰ (Figures 14 and 15). δ^{13}C values are consistent from the surface to 105 cm at -24.5‰ to -23‰. δ^{13}C increases to -22.3‰ at 110 cm and then declines to -24.5‰ at 115 cm. From 115 cm to 210 cm, values oscillate between -25.2‰ and -23.2‰. Below 210 cm, δ^{13}C values progressively decline to a minimum of -27.6‰ in the lowermost sample at 240 cm. CA1-P TOC values range from 0.04% to 0.7% (Figure 14). Values are highest from 10 cm to ~85 cm with a range of 0.5% to 0.7%. With the exception of a ~0.1% increase at 110 cm, there is a steady decrease in values from ~85 cm to 170 cm. Below 170 cm, TOC remains low to the bottom of the core. CA1-P temperature deviation, based on HPRCC 30-year average at Sublette, KS weather station (78.7 °F, 25.9 °C), ranges from -9.9 °C to -6.3 °C (Figure 15). For the majority of the profile, reconstructed temperatures are ~6.3-7.8 °C cooler than modern. From 220 cm to ~240 cm, reconstructed temperatures decrease to a range of 8.0-9.9 °C cooler than modern.

CA1-L δ^{13}C values range from –23.1‰ to –14.6‰ (Figures 16 and 17). Values from 0 cm to ~65 cm are fairly high, averaging ~-16‰, and values exhibit a decreasing trend from ~70 cm to 165 cm (though values regularly oscillate by 3‰ in less than 10 cm intervals). From 165 cm to 286 cm, δ13C has a generally increasing trend, reaching the maximum value of -14.6‰ at 286 cm. From 286 cm to 330 cm, values oscillate considerably and then exhibit a generally declining trend to depth, though values continue to oscillate by 2-3‰ in 10 cm intervals, reaching a minimum of -23.1‰ at 536 cm (14 cm above the base of the core). CA1-L TOC values range from 0.1% to 1.1% (Figure 16). TOC values are highest near the surface and steadily decrease with depth, ranging from 1.2% (surface value) to 0.3% at 70 cm. From 70 cm to ~330 cm, TOC values range between ~0.2% and 0.4%. Below 330 cm, TOC remains below 0.2%. CA1-L temperature deviation ranges from -6.8 °C to -1.0 °C (Figure 17). Reconstructed temperatures are 1-3 °C cooler than modern from the surface to ~50 cm, 2.7-5.6 °C cooler from 50 cm to ~200 cm, are generally 1-3 °C cooler than modern from ~200 cm to 370 cm, and are 4-6 °C cooler from 370 cm to the base of the core at 550 cm.

5.3.3 CA2

CA2-P δ^{13}C values range from -27.8‰ to -20.9‰ (Figure 14, 15). δ^{13}C values decrease steadily from -20.9‰ at 10 cm to -23.6‰ at 100 cm (-20.9‰ to -23.6‰) before dramatically decreasing to -27.4‰ at 135 cm. Values then progressive increase to -22.3‰ at 215 cm before steadily decreasing to the minimum value of -27.8‰ at the base of the core at 245 cm. CA2-P TOC values range from 0.2% to 0.7% (Figure 14). Values for TOC steadily decrease from the maximum value of 0.7% at 10 cm to ~0.2% in the lower ~90 cm of the core. There are two slight increases in TOC of ~0.1% at 25 cm and 40 cm and a 0.2% increase at 90 cm. CA2-P

temperature deviation, based on HPRCC 30-year average at Sublette, KS weather station (78.7 °F, 25.9 °C), ranges from –10.05 °C to –5.33 °C (Figure 15). Reconstructed temperature values steadily decrease with depth and are notably lowest in the lowermost 90 cm of the core (-8.8 °C to -10.1 °C cooler than modern).

CA2-L δ^{13}C values range from –22.2‰ to –12.9‰ (Figures 16 and 17). δ^{13}C values are highly oscillatory and exhibit several dramatic fluctuations in short intervals. From the surface to ~30 cm, δ^{13}C values increase from -18.3‰ at 10 cm to -14.6‰ at 34 cm and then steadily decline to -21.3‰ at 90 cm. From ~90 cm to ~500 cm values oscillate frequently between -15.5‰ to -22.2‰, with shifts greater than 5‰ in 10 cm intervals common. δ^{13}C values steadily increase from -18.1‰ at 500 cm to -13.6‰ at 590 cm; values then range between -12.9‰ and -18.7‰ from 590 cm to the bottom of the core at 810 cm, with several shifts of 3-5‰ in 10 cm intervals. CA2-L TOC values range from 0.03% to 1.1% (Figure 16). The greatest TOC values are at the surface and steadily decline to ~0.1% at 98 cm. From 98 cm to 526 cm, TOC is generally below 0.2% and most samples are below 0.1%. TOC increases to 0.5% at 590 cm, then declines to 0.2% at 602 cm and remains low for all samples except one value of 0.4% at 682 cm. CA2-L temperature deviation ranges from –6.3 °C to 0.1 °C (Figure 17). Reconstructed temperature is only 1 °C cooler than modern at 34 cm but declines to 5.6 °C cooler than modern at 90 cm. from 90 cm to 500 cm, temperature deviation ranges from -6.3 °C to -1.8 °C with 2-3 °C shifts in temperature in less than 10 cm intervals common. Below 500 cm, temperature deviation declines, and reconstructed temperature ranges from 3.9 °C cooler to 0.1 °C warmer than modern, with shifts of 2-3 °C in less than 10 cm intervals common.

5.3.4 SC

SC-P δ^{13}C values range from -26.7‰ to -17.4‰ (Figures 14 and 15). δ^{13}C values are greatest near the surface, with a maximum value of -17.4‰ at 20 cm, and dramatically decrease to -24.8‰ at 50 cm. Values then slightly oscillate between -23.7‰ and -26.7‰ from ~50 cm to the bottom of the core at 340 cm. SC-P TOC values range from 0.1% to 1.3% (Figure 14). TOC values have a similar trend to ^{13}C: maximum values are near the surface, values decrease to 0.2% at 50 cm, and then values slightly oscillate between 0.1% and 0.3% to the base of the core. SC-P temperature deviation, based on the HPRCC 30-year average at Healy, KS weather station (78.1 °F, 25.6 °C), ranges from -9.0 °C to -2.6 °C (Figure 15). Reconstructed temperature is ~2.5-6 °C cooler than modern for the upper 45 cm, then they are 7-9 °C cooler than modern to the base of the core

SC-L δ^{13}C values range from -24.0 ‰ to -13.6‰ (Figures 16 and 17). The only δ^{13}C values to exceed -20‰ are from the surface to 95 cm (range of -13.6‰ to -19.0‰). From 100 cm to 340 cm, δ^{13}C values generally oscillate between ~-20.1‰ and ~-24‰ and then increase from -21‰ at 340 cm to -20.5‰ at 360 cm. δ^{13}C then declines to -22.5‰ at 450 cm, increases to -19.6‰ at 465 cm, and then declines to -21.3‰ at the base of the core at 480 cm. SC-L TOC values range from 0.1% to 1.4% (Figure 16). TOC values are generally above 1% in the upper 35 cm, declines to 0.2% at 90 cm, and oscillates between 0.1% and 0.3% to the base of the core. SC-L temperature deviation ranges from –7.1 °C to 0.0 °C (Figure 17). Reconstructed temperatures are similar to modern values in the upper 45 cm, steadily decreases to -7.1 °C cooler than modern at 185 cm, remains 5.8-6.8 degrees °C than modern to 340 cm, and then exhibits a slight temperature increase to the bottom of the core.
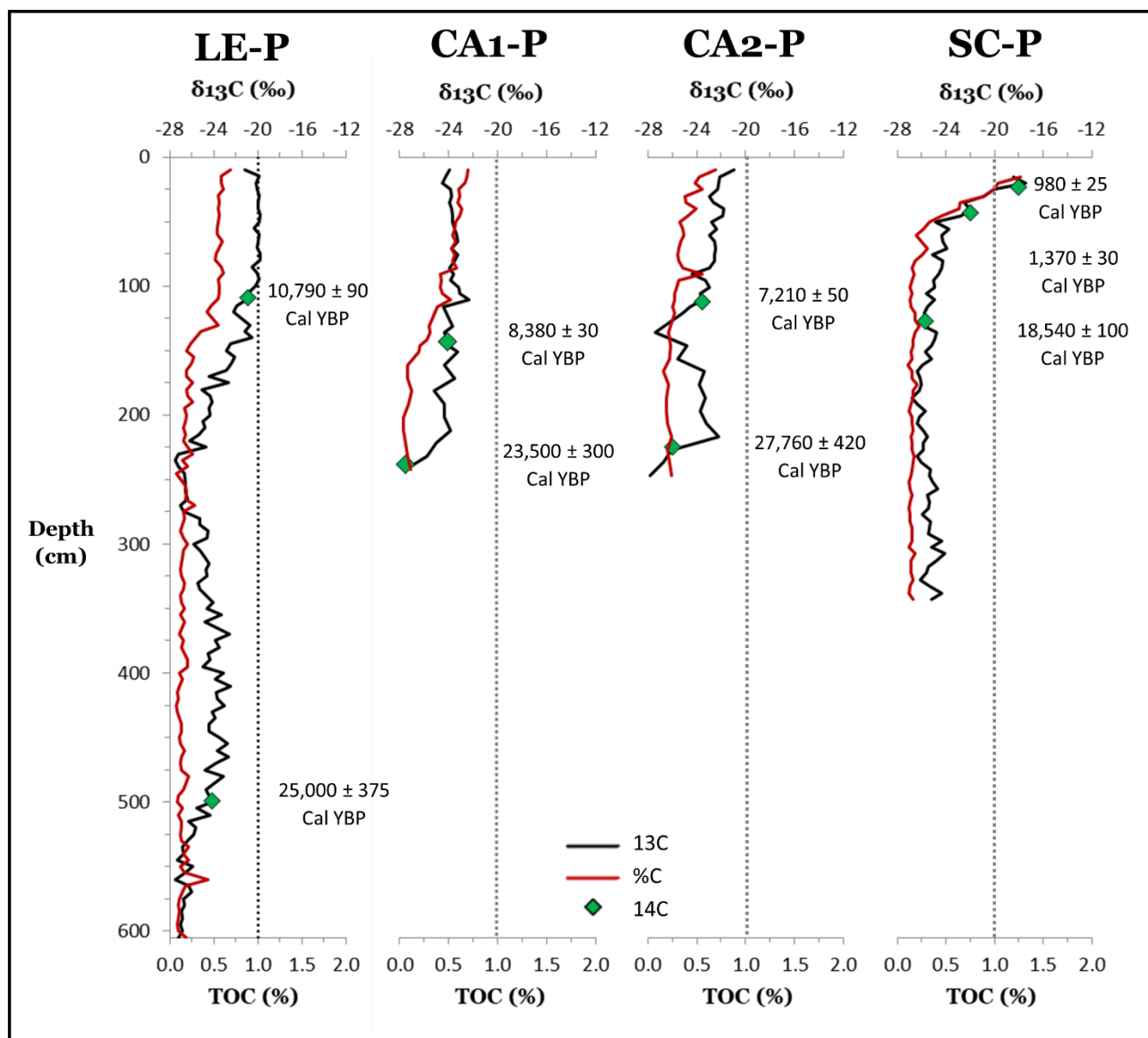
Figure 14 *Stable carbon isotope (13C) data and total organic carbon (TOC) plotted against depth. Radiocarbon dates plotted at approximate extraction depths. All playa cores.*
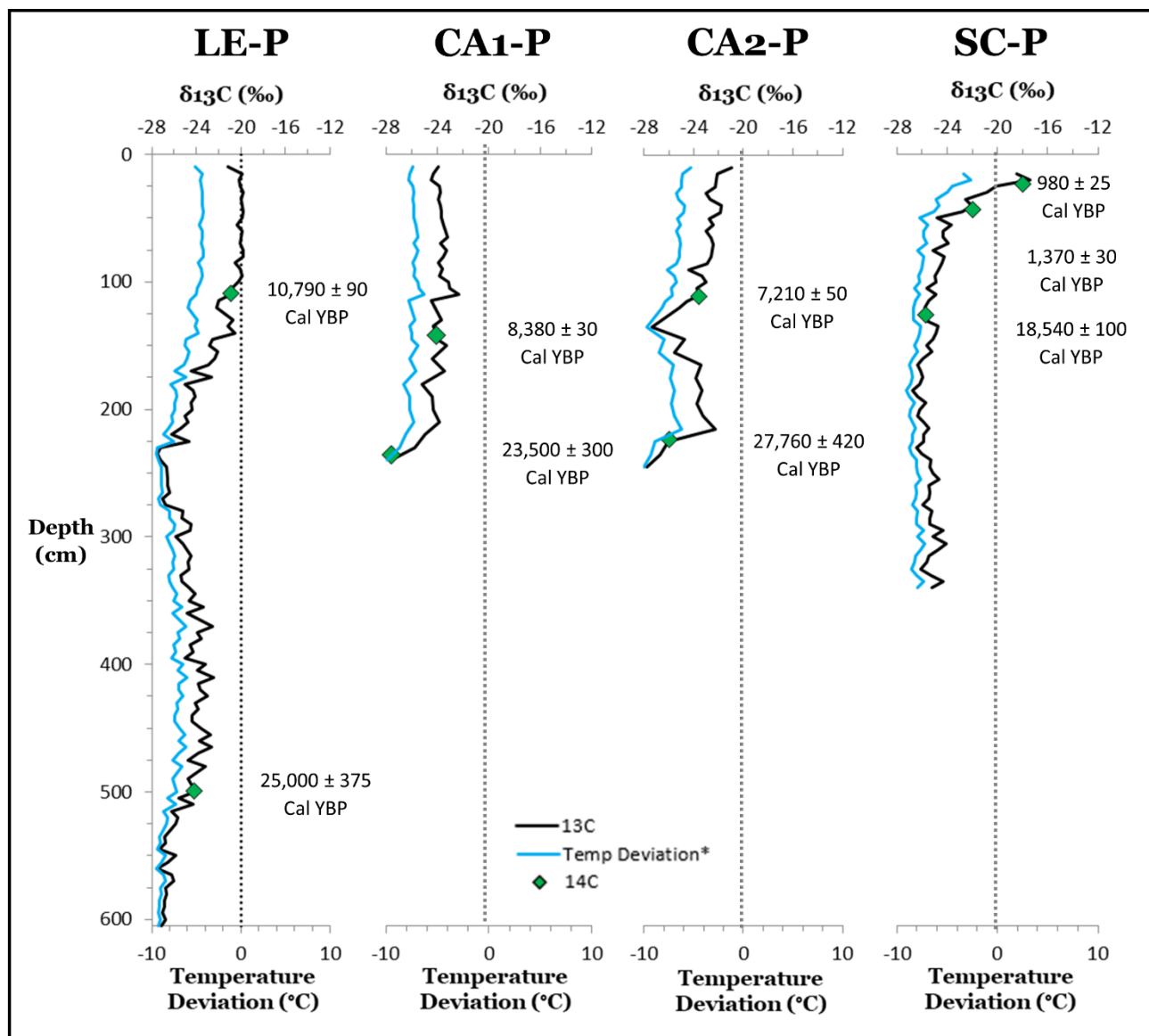
Figure 15 *Stable carbon isotope (13C) data and temperature deviation plotted against depth. Radiocarbon dates plotted at approximate extraction depths. All playa cores*
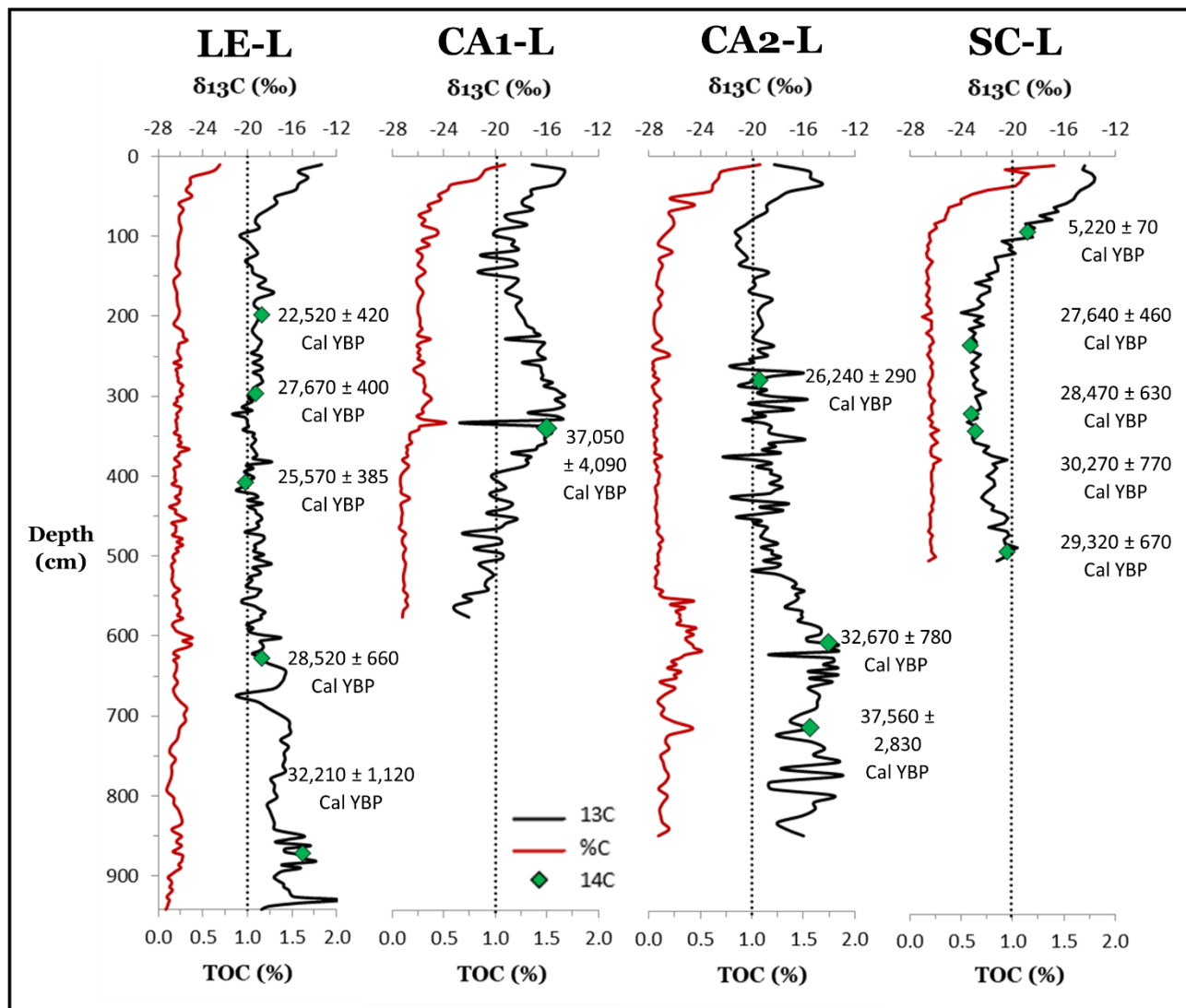
Figure 16 *Stable carbon isotope (13C) data and total organic carbon (TOC) plotted against depth. Radiocarbon dates plotted at approximate extraction depths. All lunette cores.*
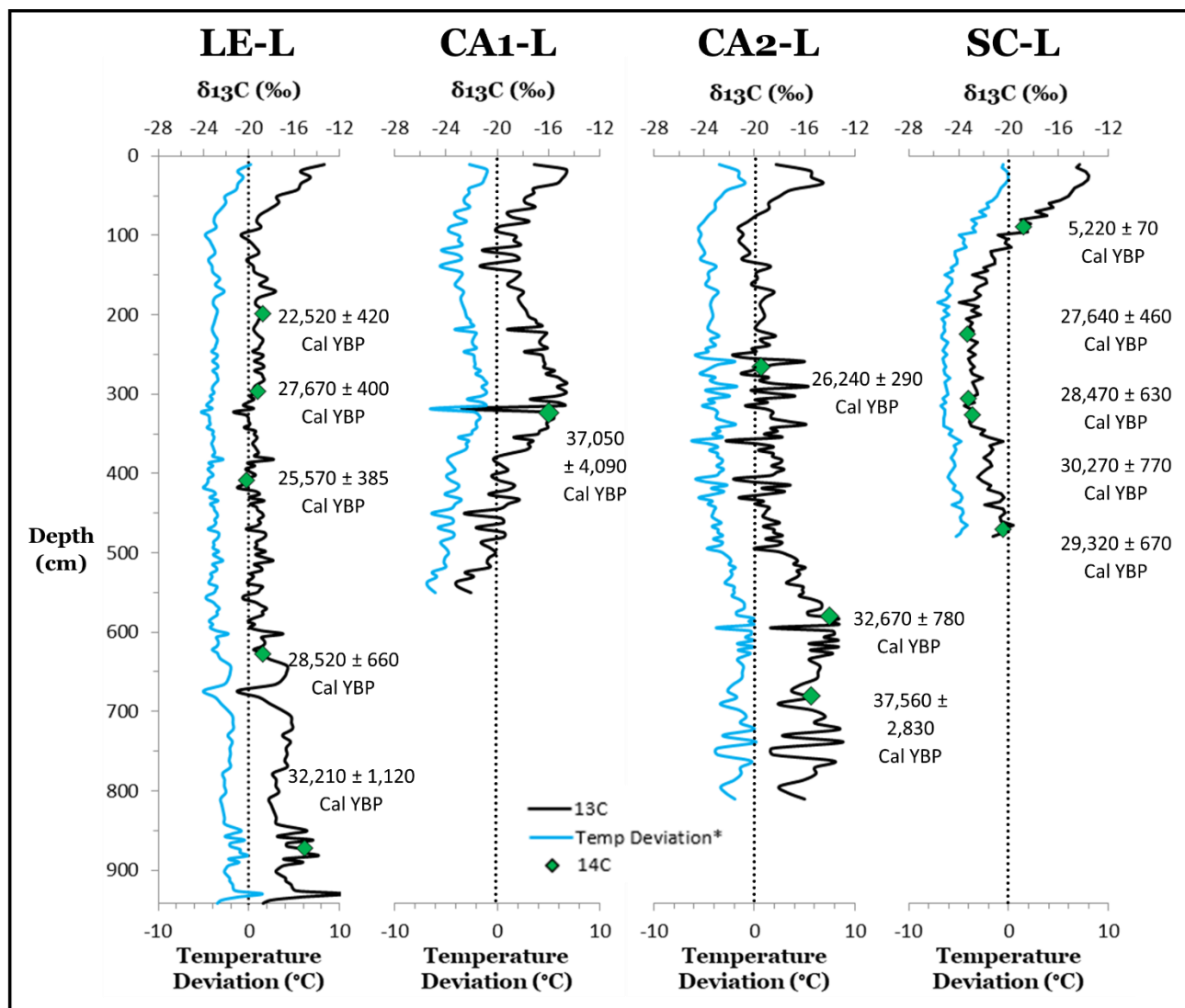
Figure 17 *Stable carbon isotope (13C) data and temperature deviation plotted against depth. Radiocarbon dates plotted at approximate extraction depths. All lunette cores.*

5.4 Particle Size Analysis

Recently, systematic problems with the particle size data were identified. Errors were due to issues related to the standard operating procedures for the Malvern Mastersizer and incomplete dispersion of aggregates during sonication. Unfortunately, these problems were not identified until PSA of all samples was complete. New standard operating procedures have been developed and samples are currently being re-analyzed after soaking in sodium hexametaphosphate for at least 24 hours. Analysis is ongoing, but the revised data were not available at time of publication of the thesis. It is anticipated that analysis will be complete in early summer 2022, and the revised data will be included in a peer-reviewed manuscript based on this thesis. Data reported below are for samples with errors and caution is urged when

examining these data. These PSA data were not used to aid in the interpretation of PLS geomorphic evolution or paleoenvironmental reconstructions but are reported to show general trends in particle size data among sites.

5.4.1 LE

Particle size distribution for LE-L is fairly consistent with small fluctuations in percent sand, silt, and clay throughout. However, the entire profile is dominated by silt, with percent silt ranging from 68.4% to 80.8% and an average silt content of 76.4% (Figure 18). Sand was the next greatest constituent, averaging 13.0% and ranging from 6.7% to 23.0%. Clay content averages 10.6% and ranges from 7.3 to 17.0%. Clay content is slightly greater and sand content slightly less between ~100 cm and 350 cm. The dominant USDA particle size class for LE-L is silt loam (90 out of 95 samples), with five samples classified as silt (Figure 19).

5.4.2 CA1

Particle size distribution for CA1-P is relatively consistent from 10 cm to 140 cm, with sand ranging from 3.5% to 6.3% and silt ranging from 82.0% and 84.2%. Silt content then decreases ~14% and sand content increases ~11% at 160 cm (Figure 18). Below 160 cm, sand content ranges from 14.1% to 20.5% for all but two samples (7.5% at 290 cm and 9.3% at 310 cm). Silt content progressively increases from 69.3% at 160 cm to 82.7% at 290 cm and then steadily declines to 72.3% at the bottom of the core at 360 cm. Clay content is relatively consistent from 10 cm to 180 cm and ranges from 10.4% to 13.7%, decreases to 9.1% at 190 cm, and ranges from 6.9% to 9.8% to the bottom of the core. USDA particle size class is predominantly silt loam (31 out of 36 samples) with five samples classified as silt (Figure 19).

CA1-L is dominated by silt and is relatively homogenous to depth. Clay content is relatively low throughout, ranging from 6.9% to 12.8% with only three samples below 7.5% and three samples above 12.0%. Sand content ranges from 6.4% to 29.2%; sand content is greatest between ~350 cm and 450 cm, which corresponds with a decrease in silt content (Figure 20). Silt content ranges from ~74% to 82% except between ~350 cm and 450 cm, where it ranges from 63.1% to 71.5%. Silt loam is the dominant USDA particle size class (51 out of 56 samples), with the lowermost four samples and one other sample classified as silt (Figure 21).

5.4.3 CA2

Particle size distribution for CA2-P is relatively consistent from 0 cm to ~110 cm with sand ranging from 2.8% to 6.6% and silt ranging from 80.9% to 85.7%. From ~110 cm to ~140 cm, there is a dramatic decrease in silt (to ~75%) and increase in sand (to ~11%). Below this, is similar to near surface values until ~225 cm, where there is another increase in sand (to ~18%) and decrease in silt (to ~72%). Clay content is relatively low throughout the core (6.6% to 14.5%) with distinct fluctuations at ~36cm, ~110 cm, and ~225 cm (Figure 18). The dominant USDA particle size class for CA2-P is silt (19 out of 25 samples) but a few samples, especially near the bottom of the core, were classified as silt loam (6 out of 25 samples) (Figure 19).

Particle size distribution for CA2-L is the most complex and highly variable of all the cores. From the surface to ~150 cm, silt is dominant, then sand becomes the dominate size class until ~550 cm, but there are large fluctuations in silt and sand content throughout. Between ~550 cm and ~650 cm, silt becomes dominant, sand dominates from ~670 cm to ~680 cm, then returns to silt dominance to depth (Figure 20). Sand content has a wide range, 1.1% to 75.3% but is greatest from ~140 cm to ~520 cm. Like sand, silt content has a wide range, 21.7% to 86.8%,

and clay percentages also have a wide range from 24.7% to 98.9% but is highest from 0 to ~140 cm and ~520 to the bottom. Clay content remains low, 2.7% to 9.6%, from 0 cm to ~690 cm, but increases from ~700 to the bottom (10% to 21%). Particle size classes reflect the wide ranges and frequent fluctuations in particle size distribution. Silt loam is the dominant USDA particle size class (41 out of 87 samples) however, silt is also predominate (37 out of 83 samples). The remaining samples are classified as silt (3 out of 83 samples), loam (1 out of 83 samples), and loamy sand (1 out of 83 samples) (Figure 21).

5.4.4 SC

Particle size distribution for SC-P is fairly consistent, with small fluctuations in sand, silt, and clay content throughout (Figure 18). However, the entire profile is dominated by silt, with percent silt ranging from 73.8% to 84.8% and an average silt content of 80.3%. Sand was the next greatest constituent, averaging 10.1% and ranging from 3.7% to 15.4%. Clay content ranges from 6.5% to 17.5% and averages 9.7%. Clay content is greatest at the top and bottom of the profile, and sand is greatest in the middle. Silt loam is the dominant USDA particle size class for this core (36 out of 67 samples), but the silt class is also common (31 out of 67 samples) (Figure 19).

Core SC-L has high variability in particle size distribution throughout the entire core; however, silt is consistently the dominate size class (Figure 20). Percent silt ranges from 63.5% to 82.2% with an average of 73.2%. Sand content has a wide range from 0.6% to 32.2%, averages 14.7%. Clay content ranges from 4.3% to 18.2% and averages 12.2%. The USDA particle size class for core SC-L is classified solely as silt loam (96 out of 96 samples) (Figure 21).
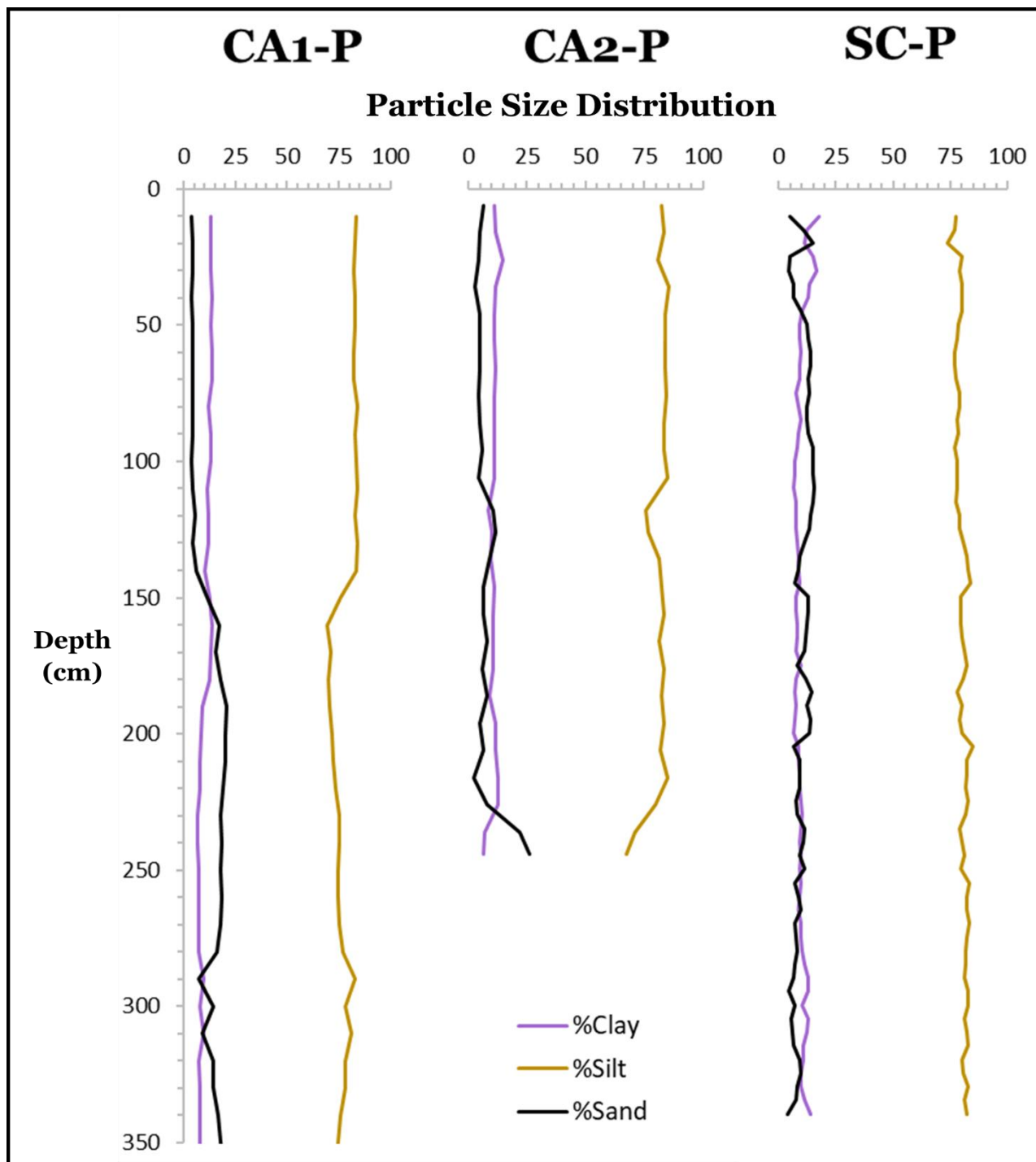
Figure 18 *Particle size distribution (percent sand, silt, and clay) plotted against depth for all playa cores.*
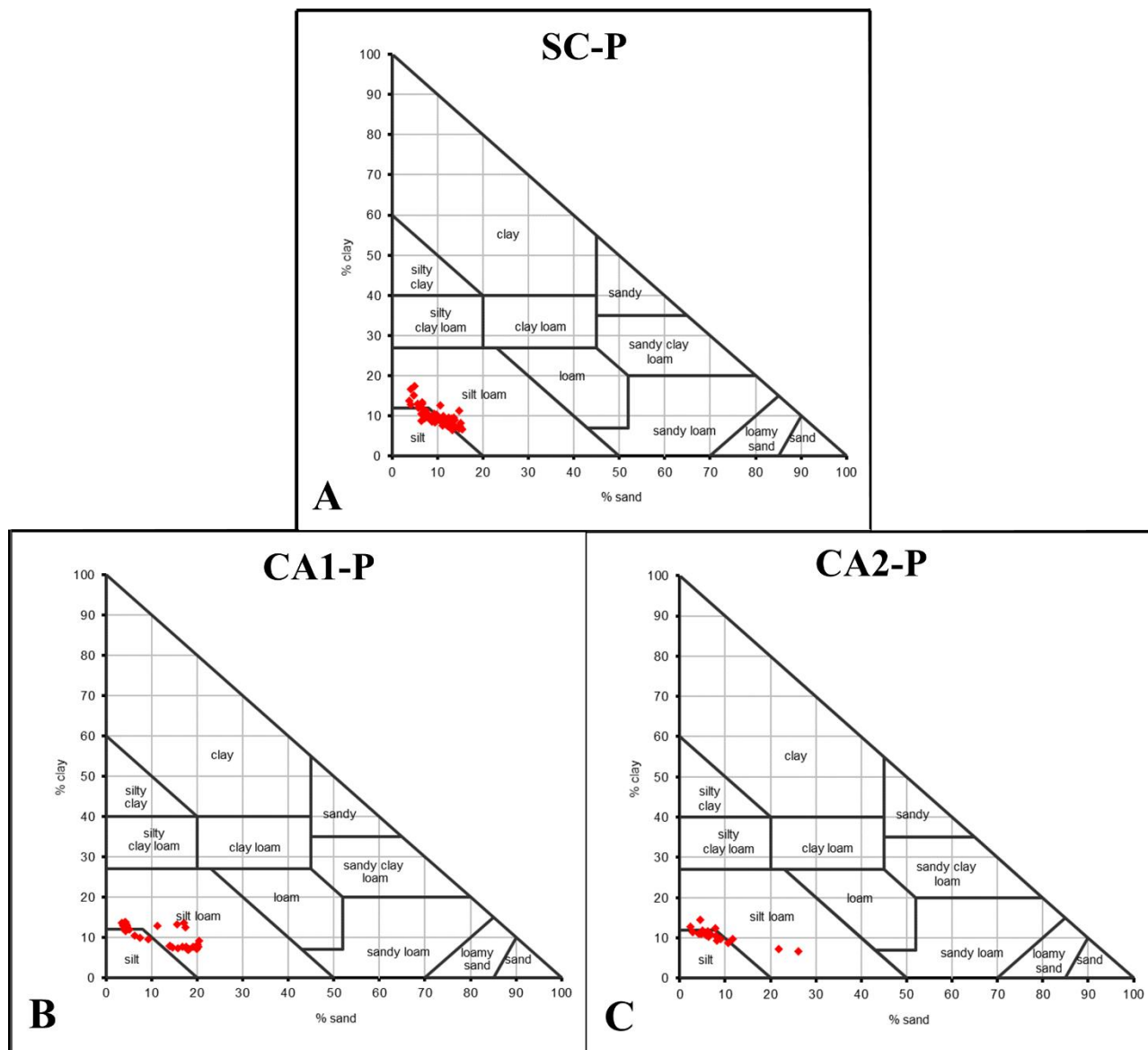
Figure 19 *Particle size class for playas based on a USDA texture triangle (Gerakis and Baer, 1999).*
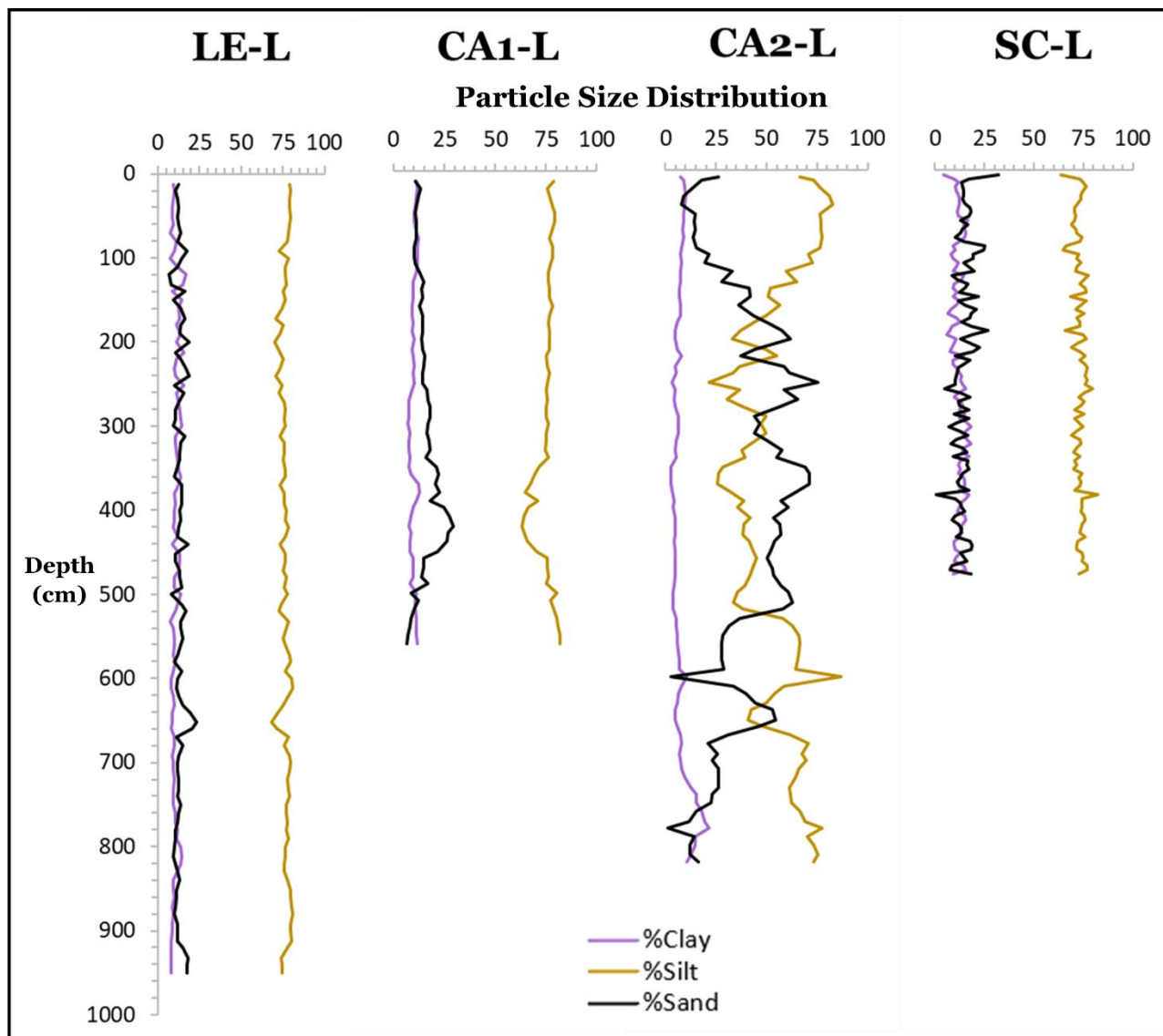
Figure 20 *Particle size distribution (percent sand, silt, and clay) plotted against depth for all lunette cores.*
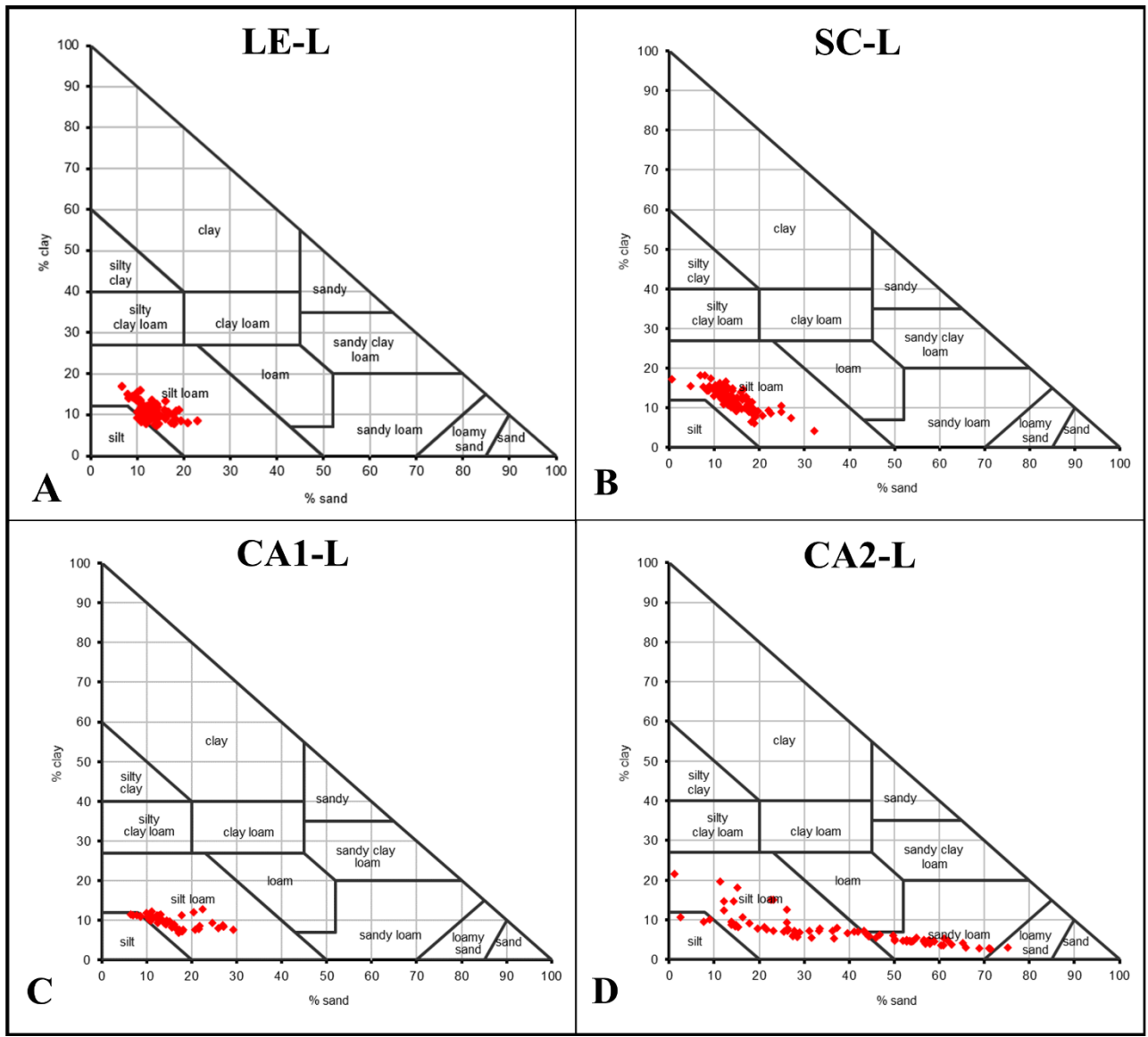
Figure 21 *Particle size class for lunettes based on a USDA texture triangle (Gerakis and Baer, 1999).*

Chapter 6 Discussion

1. Late Pleistocene (126 ka – 12.6 ka)

Regionally, the general climate during the late Pleistocene on the central Great Plains promoted C3 plant dominance associated with decreased summer precipitation correlated with diminished subtropical airflow (Feggestad et al., 2004). However, there was still high moisture availability and mesic conditions in the region (Woodburn et al., 2016). During cool and/or dry periods, glaciated and unglaciated landscapes were unstable and aeolian activity increased (Mason et al., 2007). Globally, the late Pleistocene is characterized by extreme glacial intervals, particularly in the earlier half (Pisias and Moore Jr, 1981).

Pre-LGM (~60 ka to ~25 ka)

Coring did not extend to the base of playas or lunettes, so it is difficult to discern when formation of these landforms began. Playa formation likely began at some point during marine isotope stage (MIS) 3 (~60-27 ka ago) when there was extreme climate variability associated with by Daansgard-Oeschger (D-O) events. D-O events are repeated decadal-scale warming events of 8-15°C (~14° to ~27°F) followed by century-scale cooling (Siddall et al., 2008). These abrupt oscillations in climate could have triggered PLS formation due to repeated periods of inundation and exposed floors. The main processes controlling playa formation are (1) carbonate dissolution and (2) the movement with descending groundwater of particulate organic material (Osterkamp and Wood, 1987). The dissolution of carbonates to form playas occurs when particulate organic material oxidizes in subsurfaces, releases carbon dioxide, which reacts with recharging ground water to form carbonic acid (Osterkamp and Wood, 1987). This carbonic acid dissolved the calcareous material in the Ogallala Formation. Playa initiation was dependent on

decaying vegetation which ensured a continuous supply of organic material to the subsurface decomposed to form carbonic acid and supported a positive feedback loop (Osterkamp and Wood, 1987). Therefore, when climate was moist and supporting C3 vegetation, dissolution occurred. When climate then abruptly alternated to warmer conditions, playas dried out, exposing the floors, and promoting deflation of accumulated sediment to form lunettes. CA1-L and CA2-L have several meters of sediment below our oldest radiocarbon age ($37,560 \pm 2,830$ cal YR BP), indicating they were likely on the landscape prior to this time. Therefore, playas may have formed as early as ~50,000 ka (or possibly earlier) with lunettes forming contemporaneously or immediately following initial playa formation.

Stable carbon isotope (δ^{13}C) data for playas are all generally very low (~-28‰ to ~-26‰), which suggests playa vegetation communities were composed of 94% to 100% C3 plants. Playas likely stored water regularly and for prolonged periods. Once playas formed via dissolution, they likely stored water regularly until at least ~28,000 ka ago, which continued to promote dissolution as the dominant geomorphic process. This is supported by playa stratigraphic records, all of which include the accumulation of carbonates and gleying in the lower portion of cores. While playas were storing water, wave action, driven by predominantly west/northwest winds, elongated playas. However, very little (~25 cm to ~1 m) of the pre-LGM record was captured in playa cores. This material is likely present in playas, but we were unable to core deep enough to capture it due to the abundance of heavy clays within the playas. Regional reports from Fredlund and Tieszen (1997) agree that playas in Kansas likely stored water regularly during this period. This supports my interpretation that dissolution was the dominant geomorphic process impacting my study playas. However, Bowen and Johnson (2012) report increased C4 contributions, pedogenesis, and very little water storage within playas during this period. They claim these

interpretations may have been impacted by inputs of SOC derived from playa vegetation and by the influence of near-surface groundwater on bench (between playa and lunette) plant communities (Bowen and Johnson, 2012).

δ^{13}C data for lunettes during this period are complex and highly oscillatory (~-24‰ to ~-14‰). These data indicate vegetation consisted of between 20% and 87% C4 plants (or 13% to 80% C3 plants). Reconstructed mean July temperature based on lunette δ^{13}C ranges between -13.8°C and -17.6°C (7.1°F and 0.2°F) cooler than present. This suggests that climate frequently experienced dramatic shifts in temperature and precipitation regimes. Although playas stored water regularly and supported C3 vegetation, climate oscillations reflected in lunette δ^{13}C data suggest there were times when playa floors were exposed, and deflated sediment from playas floors, as well as regional dust inputs, supplied sediment to lunettes. This is supported by lunette stratigraphy, which is complex, with ~1-10 cm thick intercalated clay-rich sediment layers and buried soils common. Several meter thick intervals of these stratified zones indicate that climate fluctuated repeatedly between approximately 45,000 to 26,000 ka, resulting in alternating periods dominated by regional aeolian deposition and by soil formation. Mason et al. (2007) reported increased regional sediment accumulation rates and/or decreased rates of pedogenic processes during this period, which supports the complex lunette stratigraphy at our study sites. Bowen and Johnson (2012) reported lunette δ^{13}C data that suggested the climate was relatively warm, with effective precipitation sufficient to promote pedogenesis. Fredlund (1995) reported mesic conditions on regional uplands. Globally, climate temperatures were much cooler than present, which initiated glacial advances, widespread aeolian transportation, and accumulation of loess (Welch and Hale, 1987).

LGM (25 - 19 ka)

Within playas, $\delta^{13}C$ data fluctuate frequently between -27‰ and -24‰, indicating playas were composed of 80% to 100% C3 plants. This suggests playas regularly stored water for prolonged periods. Playa stratigraphy for this period includes 3Ck, 2C, Cg, and C1 horizons, thick sequences of gleyed deposits, and accumulation of carbonates. This supports the hypothesis of a moist climate and frequent water storage with playas dominated by sediment delivery via overland flow, continued infiltration and dissolution, and lacustrine (i.e., wave action) geomorphic processes. Pollen analyses conducted by Karlstrom et al. (2008) indicate that spruce forest predominated in the cold climate of northeastern Kansas between ~23 ka and at least 15 ka. In Kansas, playas were storing water more frequently and/or for longer periods due to increased effective precipitation and cool temperatures (Bowen and Johnson, 2012). Bowen and Johnson (2012) also suggest that greater effective precipitation could have generated more runoff and delivered an increased sediment load to playas, similar to the thick stratigraphic units from this period observed in my study playas. This supports my interpretation of conditions for my study playas.

Generally, $\delta^{13}C$ data for lunettes during this period fluctuate between -21‰ to -16‰, excluding SC-L (-24‰ to -22‰). These intense fluctuations in lunette data suggest there were periods when up to 74% of vegetation communities were dominated by C4 plants and other periods when up to 80% were dominated by C3 plants. These differences in lunette vegetation communities indicate frequent alternating periods of cool/ moist and warm/dry conditions. Reconstructed mean July temperature based on lunette $\delta^{13}C$ ranges between -13.8°C and -16.8°C (7.1°F and 1.7°F) cooler than present. The dominant geomorphic process impacting lunettes during this period likely alternated between aeolian processes (sediment deposition via wind)

while climate was dry and pedogenesis when climate was moist. Lunettes (and the broader region) were likely experiencing infrequent pulses of loess/regional dust inputs as Rocky Mountain glaciers and the Laurentide ice sheet were advancing/retreating and meltwater was supplying pulses of sediment that were then transported by wind and deposited on lunettes. The fluctuations of dust/loess inputs and soil formation are due to moderately unstable conditions throughout the Great Plains/High Plains controlled by ice sheet activity. This is supported by lunette stratigraphy, which includes Cstrat horizons and well-developed buried soils. Regionally, climate on the Southern High Plains experienced intermittent drying and cool temperatures during the LGM (Rich, 2013). There is a notable lack of buried soils during this period, which suggests rapid deposition and/or unfavorable soil forming conditions (Welch and Hale, 1987). Globally, nearly all ice sheets had attained their maximum extents during the LGM, which corresponds with the low sea levels of the period and a general cooling trend (Clark et al., 2009). According to Bowen and Johnson (2012), PLSs evolved under a cooler climate, while effective precipitation was probably greater; however, temperature and moisture availability were highly variable, which is reflected in the complex stratified lunette stratigraphy at my study sites.

Post LGM (19 – 14.7 ka)

Playa $\delta^{13}C$ data fluctuate between ~-26‰ to ~-24‰, signifying 80% to 93% C3 plant dominance. This suggests that playas likely stored water frequently for prolonged periods. Stratigraphy for playas includes Cgk, Ck2, and C1 horizons with pale coloring, associated with gleying and water storage. Playas continued to be dominated by sediment delivery via overland flow, water storage, and infiltration as indicated by these thick sequences of gleyed deposits. Mollusk shells were collected from SC-P for this interval, indicating climate was moist and

playas stored water long enough to support semiaquatic life. Stratigraphic evidence from Bowen and Johnson (2012) indicates playa water levels were relatively high ca. 20 ka, and that from ca. 20 to 14.5 ka prevailing wind strength decreased. They also report $\delta^{13}C$ values indicative of ~95% C3 vegetation communities. These high water levels and wetland vegetation communities are reflective of our study and support our interpretation of frequent water storage.

$\delta^{13}C$ data for lunettes fluctuate between only -20‰ and -19‰, except SC-L, which fluctuates from ~-24‰ to -20‰. These values indicate vegetation communities were composed of between 20% and 53% C4 plants, indicating more mixed C3-C4 plant communities compared to preceding intervals. Reconstructed mean July temperature based on lunette $\delta^{13}C$ ranges between -14.6°C and -15.7°C (5.8 °F and 3.7 °F) cooler than present. This suggests that climate was stabilizing and shifts in vegetation communities and temperature were becoming smaller. Stratigraphy for lunettes includes C and Cstrat horizons with alternating brown and pale brown layers. The several-meter thick units in lunettes suggest landscapes were stabilizing and climate supported alternating rates of pedogenesis. Regionally, climate on the High Plains was cool with lower evaporation rates, increased effective moisture, and greater humidity (Rich, 2013). C3 vegetation was dominant in the mid-latitude regions of the Great Plains during this time (Muhs et al., 1999). Globally, C3 vegetation dominance was associated with decreased summer precipitation due to diminished subtropical airflow (Cordova et al., 2011). The C3 dominance reported in these studies is not reflective of the combination of C3 and C4 plants in my study lunettes. However, these reports do support the interpretation of decreasing temperature and increasing land stability.

2. Pleistocene-Holocene Transition (14.7 – 11.7 ka)

δ^{13}C for the Pleistocene-Holocene transition (PHT) at LE-P displays a very distinct trend, with values increasing from ~-27‰ to ~-20‰. As previously noted, LE-P and the associated watershed morphology differ from other sites. The increased watershed circularity at LE-P means that runoff has a much shorter distance to travel. Given that the LE watershed is relatively small compared to playa size, it cannot contribute as much overland flow as the other sites. Therefore, LE-P likely stored water less often and for shorter durations during mesic to arid conditions. This allowed upland grasses to establish on playa floors and promote soil development, which shifted isotopic values to less negative compared to the other sites. δ^{13}C data for LE-P suggest playa vegetation shift from exclusively C3 plants to a nearly even combination of C3 and C4 plants, which reflects a transition from consistently storing water to seasonally storing water. δ^{13}C data for all other playas fluctuate around ~-24‰, indicating playa plant communities were composed of ~80% C3 vegetation and likely stored water for prolonged periods. Playa stratigraphy includes C1, Ck2, and thick Cgk horizons with colors ranging from light yellowish-brown, pale brown to light gray. The distinct presence of carbonates and occasional gleying supports the interpretation that playas were often moist enough to store water. Sediment delivery via overland flow, water storage, and infiltration were likely the dominant processes occurring within these playas. Regionally, the climate alternated between prolonged phases of sediment deposition and brief phases of non-deposition and pedogenesis, with relatively rapid fluctuations between wet and dry conditions within playas (Holliday, 1997). Bowen and Johnson (2015) report δ^{13}C data from playa centers in western Kansas that indicate the climate was sufficiently moist to support the expansion of C3 wetland vegetation (Bowen and Johnson, 2015). However, they also reported an increase in δ^{13}C values throughout the period, which indicates that C4 plants expanded as the climate became warmer and/or drier. They

suggest that aeolian and fluvial deposition was relatively slow and lacustrine processes would have been temporary, which at least partially supports my interpretation that these playas stored water for long enough to gley occasionally.

Lunette $\delta^{13}C$ data fluctuate between -22‰ and -18‰, which indicates nearly equal contributions from C3 and C4 plants with slight shifts in C3 and C4 plant abundance as the climate alternated between slightly moister/cooler and slightly drier/warmer. Reconstructed mean July temperature based on $\delta^{13}C$ was between -14.6°C and -16.1°C (5.8°F and 3.0°F) cooler than present. Stratigraphy for lunettes includes C and Cstrat horizons with alternating brown and pale brown layers. The thick stratified units found in lunettes suggest that the landscape of the High Plains was only partially stable while environmental conditions fluctuated between periods of regional dust deposition and periods of soil formation. These fluctuations may have been influenced by the Bølling-Allerød (B-A; 14.7–12.9 cal ka) or Younger Dryas (YD; 12.9–11.7 cal ka). The central Great Plains experienced similar drying and warming trends to the rest of the world during this period, as identified in upload soil exposures in Nebraska (Woodburn et al., 2016). The loess-paleosol sequences found in the central and northern Great Plains indicate a broad peak of high effective moisture across the PHT, rather than well-defined climatic episodes corresponding to the Bølling-Allerød and Younger Dryas (Mason et al., 2008). Globally, the PHT is characterized by rapid warming at the beginning of the period followed by several decades of warming (Pillans and Naish, 2004). According to Bowen and Johnson (2012), temperature increased during the PHT, while effective precipitation probably decreased; however, precipitation remained great enough to support dense vegetative cover that stabilized the landscape and promoted pedogenesis. During periods of increased temperatures/decreased moisture, playas likely dried out for longer periods and provided sediment to lunettes. During

periods of decreased temperatures/increased moisture, playas likely stored water for longer periods. This enhanced moisture promoted pedogenesis on the lunettes. The slight shifts in plant communities and climate resulted in the thick sequences of sediment and incipient soils that dominated this interval in the soil-sediment cores.

3. Holocene (11.7 ka to present)

Regionally, the Holocene epoch commonly experienced prolonged droughts resulting in increased aeolian activity in the Great Plains (Jacobs and Mason, 2004). Playas were frequently subaerially exposed during this period due to arid to mesic conditions (Bowen and Johnson, 2015). Globally, the Holocene is characterized by a general warming trend from the PHT that was interrupted by 8 to 10 brief multi-decadal- to century-scale cold relapses with highly variable precipitation patterns (Wanner et al., 2014). Generally, the Holocene was dominated by soil formation for both playas and lunettes and buried soils are common. Playas had sufficient moisture to support wetland vegetation but had to be subaerially exposed for prolonged periods to support pedogenesis (Bowen and Johnson, 2012).

Early Holocene (11.7 - 8.2 ka)

$\delta^{13}C$ data for playas range from ~-24‰ to ~-21‰, which indicates C3 plants composed between 60-80% of vegetation communities during this period. These data suggest there was enough effective precipitation for playas to store water seasonally and support wetland vegetation. Playa stratigraphy for this period includes BC, Ck1, and Cgk, horizons with colors ranging from white, light gray to light yellowish-brown. The continuity of stratigraphy among sites and the presence of gleying and accumulation of carbonates all indicate that playas

experienced significant infiltration and translocation of carbonates between ~10,800 and ~8,300 ka ago. However, climate reconstructions from other playas in western Kansas indicate conditions transitioned from mesic to arid, and aeolian processes were dominant within playas (Bowen and Johnson, 2015). Prior studies have indicated declined trends in $\delta^{13}C$ in the central Great Plains, which was likely due to increases in drought tolerant C3 weeds in response to increased aridity and landscape instability (Bowen and Johnson, 2015; Miao et al., 2007; Feggestad et al., 2004; Mason et al., 2003; Johnson and Willey, 2000). Feggestad et al. (2004) attributed a decline in $\delta^{13}C$ in the early Holocene to increases in herbaceous C3 annuals better suited to disturbance and high rates of sediment accumulation. Bowen and Johnson (2012) report playas were predominantly influenced by regional aeolian processes with relatively high rates of loess inputs via air fall on a subaerially exposed playa floor. It is unclear why environmental conditions within the study playas appears out of phase with other playas and regional climate. Lack of more precise age control for stratigraphic units due to a dearth of dateable material may have resulted in the incorrect attribution of middle Holocene environmental conditions to the early Holocene.

Lunette $\delta^{13}C$ data for this period range from -20‰ to -15‰, which indicates a mix of C3 and C4 vegetation to C4 dominated plant communities (46% to 80% C4). Reconstructed mean July temperature based on $\delta^{13}C$ was ~2-3°C (~35-37°F) cooler than present at the beginning of the interval and increased to temperatures similar to modern. Lunette stratigraphy during the early Holocene is truncated and over-printed by later soil development that weathered sediment into Bt and BC horizons ranging in color from brown, grayish brown, to pale brown. Well-developed Bt horizons suggest there was a period of stability to support pedogenesis, which may have occurred near the end of early Holocene and into the middle Holocene. Overall, aeolian

processes likely dominated the region during this time. Globally, the early Holocene climate experienced progressive warming, especially in the Northern Hemisphere (Wanner et al., 2014). In Kansas, this period was characterized by periodic droughts that destabilized the landscape and resulted in high sediment accumulation rates (Arbogast, 1996). In Bowen and Johnson (2012), $\delta^{13}C$ data indicate that the early Holocene was characterized by increased temperatures and C4 plant composition due to continued increasing temperatures and decreasing effective precipitation.

Middle Holocene (8.2 - 4.2 ka)

Within playas, $\delta^{13}C$ data were ~-24‰, excluding LE-P (~-20‰), indicating ~80% C3 plant composition. Playas likely stored water regularly and for prolonged periods, while LE-P, with a relatively small and circular watershed was dry more often due to less water delivery to the playa. During the middle Holocene, playas would have been subaerially exposed most of the year, allowing for pedogenesis, but seasonally inundated to promote gleying. Playa stratigraphy includes thick Bt and Cgk horizons with grayish gleyed soils and an accumulation of silicate clays and carbonates. This indicates water was being stored at least seasonally by ~7,000 ka ago. Playa SC-P experienced enhanced pedogenesis and preserves a well-developed buried soil (Ab Bb) from this period. Regionally, pedogenesis was enhanced in Kansas playas (likely because of decreased precipitation variability rather than increased precipitation) (Bowen and Johnson, 2015). Enhanced pedogenesis occurred within my study playas, as indicated by the presence of thick, well-developed Bt horizons and buried soil (Bb).

Lunette $\delta^{13}C$ data generally increases (~-20‰ and ~-16‰) towards the surface, however, there are small fluctuations throughout. This suggests C4 plants initially comprised ~50% of

plant communities and then increased to ~75%. Reconstructed mean July temperatures from lunettes are similar to present. Regional climate likely had distinct seasons based on the small fluctuations in $\delta^{13}C$ data but was generally warm and/or dry based on increased C4 plant composition. Climate was cool/moist at the beginning of this period, C3 plants were dominant, and lunettes experienced enhanced pedogenesis. Climate became drier, temperature increased, and C4 plant dominance increased towards the end of this period. Lunette stratigraphy includes Bt, CB, and Cstrat horizons ranging between pale brown and brown coloring. This stratigraphy can be interpreted as decreased aeolian activity and enhanced pedogenesis during ~5,000 ka ago, resulting in well-developed soils. C4 plant expansion has been documented throughout the Great Plains (Leavitt et al., 2007; Nordt et al., 2007). Global climate during the middle Holocene is classified as warm, especially in the Northern Hemisphere, and thus has been named the "Holocene Thermal Maximum" or "Mid-Holocene Thermal Maximum" (Wanner et al., 2014; Charpentier Ljungqvist, 2011). Precipitation variability decreased or timing may have shifted during the middle Holocene such that more precipitation was delivered during the peak summer growing season for grasses, which would have increased plant productivity that stabilized the landscape, reduced sediment deposition, and allowed C4 grasses to expand relative to C3 vegetation (Bowen and Johnson, 2015). Skinner et al. (2002) observed that reduced rainfall variability during the summer growing season resulted in greater C4 productivity, while C3 productivity was relatively unaffected. These reports are all in agreement with my interpretation of lunette data, which suggests landscape stability, enhanced pedogenesis, and distinct seasons.

Late Holocene (4.2 ka to present)

Globally, the Late Holocene exhibited distinct fluctuations in climate. The Medieval Warm Period (MWP) was a time of warm climate in the North Atlantic region that lasted from 950 CE to 1250 CE. The Little Ice Age (LIA) was a period of regional cooling, particularly pronounced in the North Atlantic region, that occurred between 1350 CE and 1850 CE (Wanner et al., 2008). The LIA is characterized by lower summer insolation in the Northern Hemisphere due to orbital forcing and coincided with solar activity minima and several strong tropical volcanic eruptions (Wanner et al., 2008). Global climate during the late Holocene is classified as cool overall apart from the warmer modern Industrial Era (1760 – 1840) (Wanner et al., 2014).

δ^{13}C data from SC-P display a sharp increase from ~-22‰ to ~-18‰, indicating a significant shift from ~67% C3 plant composition to ~60% C4 plant composition. This suggests this playa stopped regularly storing water within a short span of time (~1,400 yr to ~1,000 yr). Excluding this playa, δ^{13}C data during this period range from ~-22‰ to ~-20‰, indicating there was a mix of C3 and C4 vegetation within playas. This combination may be due to either a warming climate and drought tolerant C3 weeds or strong seasonal inundation. Playas during the late Holocene are dominated by well-developed soils, with SC-P having a distinct late Holocene-aged buried soil. Playa stratigraphy includes very dark gray, dark gray, to dark grayish brown A, Ab, and Bg horizons. The grayish color coincides with strong gleying, suggesting playas were likely seasonally inundated but were primarily subaerially exposed to promote pedogenesis. Regionally, mesic conditions continued from the mid-Holocene and fluvial processes were enhanced in Kansas playas (Bowen and Johnson, 2015). Effective precipitation increased and playa water levels were higher than in prior periods, but still fluctuated considerably (Bowen, 2011). Several small-scale fluctuations in climate throughout the late Holocene may have impacted playa ecosystem functions, yet playas likely functioned like today (Bowen and

Johnson, 2015). My interpretation of seasonal inundation in playas is supported by these reports of small-scale climate fluctuations, which allowed for periods of pedogenesis and water storage based on the presence of both buried soils and gleying.

Lunette $\delta^{13}C$ data generally increases towards the surface (~-20‰ to ~-14‰), indicating 47% to 87% C4 vegetation and warming and/or drying regional climate. Reconstructed mean July temperatures are similar to present. Lunettes during the late Holocene were also dominated by pedogenesis and the formation of well-developed soils. Lunette stratigraphy includes A, AB, B, and Bt horizons with colors ranging from very dark brown, dark grayish brown to pale brown. There is evidence throughout the central Great Plains that suggests a more humid climate with lower sediment accumulation rates and greater pedogenic imprinting compared with the middle Holocene (Jacobs and Mason, 2004; Mason et al., 2003). Arbogast (1996) reports that Wilson Ridge lunette, in western Kansas, was largely stable, and influenced by warm and dry local climate as indicated by relatively high $\delta^{13}C$ values. These reports support my interpretation of a stable landscape undergoing warming and/or drying climate.

Chapter 7 Conclusion

In this study, I 1) collected soil-sediment cores from four playa-lunette systems, described and analyzed their stratigraphic units; (2) determined the age of stratigraphic units using 14C dating techniques; and (3) reconstructed paleoenvironmental conditions (i.e., regional climate, playa hydrology, and PLS vegetation communities) and geomorphic processes using stable carbon isotope and particle size distribution data. I hypothesized that playa-lunette systems began forming during the late Pleistocene with playa formation occurring via dissolution during wet periods followed by deflation of sediment from playa floors and accumulation immediately downwind (along with regional dust inputs) to form the lunettes during arid periods. This hypothesis on the timing for PLS formation is supported by the fact that there are several meters of sediment underneath our oldest radiocarbon ages of ~37,000 ka. This suggests that playa on the Central High Plains may have formed as early as ~50,000 ka with lunettes forming contemporaneously or immediately following initial playa formation.

Pre-LGM
- Playas stored water regularly and promoted dissolution as the dominant geomorphic process
- Lunettes underwent alternating periods dominated by regional aeolian deposition and by soil formation.
- Climate was similar to modern conditions, though temperature fluctuated by several degrees over several decade to century scales; precipitation also likely experienced extreme shifts over similar timescales

LGM
- Playas stored water frequently and promoted dissolution and fluvial and lacustrine (i.e., wave-action) geomorphic processes and sediment accumulation

- Lunettes were influenced by meltwater from Rocky Mountain glaciers and the Laurentide Ice Sheet supplying pulses of sediment that were then transported and deposited by aeolian processes

- Climate was cooler and wetter than modern condition with slight oscillations (i.e., 0.5-1.0° C) common over decadal to century scales, resulting in infrequent pulses of loess/regional dust as glaciers were advancing/retreating

Post-LGM

- Playas likely stored water frequently for prolonged periods and were dominated by dissolution, fluvial/lacustrine geomorphic processes, and sediment accumulation

- Lunettes experienced enhanced pedogenesis

- Climate was stabilizing and warming following the LGM and shifts in both δ^{13}C and temperature were becoming smaller

P-H Transition

- Playas likely still stored water for prolonged periods, so dissolution and fluvial/lacustrine processes were likely dominant, but frequency and duration of inundation were likely declining

- Lunettes were influenced by fluctuations in aeolian activity (deflated playa sediment and regional dust deposition) and periods of pedogenesis

- Climate alternated between slightly moister and/or cooler and slightly drier and/or warmer

Early Holocene

- Playas were primarily subaerial exposed but effective precipitation was sufficient to allow playas store water seasonally; fluvial/lacustrine processes continued to influence playas, but aeolian deflation was also an important geomorphic process when playas were dry

- The early Holocene is poorly preserved in lunettes, suggesting they were sparsely vegetated and unstable

- Climate began a distinct warming (and drying) trend that continued throughout much of the Holocene

Middle Holocene

- Playas likely stored water seasonally with pedogenesis occurring at several sites

- Lunettes received minor inputs from aeolian deposition and experienced enhanced pedogenesis

- Climate likely had distinct seasons but was generally dominated by a warming and/or drying trend

Late Holocene

- Playas were likely seasonally inundated but were primarily subaerially exposed to promote pedogenesis

- Lunettes were dominated by pedogenesis

- Climate continued a warming and/or drying trend and conditions were similar to modern for much of the late Holocene

7.1 Significance of Study

The scientific community specifically involved in PLS research is relatively small despite the importance of these landforms. From the few playa, lunette, and PLS experts, hypotheses have been proposed concerning their formation and geomorphic evolution. Deflation hypotheses suggest initial playa formation may have begun with the collection of water in a small depression, which is then elongated by wave action (Reeves, 1966). Dissolution hypotheses suggest that underlying carbonate or evaporite beds form voids where there are fluctuations of a high-water table which then subside, creating the depression that evolves into a playa (Wood et al., 1992). Vance Holliday has published extensively on this issue (2001, 2000, 1997, 1996). Arbogast (1996) and Bowen and Johnson (2017, 2015, 2012) examined PLSs in Kansas and reconstructed regional environmental conditions and geomorphic processes for playas on the Central High Plains. Rich (2013) has published important data regarding lunette formation and evolution on the SHP. The data I produced in this study complement these data and help validate prior hypotheses regarding PLS formation and evolution. Importantly, we provided new radiocarbon ages that indicate PLSs were integral features of the High Plains as early as ~40,000

ka (pre-LGM) and possibly much earlier. My research contributes to our understanding of the timing and magnitude of PLS formation and evolution and the environmental conditions and geomorphic processes controlling these systems.

A key goal in most climate (or paleoclimate) research is to gain an understanding of how climate has changed in the past, is changing now, and will change in the future. In regard to my research, paleoclimate proxy data including particle size and stable carbon isotopes were generated. These data can be used in models that produce climate reconstructions for the Great Plains such as those from Modala et al. (2017), McIntrye et al. (2014), Liu et al. (2013), Islam et al. (2012), Ko et al. (2012), among others or in larger scale predictions like that of the UN's Intergovernmental Panel on Climate Change (IPCC). There is a notable lack of long-term records on the High Plains, so PLSs represent an important yet underutilized record of environmental change. By providing a unique but complementary record of past climate, we can more easily predict how future climate will impact the people, economies, water resources, landforms and landscapes, and way of life on the High Plains. This semi-arid agriculturally dominated region is particularly sensitive to the impacts of climate change, so providing a more robust understanding of potential effects of climate change on this region is essential.

In addition to contributing to our understanding of climate change and the potential impacts to the High Plains, my research is directly relevant to people living in the region and beyond due to the importance of the ecological functions playas provide and the role of the High Plains in feeding the world. Playas provide a wide range of essential ecological functions such as groundwater recharge, surface water storage, wetland habitat, plant biomass storage and carbon sequestration, biodiversity, flood mitigation, sediment and pollutant filtering, and nutrient cycling (Smith et al., 2011; Smith, 2003). Playas on the High Plains have shrink-swell clay floors

that store water and provide recharge to the Ogallala (High Plains) Aquifer. The primary function of this massive aquifer is to provide irrigation water for this agriculturally dominated landscape of the central US. However, it also provides drinking water to a small population of people (primarily involved in agriculture) distributed over a large area, and provides an important source to wildlife where it returns to the surface via springs and seeps. Another key function playas provide is improving water quality by nutrient and pesticide removal via wetland plants (and other aquatic organisms) and sediment trapping (Howell et al., 2019). If it were not for playas recharging the aquifer and improving water quality, groundwater levels would have declined even more rapidly and the aquifer would be impaired by excess nutrients and pesticides from infiltrating waters, which would result in disaster for the people and economies that rely on a clean and functioning aquifer. Playas provide habitat for waterfowl (including millions of migrating birds), small mammals, and aquatic/semi aquatic life, which increases biodiversity by over 300% compared to similar areas of short-grass prairie not containing a playa (Smith, 2003). Thus, playas support biodiversity at local to continental scales. Landowners that have playas on their property can lease land to hunters (primarily for waterfowl) at an average rate of ~$10 per acre, which provides important supplemental income for landowners and recreational opportunities for the public (Brockus, 2016). This is particularly important on the High Plains, where most of the land is privately owned. In fact, in Kansas, Nebraska, Oklahoma, and Texas 95% to 98% of land is privately owned (US Bureau of the Census, 1991). Aside from these tangible benefits, playas are important for aesthetic purposes. Their presence serves as an oasis in the vast sea of agricultural lands by breaking up the visual monotony and increasing the presence and diversity of plants and animals in the region.

PLSs were ideal camping grounds for ancient native communities since they provided water, shelter, important plant resources, and ample hunting ground. In fact, the use of playas and lunettes by native peoples has been documented throughout the High Plains, including Paleoindian sites in New Mexico (Hill et al., 1995), Texas (Litwinionek et al., 2003; Holliday, 1997), Oklahoma (LaBelle et al., 2003), Colorado (Stanford, 1979), and Kansas (Mandel and Hofman, 2003; Witty, 1989). A study by Witty (1989) identified an archeological site associated with a lunette in Lane County, Kansas that preserved a continuous record of lithic artifacts (i.e., arrowheads, spear points, etc.) from Paleoindian (i.e., Clovis; ~13-11 ka) to the Historic Period (i.e., 1600-1700 AD) and contained worked mammoth (*Mammuthus*, species unknown), ancient bison (*Bison antiquus*), the American horse (*Equus scotti*), and North American camel (*Camelops*, species unknown). This suggests that PLSs can serve as critical archaeological sites since they may preserve evidence of occupation extending over several thousand years, including preserving evidence of the earliest known cultures in the Americas. Thus, there is potential to improve our understanding of the peopling of the Americas (i.e., determining when humans entered and spread throughout the Americas) by utilizing archaeological records preserved in PLSs.

One of my passions is to share and communicate science in a way that is approachable enough for the general public to understand and have interest in. If this research can help scientists understand the importance of PLSs, hopefully they can convey this message to farmers who can then help spread this information throughout their communities. When the communities living on the High Plains understand the conditions needed for PLS development and evolution and the importance of maintaining healthy, functioning playas, they may be more inclined to

adapt their farming practices to help conserve these essential resources. Writing a master's thesis may not be enough to do that, but by contributing to a growing body of knowledge it may help.

7.2 Future Work

Debatably the most exciting outcome of this study are the data showing PLS were an integral part of the High Plains landscape for more than 40,000 years (i.e., potentially pre-dating the last glacial period). In the future, it may be beneficial to core these sites, or comparable sites, to further depths to reach the base of these features and the contact with underlying material to determine precisely when these features appeared on the landscape. It may be necessary to use additional forms of age control, such as optically stimulated luminescence dating (OSL) because these features may extend beyond the timeframe of radiocarbon dating (i.e., >50,000 years) and may not contain suitable material (i.e., carbon) for radiocarbon dating. Utilizing additional proxy records, such as magnetic susceptibility, phytoliths, fossil pollen, and aquatic invertebrate (i.e., mollusk and gastropod shells) would provide greater insight and potentially lines of converging evidence regarding environmental conditions within and surrounding PLSs. Finally, incorporating GIS modelling at these sites, particularly using high-resolution LiDAR topographic data, could provide insight into rainfall-runoff relationships to better understand how changes to environmental conditions (i.e., climate and vegetation patterns) directly affects playa hydrology.

References

Arbogast, A.F., 1996. Late Quaternary Evolution of a Lunette in the Central Great Plains: Wilson Ridge, Kansas. Physical Geography 17, 354–370.

Bowen, M.W., 2011. Spatial distribution and geomorphic evolution of playa-lunette systems on the central High Plains of Kansas (Doctoral Dissertation). University of Kansas, Lawrence, Kansas, USA.

Bowen, M.W., Johnson, W.C., 2019. Sediment accumulation and sedimentation rates in playas on the High Plains of western Kansas, USA. Geomorphology 342, 117–126.

Bowen, M.W., Johnson, W.C., 2017. Anthropogenically accelerated sediment accumulation within playa wetlands as a result of land cover change on the High Plains of the central United States. Geomorphology 294, 135–145.

Bowen, M.W., Johnson, W.C., 2015. Holocene records of environmental change in High Plains playa wetlands, Kansas, US. The Holocene 25, 1838–1851.

Bowen, M.W., Johnson, W.C., 2012. Late Quaternary environmental reconstructions of playa-lunette system evolution on the central High Plains of Kansas, United States. Geological Society of America Bulletin 124, 146–161. https://doi.org/10.1130/b30382.1

Bowen, M.W., Johnson, W.C., 2011. Lunette Distribution on the High Plains of Kansas—A Guide to Seeking Paleoindian Sites. Current Research in the Pleistocene 28, 129–131.

Bowen, M.W., Johnson, W.C., King, D.A., 2018. Spatial distribution and geomorphology of lunette dunes on the High Plains of Western Kansas: implications for geoarchaeological and paleoenvironmental research. Physical Geography 39, 21–37.

Bowen, M.W., Johnson, W.C., Klopfenstein, S.T., Dunham, J.W., 2009. Developing a Geospatial Database of Playas within the High Plains of Kansas. Current Research in the Pleistocene 26, 191–193.

Briere, P.R., 2000. Playa, playa lake, sabkha: Proposed definitions for old terms. Journal of Arid Environments 45, 1–7.

Brockus, K., 2016. 2016 River Valley Extension Lease Survey Summary.

Brostoff, W., Lichvar, R., Sprecher, S., 2001. Deliniating Playas in the Arid Southwest - A Literature Review. Engineer Research and Development Center TR-01-4.

Buchanan, R., McCauley, J.R., 2010. Roadside Kansas: A Traveler's Guide to its Geology and Landmarks: Lawrence, Kansas.

Buchanan, R.C., Wilson, B.B., Buddemeier, R.R., Bulter, J.J.J., 2015. The High Plains aquifer: Kansas Geological Society. Public Information CIrcular 18, 6.

Charpentier Ljungqvist, F., 2011. The spatio-temporal pattern of the mid-Holocene thermal maximum. Geografie–Sborník ČGS 116, 91–110.

Clark, P.U., Dyke, A.S., Shakun, J.D., Carlson, A.E., Clark, J., Wohlfarth, B., Mitrovica, J.X., Hostetler, S.W., McCabe, A.M., 2009. The Last Glacial Maximum. Science, New Series 325, 710–714.

Cooke, R., Warren, A., Goudie, A., 1993. Desert Geomorphology. UCL Press, London.

Cordova, C.E., Johnson, W.C., Mandel, R.D., Palmer, M.W., 2011. Late Quaternary environmental change inferred from phytoliths and other soil-related proxies: case studies from the central and southern Great Plains, USA. Catena 85, 87–108.

Fairbanks, R.G., Mortlock, R.A., Chiu, T.C., Cao, L., Kaplan, A., Guilderson, T.P., Fairbanks, T.W., Bloom, A.L., Grootes, P.M., Nadeau, M.J., 2005. Radiocarbon Calibration Curve Spanning 0 to 50,000 Years BP Based on Paired 230Th/234U/238U and 14C dates on Pristine Corals. Quaternary Science Reviews 24, 1781–1796.

Feggestad, A.J., Jacobs, P.M., Miao, X., Mason, J.A., 2004. Stable carbon isotope record of Holocene environmental change in the Central Great Plains. Physical Geography 25, 170–190.

Feng, Z.-D., Johnson, W.C., Sprowl, D.R., Lu, Y., 1994. Loess accumulation and soil formation in central Kansas, United States, during the past 400,000 years. Earth Surface Processes and Landforms 19, 55–67.

Fenneman, N.M., 1931. Physiography of Western United States. McGraw-Hill, New York, NY, USA.

Fish, E.B., Atidnson, E.L., Shanks, C.H., Brenton, C.M., Mollhagen, T.R., 1998. Playa lakes digital database for the Texas portion of the Playa Lakes Joint Venture Region. CD-ROM with maps, data and manuscript.

Fredlund, G.G., 1995. Late Quaternary Pollen Record from Cheyenne Bottoms, Kansas. Quaternary Res 43, 67–79.

Fredlund, G.G., Tieszen, L.T., 1997. Calibrating grass phytolith assemblages in climatic terms: Application to late Pleistocene assemblages from Kansas and Nebraska. Palaeogeography, Palaeoclimatology, Palaeoecology 136, 199–211.

Frye, J.C., Leonard, A.B., 1951. Stratigraphy of the Late Pleistocene Loesses of Kansas. The Journal of Geology 59, 287–305.

Gerakis, A., Baer, B., 1999. A computer program for soil textural classification [WWW Document]. URL https://nowlin.css.msu.edu/software/triangle_form.html (accessed 1.17.21).

Gibbard, P., Head, M., J.C., W., Alloway, B., Beu, A., Coltorti, M., V.M., H., J., L., Knudsen, K., Kolfschoten, T., T., L., Marks, L., J., M., T.C., P., Piotrowski, J., Pillans, B., Rousseau, D.-D., Suc, J.-P., Tesakov, A., Turner, C., 2010. Formal ratification of the Quaternary System/Period and the Pleistocene Series/Epoch with a base at 2.58 Ma. Journal of Quaternary Science 25, 96–102. https://doi.org/10.1002/jqs.1338

Gilbert, G.K., 1895. Lake Basins Created by Wind. The Journal of Geology 3, 47–49.

Gurdak, J.J., Roe, C.D., 2009. Recharge rates and chemistry beneath playas of the High Plains Aquifer - A literature review and synthesis (No. Circular 1333). U.S. Department of the Interior, Geological Survey, Reston, VA, USA.

Gustavson, T., Holliday, V., Hovorka, S., 1995. Origin and development of playa basins, sources of recharge to the Ogallala aquifer, Southern High Plains, Texas and New Mexico. University of Texas Bureau of Economic Geology Report of Investigations 229 44.

Gustavson, T.C., Holliday, V.T., Hovorka, S.D., 1994. Development of playa basins, Southern High Plains, Texas and New Mexico. Presented at the Proceedings of the playa basin symposium. Water Resources Center, Texas Tech University, Lubbock, pp. 5–14.

High Plains Regional Climate Center, 2020. High Plains Regional Climate Center [Online] [WWW Document]. URL http://www.hprcc.unl.edu (accessed 11.2.20).

Hill, M.G., Holliday, V.T., Stanford, D.J., 1995. A further evaluation of the San Jon site, New Mexico. The Plains Anthropologist 369–390.

Holliday, V.T., 2001. Stratigraphy and geochronology of upper Quaternary eolian sand on the Southern High Plains of Texas and New Mexico, United States. Geological Society of America Bulletin 113, 88–108.

Holliday, V.T., 2000. Folsom drought and episodic drying on the Southern High Plains from 10,900-10,200 C-14 yr BP. Quaternary Research 53, 1–12.

Holliday, V.T., 1997. Origin and Evolution of Lunettes on the High Plains of Texas and New Mexico. Quaternary Research 47, 54–69.

Holliday, V.T., 1996. Lithostratigraphy and geochronology of fills in small playa basins on the Southern High Plains, United States. Geological Society of America Bulletin 13.

Holliday, V.T., Hovorka, S.D., Gustavson, T.C., 1996. Lithostratigraphy and Geochronology of Fills in Small Playa Basins on the Southern High Plains, United States. Geological Society of America Bulletin 108, 953–956.

Holliday, V.T., Mayer, J.H., Fredlund, G.G., 2008. Late Quaternary sedimentology and geochronology of small playas on the Southern High Plains, Texas and New Mexico, U.S.A. Quaternary Research 70, 11–25.

Holliday, V.T., Meltzer, D.J., Mandel, R., 2011. Stratigraphy of the Younger Dryas Chronozone and paleoenvironmental implications: Central and Southern Great Plains. Quaternary International 242, 520–533. https://doi.org/10.1016/j.quaint.2011.03.047

Howell, N.L., Butler, E.B., Guerrero, B., 2019. Water quality variation with storm runoff and evaporation in playa wetlands. Science of The Total Environment 652, 583–592.

Islam, A., Ahuja, L.R., Garcia, L.A., Ma, L., Saseendran, A.S., Trout, T.J., 2012. Modeling the impacts of climate change on irrigated corn production in the Central Great Plains. Agricultural water management 110, 94–108.

Jacobs, P.M., Mason, J.A., 2007. Late Quaternary climate change, loess sedimentation, and soil profile development in the central Great Plains: A pedosedimentary model. Geological Society of America Bulletin 119, 462–475.

Jacobs, P.M., Mason, J.A., 2004. Paleopedology of soils in thick Holocene loess, Nebraska, USA. Revista Mexicana de Ciencias Geológicas 21, 54–70.

Johnson, W.C., Willey, K.L., 2000. Isotopic and Rock Magnetic Expression of Environmental Change at the Pleistocene-Holocene Transition in the Central Great Plains. Quaternary International 67, 89–106.

Johnson, W.C., Willey, K.L., Mason, J.A., May, D.W., 2007. Stratigraphy and Environmental Reconstruction at the Middle Wisconsinan Gilman Canyon Formation Type Locality, Buzzard's Roost, Southwestern Nebraska, USA. Quaternary Research 67, 474–486.

Kansas Biological Society, 2017. Kansas Land Cover Maps [WWW Document]. Kars.ku.edu. URL http://kars.ku.edu/agol-maps/kansaslandcover/ (accessed 1.17.21).

Kansas Department of Agriculture, 2019. Kansas Farm Facts.

Kansas State University, 2020. Kansas Climate [WWW Document]. URL https://climate.k-state.edu/basics/ (accessed 1.17.21).

Kapp, R.O., 1965. Illinoian and Sangamon vegetation in southwestern Kansas and adjacent Oklahoma.

Karlstrom, E.T., Oviatt, C.G., Ransom, M.D., 2008. Paleoenvironmental interpretation of multiple soil–loess sequence at Milford Reservoir, northeastern Kansas. CATENA 72, 113–128. https://doi.org/10.1016/j.catena.2007.04.009

Ko, J., Ahuja, L.R., Saseendran, S., Green, T.R., Ma, L., Nielsen, D.C., Walthall, C.L., 2012. Climate change impacts on dryland cropping systems in the Central Great Plains, USA. Climatic Change 111, 445–472.

Kuchler, A.W., 1974. A New Vegetation Map of Kansas. Ecology 55, 586–604.

Kustu, D.M., Fan, Y., Robock, A., 2010. Large-scale water cycle peturbation due to irrigation pumping in the US High Plains: A synthesis of observed streamflow changes. Journal of Hydrology 222–244.

LaBelle, J.M., Holliday, V.T., Meltzer, D.J., 2003. Early Holocene Paleoindian Deposits at Nall Playa, Oklahoma Panhandle, U.S.A. Geoarchaeology: An International Journal 18, 5–34.

Laity, J., 2014. Lunette, in: Encyclopedia of Planetary Landforms. Springer New York, New York, NY, pp. 1–4. https://doi.org/10.1007/978-1-4614-9213-9_494-1

Leavitt, S.W., Follett, R.F., Kimble, J.M., Pruessner, E.G., 2007. Radiocarbon and delta C-13 depth profiles of soil organic carbon in the US Great Plains: A possible spatial record of paleoenvironment and paleovegetation. Quaternary International 162, 21–34.

Litwinionek, L., Johnson, E., Holliday, V., 2003. The playas of the Southern High Plains: An archipelago of human occupation for 12,000 years on the North American grasslands. Islands on the plains: Ecological, social, and ritual use of landscapes 21–43.

Liu, Y., Goodrick, S.L., Stanturf, J.A., 2013. Future US wildfire potential trends projected using a dynamically downscaled climate change scenario. Forest Ecology and Management 294, 120–135.

Ludlow, M.M., Troughton, J.H., Jones, R.J., 1976. Technique for Determining Proportion of C3 and C4 Species in Plant Samples Using Stable Natural Isotopes of Carbon. Journal of Agricultural Science 87, 625–632.

Luo, H.-R., Smith, L.M., Haukos, D.A., Allen, B.L., 1999. Sources of Recently Deposited Sediments in Playa Wetlands. Wetlands 19, 176–181.

Maat, P.B., Johnson, W.C., 1996. Thermoluminescence and new 14C age estimates for late Quaternary loesses in southwestern Nebraska. Geomorphology 17, 115–128.

Macfarlane, A.P., Brownie, W.B., 2006. Enhancement of teh Bedrock-surface-elevation Map Beneath the Ogallala Portion of the High Plains Aquifer, Western Kansas, 20. Kansas Geological Survey.

Mandel, R.D., Hofman, J.L., 2003. Geoarchaeological investigations at the Winger site: A late Paleoindian bison bonebed in southwestern Kansas, USA. Geoarchaeology 18, 129–144.

Martin, C.W., 1993. Radiocarbon ages on late Pleistocene loess stratigraphy of Nebraska and Kansas, central Great Plains, U.S.A. Quaternary Science Reviews 12, 179–188.

Mason, J.A., Jacobs, P.M., Hanson, P.R., Miao, X., Goble, R.J., 2003. Sources and paleoclimatic significance of Holocene Bignell Loess, central Great Plains, USA. Quaternary Research 60, 330–339.

Mason, J.A., Joeckel, R.M., Bettis, E.A., 2007. Middle to Late Pleistocene loess record in eastern Nebraska, USA, and implications for the unique nature of Oxygen Isotope Stage 2. Quaternary Science Reviews 26, 773–792. https://doi.org/10.1016/j.quascirev.2006.10.007

Mason, J.A., Kuzila, M.S., 2000. Episodic Holocene loess deposition in central Nebraska. Quatern Int 67, 119–131.

Mason, J.A., Miao, X., Hanson, P.R., Johnson, W.C., Jacobs, P.M., Goble, R.J., 2008. Loess record of the Pleistocene–Holocene transition on the northern and central Great Plains, USA. Quaternary Science Reviews 27, 1772–1783. https://doi.org/10.1016/j.quascirev.2008.07.004

McGuire, V.L., 2017. Water-level and recoverable water in storage changes, high plains aquifer, predevelopment to 2015 and 2013-2015. (No. Scientific Investigations Report 2328-0328)). U.S. Department of the Interior, Geological Survey, Reston, VA, USA.

McIntyre, N.E., Wright, C.K., Swain, S., Hayhoe, K., Liu, G., Schwartz, F.W., Henebry, G.M., 2014. Climate forcing of wetland landscape connectivity in the Great Plains. Frontiers in Ecology and the Environment 12, 59–64.

Miao, X.D., Mason, J.A., Johnson, W.C., Wang, H., 2007. High-resolution proxy record of Holocene climate from a loess section in Southwestern Nebraska, USA. Palaeogeogr Palaeocl 245, 368–381. https://doi.org/10.1016/j.palaeo.2006.09.004

Modala, N.R., Ale, S., Goldberg, D.W., Olivares, M., Munster, C.L., Rajan, N., Feagin, R.A., 2017. Climate change projections for the Texas high plains and rolling plains. Theoretical and Applied Climatology 129, 263–280.

Muhs, D.R., Bettis, E.A., 2003. Quaternary loess-paleosol sequences as examples of climate-driven sedimentary extremes., in: Geological Society of America Special Paper 370. Geological Society of America, Boulder, CO, USA, pp. 53–73.

Muhs, D.R., Swinehart, J.B., Loope, D.B., Aleinikoff, J.N., Been, J., 1999. 200,000 Years of Climate Change Recorded in Eolian Sediments of the High Plains of Eastern Colorado and Western Nebraska, in: Lageson, D.R., Lester, A.P., Trudgill, B.D. (Eds.), Colorado and Adjacent

Areas: Geological Society of America Field Guide 1. Geological Society of America, Boulder, CO, USA, pp. 71–91.

Natural Resources Conservation Service, 2018. Official Series Description - Buffalo Park Series [WWW Document]. URL https://soilseries.sc.egov.usda.gov/OSD_Docs/B/BUFFALO_PARK.html (accessed 1.13.22).

Natural Resources Conservation Service, 2017. Official Series Description - Ulysses Series [WWW Document]. URL https://soilseries.sc.egov.usda.gov/OSD_Docs/U/ULYSSES.html (accessed 12.15.20).

Natural Resources Conservation Service, 2007. Official Series Description - Uly Series [WWW Document]. URL https://soilseries.sc.egov.usda.gov/OSD_Docs/U/ULY.html (accessed 1.13.22).

Natural Resources Conservation Service, 2006a. Official Series Description - Richfield Series [WWW Document]. URL https://soilseries.sc.egov.usda.gov/OSD_Docs/R/RICHFIELD.html (accessed 12.15.20).

Natural Resources Conservation Service, 2006b. Official Series Description - Ness Series [WWW Document]. URL https://soilseries.sc.egov.usda.gov/OSD_Docs/N/NESS.html (accessed 12.15.20).

Natural Resources Conservation Service, 1997. Official Series Description - Harney Series [WWW Document]. URL https://soilseries.sc.egov.usda.gov/OSD_Docs/H/HARNEY.html (accessed 1.13.22).

Nordt, L., von Fischer, J., Tieszen, L., 2007. Late Quaternary temperature record from buried soils of the North American Great Plains. Geology 35, 159–162.

Nordt, L.C., Boutton, T.W., Hallmark, C.T., Waters, M.R., 1994. Late Quaternary vegetation and climate changes in Central Texas based on the isotopic composition of organic carbon. Quaternary Research 41, 109–120.

NRCS, U., 2006. Land resource regions and major land resource areas of the United States, the Caribbean, and the Pacific Basin. US Department of Agriculture Handbook 296.

Osterkamp, W.R., Wood, W.W., 1987. Playa-Lake Basins on the Southern High Plains of Texas and New Mexico: Part 1. Hydrologic, Geomorphic, and Geologic Evidence for their Development. Geological Society of America Bulletin 99, 215–223.

Peel, M.C., Finlayson, B.L., McMahon, T.A., 2007. Updated world map of the Köppen-Geiger climate classification. Hydrology and earth system sciences discussions 4, 439–473.

Pillans, B., Naish, T., 2004. Defining the Quaternary. Quaternary Science Reviews 23, 2271–2282.

Pisias, N.G., Moore Jr, T., 1981. The evolution of Pleistocene climate: a time series approach. Earth and Planetary Science Letters 52, 450–458.

Prescott, G.C., 1951. Geology and Ground-Water Resources of Lane County, Kansas (No. Bulletin 93). Kansas Geological Survey, Lawrence, KS, USA.

Reeves, C.C., 1966. Pluvial Lake Basins of West Texas. The Journal of Geology 74, 269–291.

Reimer, P.J., Austin, W.E., Bard, E., Bayliss, A., Blackwell, P.G., Ramsey, C.B., Butzin, M., Cheng, H., Friedrich, M., 2020. The IntCal20 Northern Hemisphere radiocarbon age calibration curve (0–55 cal kBP). Radiocarbon 62, 725–757.

Rich, J., 2013. A 250,000-year record of lunette dune accumulation on the Southern High Plains, USA and implications for past climates. Quaternary Science Reviews 62, 1–20.

Sabin, T.J., Holliday, V.T., 1995. Playas and Lunettes on the Southern High Plains: Morphometric and Spatial Relationships. Annals of the Association of American Geographers 85, 286–305.

Schaetzl, R., Anderson, S., 2005. Soils Genesis and Geomorphology. Cambridge University Press, Cambridge, MA, USA.

Siddall, M., Rohling, E.J., Thompson, W.G., Waelbroeck, C., 2008. Marine isotope stage 3 sea level fluctuations: Data synthesis and new outlook. Reviews of Geophysics 46.

Skinner, R.H., Hanson, J.D., Hutchinson, G.L., Schuman, G.E., 2002. Response of C3 and C4 grasses to supplemental summer precipitation. Journal of range management 517–522.

Smith, L.M., 2003. Playas of the Great Plains. University of Texas Press, Austin, TX, USA.

Smith, L.M., Haukos, D.A., McMurry, S.T., LaGrange, T., Willis, D., 2011. Ecosystem services provided by playas in the High Plains: potential influences of USDA conservation programs. Ecological Applications 21, 82–92.

Soil Survey Staff, Natural Resources Conservation Service, U.S. Department of Agriculture, 2019a. Web Soil Survey [WWW Document]. URL Available: https://websoilsurvey.nrcs.usda.gov/ (accessed 6.7.19).

Soil Survey Staff, Natural Resources Conservation Service, U.S. Department of Agriculture, 2019b. Web Soil Survey [WWW Document]. URL Available: https://websoilsurvey.nrcs.usda.gov/ (accessed 6.7.19).

Spinazola, J.M., Dealy, M.T., 1983. Hydrology of the Ogallala aquifer in Ford County, southwestern Kansas (No. 83–4226), Water-Resources Investigations Report. U.S. Geological Survey.

Stanford, D., 1979. The Selby and Dutton sites: evidence for a possible pre-Clovis occupation of the High Plains. Pre-Llano Cultures of the Americas: Paradoxes and Possibilities. The Anthropological Society of Washington, Washington, DC 101–123.

Steffensen, J.P., Andersen, K.K., Bigler, M., Clausen, H., Dahl-Jensen, D., Fischer, H., Popp, T., Rasmussen, S., Rothlisberger, R., Ruth, U., Stauffer, B., Siggaard-Andersen, M., Sveinbjorndottir, L., Svensson, A., White, A., C., J.W., 2008. High-resolution Greenland ice core data show abrupt climate change happens in few years. Science 321, 680–684.

Stuiver, M., 1980. Workshop on 14C data reporting. Radiocarbon 22, 964–966.

Stuiver, M., Polach, H.A., 1977. Discussion reporting of 14C data. Radiocarbon 19, 355–363.

Stuiver, M., Reimer, P.J., Reimer, R.W., 2022. CALIB 8.20 [WWW Document]. URL http://calib.org (accessed 1.17.22).

Sun, D.H., Bloemendal, J., Rea, D.K., Vandenberghe, J., Jiang, F.C., An, Z.S., Su, R.X., 2002. Grain-size distribution function of polymodal sediments in hydraulic and aeolian environments, and numerical partitioning of the sedimentary components. Sediment Geol 152, 263–277.

Telfer, M.W., Thomas, D.S.G., 2006. Complex Holocene lunette dune development, South Africa: Implications for paleoclimate and models of pan development in arid regions. Geology 34, 853–856.

The KU News Service, 2020. Water levels mostly level in western Kansas [WWW Document]. The Garden City Telegram. URL https://www.gctelegram.com/news/20190419/water-levels-mostly-steady-in-western-kansas (accessed 12.17.20).

US Bureau of the Census, 1991. Statistical Abstract of the United States: 1991 (11th ed.) Washington, DC.

Waite, H.A., 1947. Geology and Groundwater Resources of Scott County, Kansas (No. Bulletin 66). Kansas Geological Survey, Lawrence, KS, USA.

Walker, M., 2005. Quaternary Dating Methods. Wiley.

Walker, M., Head, M., Berkelhammer, M., Björck, S., Cheng, H., Cwyna, L., Fisher, D., Gkinis, V., Long, A., Lowe, J., Newnham, R., Weiss, H., 2018. Formal ratification of the subdivision of the Holocene Series/ Epoch (Quaternary System/Period): Two new Global Boundary Stratotype Sections and Points (GSSPs) and three new stages/ subseries. Episodes 41. https://doi.org/10.18814/epiiugs/2018/018016

Wang, Y., Amundson, R., Trumbore, S., 1996. Radiocarbon dating of soil organic matter. Quaternary Research 45, 282–288.

Wanner, H., Beer, J., Bütikofer, J., Crowley, T.J., Cubasch, U., Flückiger, J., Goosse, H., Grosjean, M., Joos, F., Kaplan, J.O., others, 2008. Mid-to Late Holocene climate change: an overview. Quaternary Science Reviews 27, 1791–1828.

Wanner, H., Mercolli, L., Grosjean, M., Ritz, S.P., 2014. Holocene climate variability and change; a data-based review. Journal of the Geological Society 172, 254–263. https://doi.org/10.1144/jgs2013-101

Ward, C.R., Huddleson, E.W., 1972. Multipurpose modíficatíon of playa lakes. No.4 Texas Tech University, Lubbock, Texas.

Weeks, J.B., Gutentag, E.D., Heimes, F.J., Luckey, R.R., 1988. Summary of the High Plains Regional Aquifer-System Analysis In Parts of Colorado, Kansas, Nebraska, New Mexico, Oklahoma, South Dakota, Texas, and Wyoming, U.S. Geological Survey Professional Paper.

Welch, J.E., Hale, J.M., 1987. Pleistocene loess in Kansas--status, present problems, and future considerations. Kansas Geological Survey, Lawrence, Kansas.

Wishart, D., 2004. Encyclopedia of the Great Plains. University of Nebraska Press.

Witty, T.A., 1989. The Ehmke Site Discussed (14LA311) (Kansas State Historical Society Unpublished Report).

Wood, W.W., Sanford, W.E., Reeves, C.C., 1992. Large Lake Basins of the southern High Plains: Ground-water control of their origin? Geology Vol. 20., 535–538.

Woodburn, T.L., Johnson, W.C., Mason, J.A., Bozarth, S.R., Halfen, A.F., 2016. Vegetation dynamics during the Pleistocene–Holocene transition in the central Great Plains, USA. The Holocene 0959683616652710.

Zartman, R.E., Ramsey, R.H., Evans, P.W., Koenig, G., Truby, C., Kamara, L., 1996. Outerbasin, Annulus and Playa Basm Infíltíation Studies. Texas Joumal of Agricultural Natural Resources. Vol. 9.